

1. REPORT NUMBER CA13-2380	2. GOVERNMENT ASSOCIATION NUMBER	3. RECIPIENT'S CATALOG NUMBER
4. TITLE AND SUBTITLE Implementation of New Quieter Pavement Research: Accelerated Pavement Testing and Laboratory Evaluation of Different Open-Graded Hot-Mix Asphalt Materials	5. REPORT DATE 10/22/2013	
	6. PERFORMING ORGANIZATION CODE	
7. AUTHOR R. Wu, I. Guada, E. Coleri, A. Rezaei, M. Kayhanian, and J.T. Harvey	8. PERFORMING ORGANIZATION REPORT NO. UCPRC-RR-2013-04	
9. PERFORMING ORGANIZATION NAME AND ADDRESS University of California Pavement Research Center UC Davis, UC Berkeley One Shields Avenue Davis, CA 95616	10. WORK UNIT NUMBER	
	11. CONTRACT OR GRANT NUMBER 65A0394	
12. SPONSORING AGENCY AND ADDRESS California Department of Transportation Division of Research, Innovation, and System Information P.O. Box 942873 Sacramento, CA 94273-0001	13. TYPE OF REPORT AND PERIOD COVERED Research Report February 2013 - October 2013	
	14. SPONSORING AGENCY CODE	
15. SUPPLEMENTARY NOTES		

16. ABSTRACT

This study presented in this report is part of a long-term effort that started in 2005 to develop the specifications, guidelines, standardized laboratory and field test methods, and other information needed for quieter pavement research to be incorporated into standard Caltrans practices, and lead to quieter pavements. Based on an earlier laboratory study, several open-graded friction course (OGFC) mixes were selected for further evaluation with accelerated pavement testing using the Heavy Vehicle Simulator (HVS) and laboratory testing on plant-produced materials. These selected mixes had shown good overall laboratory performance in terms of durability and sound absorption, which is correlated with tire/pavement noise.

The five test cells included three new OGFC mixes, with the Caltrans 3/8 inch mix serving as the control mix. The study examined the performance of the selected OGFC mixes in terms of their constructability, rutting performance, moisture damage susceptibility, surface texture, permeability, clogging susceptibility, clogging and rutting mechanisms, and tire/pavement noise.

The #4P mixes offer superior noise and mechanical durability compared with the control mix. They have similar skid resistance as measured by Caltrans Test 342 and surface permeability. The Georgia 1/2 inch mix is likely to provide superior skid resistance and rutting performance compared to the control mix, although it could not be fully investigated in this project due to difficulties in getting it produced by local plants as designed. Based on the results from this study, it is recommended that several pilot sections be placed using a rubberized binder.

17. KEY WORDS Open Graded Friction Course, Accelerated Pavement Testing, Rutting, Surface Texture, Permeability	18. DISTRIBUTION STATEMENT No restrictions	
19. SECURITY CLASSIFICATION (of this report) Unclassified	20. NUMBER OF PAGES 164	21. COST OF REPORT CHARGED

DISCLAIMER STATEMENT

This document is disseminated in the interest of information exchange. The contents of this report reflect the views of the authors who are responsible for the facts and accuracy of the data presented herein. The contents do not necessarily reflect the official views or policies of the State of California or the Federal Highway Administration. This publication does not constitute a standard, specification or regulation. This report does not constitute an endorsement by the Department of any product described herein.

For individuals with sensory disabilities, this document is available in alternate formats. For information, call (916) 654-8899, TTY 711, or write to California Department of Transportation, Division of Research, Innovation and System Information, MS-83, P.O. Box 942873, Sacramento, CA 94273-0001.

Implementation of New Quieter Pavement Research: Accelerated Pavement Testing and Laboratory Evaluation of Different Open-Graded Hot-Mix Asphalt Materials

Authors:

R. Wu, I. Guada, E. Coleri, A. Rezaei,
M. Kayhanian, and J.T. Harvey

Partnered Pavement Research Program (PPRC) Contract Strategic Plan Element 3.21.1:
Implementation of New Quieter Pavement Research

PREPARED FOR:

California Department of Transportation
Division of Research, Innovation,
and System Information (DRISI)
Office of Roadway Research
California Department of Resources Recycling and
Recovery
Division of Materials Management and Local Assistance
Materials Management Section

PREPARED BY:

University of California
Pavement Research Center
UC Davis, UC Berkeley



DOCUMENT RETRIEVAL INFORMATION **Research Report: UCPRC-RR-2013-04**

Title: Implementation of New Quieter Pavement Research: Accelerated Pavement Testing and Laboratory Evaluation of Different Open-Graded Hot-Mix Asphalt Materials

Authors: R. Wu, I. Guada, E. Coleri, A. Rezaei, M. Kayhanian, and J.T. Harvey

Caltrans Technical Lead: Rupinder Dosanjh; **CalRecycle Technical Leads:** Robert Fujii and Nathan Gauff

Prepared for: Caltrans Division of Research, Innovation, and System Information (DRISI); and CalRecycle Division of Materials Management and Local Assistance

FHWA No.: CA142380A	Date Work Submitted: October 22, 2013	Date February 2013
Strategic Plan Element No: 3.21.1	Status: Stage 6 final version	Version No.: 1

Abstract:

This study presented in this report is part of a long-term effort that started in 2005 to develop the specifications, guidelines, standardized laboratory and field test methods, and other information needed for quieter pavement research to be incorporated into standard Caltrans practices, and lead to quieter pavements. Based on an earlier laboratory study, several open-graded friction course (OGFC) mixes were selected for further evaluation with accelerated pavement testing using the Heavy Vehicle Simulator (HVS) and laboratory testing on plant-produced materials. These selected mixes had shown good overall laboratory performance in terms of durability and sound absorption, which is correlated with tire/pavement noise. Specifically, the following HVS test cells were constructed for this experiment:

- Cell A: Caltrans 3/8 inch mix with PG 76-22PM binder, average as-built thickness = 0.06 ft
- Cell B1: #4P mix with PG 76-22PM binder, average as-built thickness = 0.06 ft
- Cell B2: Same mix as Cell B1, average as-built thickness = 0.07 ft
- Cell C: #4P mix with PG 64-16 binder, average as-built thickness = 0.05 ft
- Cell D: Georgia 1/2 inch mix with PG 58-34PM, average as-built thickness = 0.15 ft

The #4P mixes had nominal maximum aggregate size of 4.75 mm (#4 sieve) with “P” indicating a coarser aggregate gradation identified in the earlier laboratory study. The five test cells included three new OGFC mixes, with the Caltrans 3/8 inch mix serving as the control mix.

The study examined the performance of the selected OGFC mixes in terms of their constructability, rutting performance, moisture damage susceptibility, surface texture, permeability, clogging susceptibility, clogging and rutting mechanisms, and tire/pavement noise. Recommendations are made regarding further work with the #4 mixes, and temperatures for OGFC construction. While all of the mixes are feasible for a given project, the preliminary indications with regard to differences in expected performance are:

- The #4P mixes offer superior noise and mechanical durability compared with the control mix. They have similar skid resistance as measured by Caltrans Test 342 (CST) and surface permeability. They have lower macrotexture than the control, but more than dense-graded mixes. A rubberized binder may improve moisture sensitivity and rutting performance, which were better or worse than the control mix depending on the binder type.
- The Georgia 1/2 inch mix is likely to provide superior skid resistance and rutting performance compared to the control mix, although it could not be fully investigated in this project due to difficulties in getting it produced by local plants as designed. This mix is also likely to cost more because of the lime treatment and fibers recommended by the Georgia DOT in addition to the polymer-modified binder.

Based on the results from this study, it is recommended that several pilot sections be placed using a rubberized binder. For these mixes to be placed, the gradations may need to be adjusted somewhat to be producible using current crushed stone bin gradations. Consideration should be given to increasing the minimum surface and air temperatures for paving of open-graded mixes.

Keywords: Open Graded Friction Course, Accelerated Pavement Testing, Rutting, Surface Texture, Permeability

Proposals for implementation: Based on the results of this research it is recommended that adjustments be made to the gradation of the No. 4 maximum size aggregate open-graded mix used in this study so that it can be produced by a larger number of quarries in California. It is also recommended that several pilot sections be built in the field using the revised mix following the construction recommendations included in this report.

Related documents:

- *Laboratory Evaluation of the Noise and Durability Properties of Asphalt Surface Mixes*, by Q. Lu, P.C. Fu, and J.T. Harvey. 2010. UCPRC-RR-2009-07.

Signatures:

R. Wu 1st Author	J.T. Harvey Technical Review	D. Spinner Editor	J.T. Harvey Principal Investigator	R. Dosanjh Caltrans Technical Lead	T.J. Holland Caltrans Contract Manager
----------------------------	--	-----------------------------	--	--	--

DISCLAIMER

This document is disseminated in the interest of information exchange. The contents of this report reflect the views of the authors who are responsible for the facts and accuracy of the data presented herein. The contents do not necessarily reflect the official views or policies of the State of California or the Federal Highway Administration. This publication does not constitute a standard, specification or regulation. This report does not constitute an endorsement by the California Department of Transportation (Caltrans) of any product described herein.

For individuals with sensory disabilities, this document is available in braille, large print, audiocassette, or compact disk. To obtain a copy of this document in one of these alternate formats, please contact: the California Department of Transportation, Division of Research Innovation, and Systems Information, MS-83, P.O. Box 942873, Sacramento, CA 94273-0001.

PROJECT OBJECTIVES

The goal of this project, Partnered Pavement Research Center Strategic Plan Element (PPRC SPE) 3.21, titled “Implementation of New Quieter Pavement Research,” is to continue to support the development of specifications, guidelines, and standardized laboratory and field test methods that will result in quieter pavements. To further the application of recent laboratory research in PPRC SPEs 4.20 and 4.29 for both flexible and rigid pavements, tasks within this project include testing of new quieter HMA mixes under accelerated pavement testing with the Heavy Vehicle Simulator, monitoring of Caltrans pilot projects that use technologies for quieter rigid pavements, and monitoring of Caltrans pilot projects that use technologies for quieter flexible pavements. The performance-monitoring includes measurement of on-board sound intensity (OBSI), friction, texture, and permeability. This project’s results are to be used to further incorporate quieter pavement research into standard Caltrans practice, and may serve as a basis for changes in specifications and Quieter Pavement policy.

The goal of this project will be achieved through the following tasks:

- Accelerated pavement testing with the Heavy Vehicle Simulator and other field and laboratory testing to estimate performance of asphalt mixes identified in PPRC SPE 4.20, “Laboratory Evaluation of Durability and Noise Properties of Asphalt Surface Mixes”;
- Monitoring of surface characteristics on projects that use technologies for quieter rigid and flexible pavements through the construction process and the service life.

This report presents the results of the first task. The second task is the subject of another report regarding new concrete pavement surface technologies.

ACKNOWLEDGMENTS

The University of California Pavement Research Center acknowledges the following individuals and organizations who contributed to the project:

- Dr. Joseph Holland, Caltrans Division of Research, Innovation and System Information
- Rupinder (Bobby) Dosanjh and Linus Motumah, Caltrans Office of Pavement
- Bob Fujii and Nathan Gauff, CalRecycle
- The Dynatest/UCPRC Heavy Vehicle Simulator Crew under the leadership of Mr. Peter Millar

EXECUTIVE SUMMARY

The University of California Pavement Research Center (UCPRC) has been investigating quieter pavement technologies since 2005 by performing extensive field, laboratory, and modeling studies. The initial investigations were first carried out under the direction of the California Department of Transportation (Caltrans) Quieter Pavement Research (QPR) Task Group, and later by the Caltrans Office of Pavement. The goal of this quieter pavement research program is to help reduce tire/pavement and roadside noise by producing results required to develop specifications, guidelines, standardized laboratory and field test methods, and other information needed for quieter pavement research to be incorporated into standard Caltrans practice. This work has considered existing asphalt and concrete pavement surface types, and the development and/or evaluation of new types of asphalt and concrete surfaces.

In Caltrans Standard Specifications, open-graded friction courses (OGFC) include open-graded hot-mix asphalt (HMA-O), open-graded rubberized hot-mix asphalt (RHMA-O), and high-binder rubberized open-graded hot-mix asphalt (RHMA-O-HB). A previous UCPRC noise research project on asphalt pavements identified several new OGFC mix types from studies by other agencies in the U.S. and Europe, and developed several new mix designs based on the recommendations from the first two years of available noise data on flexible pavements. In a separate laboratory testing study completed in 2009 and published in 2010, the durability and acoustical properties of these new OGFC mix designs were evaluated.

A follow-up project to evaluate those new mixes was then undertaken as part of Partnered Pavement Research Center Strategic Plan Element 3.21 (PPRC SPE 3.21), and it included construction of a Heavy Vehicle Simulator (HVS) test track at the UCPRC research site on the UC Davis campus. Results from the HVS testing would provide additional information about the construction and performance of the new open-graded mixes. This report contains details of that construction, the HVS and other testing conducted, and the related laboratory evaluation of the materials placed on the test track. The results presented include evaluation of constructability, surface texture, tire/pavement noise, moisture damage susceptibility, permeability, clogging susceptibility, durability, and rutting performance. A current typical Caltrans OGFC mix per the 2006 Caltrans Standard Specification was included as the control for comparison with the results from the new mixes.

Specifically, the following HVS test cells were constructed for this experiment:

- Cell A: Caltrans 3/8 inch mix with PG 76-22PM binder, average as-built thickness = 0.06 ft
- Cell B1: #4P mix with PG 76-22PM binder, average as-built thickness = 0.06 ft
- Cell B2: Same mix as Cell B1, average as-built thickness = 0.07 ft
- Cell C: #4P mix with PG 64-16 binder, average as-built thickness = 0.05 ft
- Cell D: Georgia 1/2 inch mix with PG 58-34PM, average as-built thickness = 0.15 ft

The #4P mixes had nominal maximum aggregate size of 4.75 mm (#4 sieve), with “P” indicating a coarser aggregate gradation identified in the earlier laboratory study (Lu et al. 2009). The five test cells included three new OGFC mixes, with the Caltrans 3/8 inch mix serving as the control mix.

The results from the HVS and related field and laboratory testing programs included in this report were developed to answer the following questions about the selected OGFC mixes:

- **Will these OGFC mixes be quieter than the control mix as measured with on-board sound intensity (OBSI) in the field?** This was answered by running the OBSI noise test vehicle at reduced speed (35 mph instead of the normal 60 mph) over the test tracks after construction.
- **Will the texture benefits of these OGFC mixes last in the field relative to the control mix?** This was answered by monitoring the surface texture change of OGFC mixes during HVS testing.
- **Will these OGFC mixes be more susceptible to moisture damage in the field than the control mix?** An attempt was made to answer the question by applying HVS loading with water heated to around 75°F (25°C) ponded on the surface. Structural failure of the pavement occurred before moisture damage was observed in the OGFC layer.
- **Will the voids in these OGFC mixes be more prone to clogging than the control mix in the field?** This was answered differently depending on the clogging mechanism:
 - Clogging due to compression of voids caused by rutting was evaluated by monitoring the permeability in the wheelpath during HVS testing.
 - Clogging due to material deposited on the pavement surface being carried into the voids by rainfall was evaluated by rainfall simulation and use of x-ray computerized tomography (CT) scans to examine the air-void content and distribution before and after clogging simulation.
 - Clogging due to airborne dust deposition on the surface being pushed into the voids by traffic was evaluated by spreading dry dust on pavement surface before and during HVS testing along the wheelpath and monitoring the permeability during HVS testing.
- **Will these OGFC mixes rut more in the field than the control mix?** This was answered by applying HVS loading and measuring rutting with the pavement surface heated to 122°F (50°C) under dry conditions. The OGFC layer thickness change was separated from the total deformation to determine the rutting in the OGFC layer.
- **Will these mixes have better laboratory rutting performance than the control mix?** This was answered by performing Hamburg Wheel-Track Testing in the laboratory.
- **How durable are these OGFC mixes compared to the control mix?** This was answered by performing Cantabro tests, which provide an evaluation of the mechanical durability of the mix and the resistance to mix disintegration or raveling under traffic.

The results of this project are organized in this report as follows:

- Chapter 2 describes the HVS test track design, construction, as-built materials, and structure.
- Chapter 3 presents the experimental plan for the HVS tests and laboratory evaluation, and the testing methods, for CT scans of microstructure changes, surface texture, tire/pavement noise, permeability and clogging.
- Chapter 4 presents surface texture measurements from the HVS test track and in the laboratory, friction testing results, and noise measurements taken on the HVS test track.
- Chapter 5 details HVS test results related to moisture susceptibility performance.
- Chapter 6 presents the results and findings from the permeability and clogging evaluation on the test track, including clogging caused by simulated rain that contains suspended solids, from rutting, and from airborne dust.
- Chapter 7 documents the HVS and laboratory test results related to rutting performance.
- Chapter 8 presents open-graded layer microstructure changes caused by HVS trafficking.
- Chapter 9 documents the laboratory durability test results for the open-graded mixes.
- Chapter 10 provides a summary, conclusions, and recommendations based on this study.

Regarding the selection of the mixes for inclusion in the study, a comprehensive review of national and international experience with OGFC mixtures and subsequent laboratory testing on several mixes at the UCPRC recommended further evaluation of three mix types in either field or HVS test sections. These three mix types had been shown to have good overall laboratory performance in terms of sound absorption, which is correlated with tire/pavement noise, and for other performance-related properties determined with other laboratory tests:

- OGFC mixes with #4 (4.75 mm) nominal maximum aggregate size (NMAS), containing either an asphalt rubber or polymer-modified binder (referred to in this report as *#4 mixes*). Two #4 mixes were developed and were designated #4 and #4P due to small differences in aggregate gradation requirements. Compared with current Caltrans OGFC mix types, the smaller maximum aggregate size was expected to permit paving in thinner lifts, and to reduce noise by maintaining relatively high permeability but with reduced positive texture.
- Georgia OGFC mix with 1/2 inch (12.5 mm) NMAS (hereafter referred to as *Georgia 1/2 inch mix*).
- European double-layer porous asphalt (DLPA) mix, which uses an OGFC mix with a 5/16 inch (8 mm) NMAS as the upper layer and an OGFC mix with 5/8 inch (16 mm) NMAS as the lower layer.

Based on these recommendations and the limited space available on the HVS test track, a decision was made to construct HVS test sections using the #4 mixes and the 1/2 inch Georgia mix, as well as a standard Caltrans OGFC mix that would serve as the control. The European DLPA mixes were not selected for further testing due to limited space and the expected greater cost and construction difficulty compared to the other mixes.

Several local asphalt plants near Davis and in other parts of Northern California area had difficulty producing the required gradations with their current crushing and sorting set-ups. For example, operators of alluvial deposit quarries in the Central Valley were unable to produce either #4 or #4P NMAS gradations. Alluvial mining operations in southern California who were approached had similar difficulties producing these gradations with their current set-ups. Both of these alluvial quarry operators said that they could meet the gradation if they changed some parts of their operations; however, they could not do that for a reasonable cost to produce the small test sections for this study.

Two hard rock mines in the San Francisco Bay Area were able to produce the #4 NMAS gradation, but with difficulty: it required material losses of up to 50 percent to obtain the gradation. Similarly, with some material loss, the #4P NMAS gradation could also be produced. It was determined that to produce the #4 NMAS gradation for commercial production would require significant changes in the mining and grading processes, which would only be warranted if a sufficiently large market for these materials were to be created.

Mix designs conformed to California Test 368 (2003) to determine the optimum binder content (OBC) of the rubberized hot-mix asphalt, Type O (RHMA-O), except that the base binder used was PG 64-10 instead of AR4000. Following the mix design procedure, the OBC calculated was multiplied by 1.2 to determine the binder content with asphalt rubber-modified binder.

Table 2.6 in the report shows the binder type and binder content proposed in the initial mix designs for the four mixes, as well as the ones that were actually used in construction. As the table shows, the initial mix designs proposed an asphalt rubber and a polymer-modified binder; however last-minute difficulties in procuring the proposed binder types (see Section 2.4.1) led to changes in both the binder type and binder content of the mixes that were eventually constructed (as is shown in the table). Another late decision was to include Evotherm™ warm mix additive because of low temperatures anticipated on the days of construction. In addition, the Georgia Department of Transportation (GDOT) normally specifies a PG 70-22 binder for the Georgia mix, however that binder was unavailable when the mix was produced for the test sections. A decision was made to proceed in order to measure the permeability obtained for this gradation, understanding that other types of performance of the mix would not be to the expected standards of the GDOT specifications.

On the first day of paving, the weather was warm and clear, and the Georgia 1/2 inch mix was delivered for paving first. As unloading proceeded, it was found that the first load could not be completely discharged. Twenty-five to 35 percent (by visual estimate) of the mix stuck to the truck bed due to binder draindown, which prevented the second load, the transfer load, from being quickly discharged. The draindown was likely caused by excess binder in the mix, which normally would be been taken up by the fibers that were eliminated at the last minute. In addition, the combination of a long haul time and the use of the tarps, which were used for the

long haul distance to retain heat, may have contributed to the draindown. Another contributor to the problem may have been excessive binder in the mix, although the amount of draindown made measurement of binder content from sampling impossible. Using material that could be salvaged, construction of Cell D continued, but its total constructed length was shortened.

Based on these binder issues, a decision was made to find a stiffer polymer-modified binder for the remaining mixes. Paramount Petroleum was contacted regarding the use of PG 76-22PM (polymer-modified binder) and Telfer Oil was contacted regarding the use of warm-mix additives. Both companies were willing to supply the requested materials, which were unavailable at the time of the Georgia mix construction. The remaining UCPRC mix designs were re-run to account for these changes, with a resulting binder content reduction of about 0.5 percent for the #4P mixes, mixes B and C.

The weather was also warm and clear on the second day of paving. The test cells with revised mixes A (Caltrans 3/8 inch mix, now with polymer-modified binder) and B (#4P mix, now with polymer-modified binder) were paved. Air temperature at the start of paving was 62°F (17°C) and the pavement surface temperature was 55°F (13°C). Insufficient aggregate was available to pave Mix C (#4P mix, now with unmodified binder) on this day.

As seen in Figure 2.6, there were difficulties with spreading and compacting the two mixes, due to the crusting of the mix in the truck and the cooling of the thin lift. The scarred mat was caused by chunks of crusted material being dragged by the paver. The mixing temperature for the mixes (i.e., the Caltrans 3/8 inch mix and the two #4P mixes) with the warm mix additive was approximately 295°F (146°C), as reported by the plant operator. Initial mix temperatures taken from the paver hopper measured between 248°F (120°C) and 302°F (150°C). As with Mix D, these mixes cooled quickly after laydown. The mat temperature dropped more than 54°F (30°C) in five minutes.

Test Cell C with revised Mix C (#4P mix with unmodified binder) was constructed on the third day of paving, October 28, 2011, in the late afternoon, under the best conditions of all the paving days for this project: sunny and warm with no wind. The air temperature at the start of paving was 86°F (30°C) and the pavement surface temperature was 97°F (36°C). No problems were encountered during paving.

The as-built thicknesses show that the thickness was difficult to control during construction. The thickness differences among the four cells were relatively small. This made it impractical to evaluate the effect of OGFC layer thickness on performance, and cells B1 and B2 became replicates.

The following items summarize several important observations made about mix constructability and the relative performance of the different OGFC mixes compared to the control mix:

- Constructability:
 - The #4P gradation was selected because the original #4 gradation could not be produced in northern California with current crushed rock bin size gradations without excessive waste of unused aggregate. If there is a market for the #4P mixes, producers indicated a potential willingness to produce additional bin sizes to economically produce this gradation.
 - The lime treatment and mineral fiber additive required for the Georgia 1/2 inch mix (according to GDOT specifications) were not readily available for the mixing plants near Davis, California, and therefore they were not added to the mixes.
 - The design thicknesses of the OGFC layers ranged from 0.05 to 0.08 ft but all were constructed with roughly the same thickness, an indication of the difficulty in meeting such a fine distinction in thickness specifications using conventional paving equipment.
 - As with all OGFC construction, paving at cool temperatures can cause difficulties. It may be worthwhile to increase the minimum surface temperature and air temperatures in the standard specifications when paving thin layers of OGFC.
- Rutting performance:
 - Based on the HVS testing results, the #4P mix with PG 64-16 binder and the Georgia 1/2 inch mix with PG 58-34PM performed better than the control mix, while the #4P mix with PG 76-22PM binder performed either the same as or worse than the control.
 - Based on Hamburg Wheel-Tracking Test (HWTT) results, the #4P mix with PG 76-22PM binder was slightly better than the control mix, while the #4P mix with PG 64-16 binder and the Georgia 1/2 inch mix with PG 58-34PM were worse than the control.
 - HWTT and HVS testing yielded results that were completely opposite in terms of rutting performance ranking. It is believed this occurred due to their different testing conditions, with the submersion in water in the HWTT affecting the performance of the PG 64-16 mix, and that this indicates the importance of HVS testing for rutting.
- Moisture damage susceptibility:
 - The HVS was found to be ineffective for evaluating the moisture damage susceptibility of OGFC mixes.
 - The crumbling of finished HWTT specimens that contained the #4P mix with PG 64-16 binder indicates that this mix is much more susceptible to moisture damage than the control mix.

- Surface texture:
 - The three OGFC mixes had lower mean profile depths (MPD), and the same or longer outflow times than the control mix. The MPD values for the #4P mixes were within the range of MPD values measured using an inertial profiler on new OGFC and rubberized open-graded mixes across the state as part of the asphalt pavement noise study. The value for the control mix built for this study is high compared to values statewide.
 - California Portable Skid Tester (CST) measurements taken after HVS trafficking indicated that all three new OGFC mixes had roughly the same coefficient of friction.
 - Based on dynamic friction tester (DFT) measurements taken on the HVS test track, all three new mixes showed higher surface friction than the control mix. On the other hand, laboratory-prepared ingot specimens of the two #4P mixes showed lower DFT surface friction than the control mix.
 - MPD, dynamic friction measured by the DFT, and coefficient of friction measured by the CST for all mixes satisfied the minimum requirements throughout HVS testing,
- Mechanical durability:
 - The two #4P mixes had better durability than either the control mix or the Georgia 1/2 inch mix under mechanical tumbling in Cantabro testing.
- Permeability before being subjected to environmental or traffic loading:
 - The two #4P mixes had roughly the same permeability as the control mix, while the Georgia 1/2 inch mix had much higher permeability compared than the control mix.
- Clogging susceptibility:
 - After HVS trafficking, the two #4P mixes showed more a severe reduction in permeability caused by rutting than the control mix, while the Georgia 1/2 inch with PG 58-34PM binder showed a smaller reduction compared to the control mix.
 - Clogging from simulated rainfall with suspended solids induced a similar amount of air void reduction in all three mixes compared to the control.
 - Airborne dust was not found to lead to clogging in any of the OGFC mixes.
- Tire/pavement noise:
 - All three new #4P OGFC mixes had lower noise levels than the control mix. Noise was not tested on the Georgia 1/2 inch mix due to the short length of the section. The overall OBSI noise reduction of the #4P mixes ranged between 0.8 and 1.6 dBA, which would be barely perceptible, if at all, for human hearing. All of the reduction in noise was at higher frequencies, and the change in frequency content of the noise would likely be perceptible to humans.

Table 10.1 summarizes the comparative performance of the three new OGFC mixes and the control mix. As the table shows, all three new #4P mixes had pros and cons compared to the control mix. The study did validate that the pavements using these new OGFC mixes had lower tire/pavement noise. Considering the fact that all of the mixes satisfied the surface texture requirements, the following recommendations are made based on Table 10.1:

- For #4P mix with PG 76-22PM binder: This mix is recommended for places where rutting is not an issue. Clogging of this mix can mostly be avoided by limiting rutting.
- For #4P mix with PG 64-16 binder: This mix is recommended for places where moisture damage can be avoided. The mix had good rutting performance but is prone to moisture damage.
- For Georgia 1/2 inch mix with PG 58-34PM binder: This mix is recommended if lime treatment and mineral fiber additives can be accommodated, and the cost is determined to be feasible.
- When all of the mixes are feasible for a given project, the preliminary indications are:
 - The #4P mixes offer superior noise and mechanical durability compared with the control mix. Their skid resistance, as measured by Caltrans Test 342 (CST), and surface permeability are similar. They have less macrotexture than the control, but more than dense-graded mixes. A rubberized binder may improve moisture sensitivity and rutting performance, which were better or worse than the control mix depending on the binder type.
 - The Georgia 1/2 inch mix is likely to provide superior skid resistance and rutting performance compared to the control mix, although it could not be fully investigated in this project due to difficulties in getting it produced as designed by local plants. It is also likely to cost more because of the lime treatment and fibers in addition to the polymer-modified binder.
- Based on the results from this study, it is recommended that several pilot sections be placed using a rubberized binder. For these mixes to be placed, the gradations may need to be adjusted somewhat to be producible using current crushed stone bin gradations.
- Consideration should be given to increasing the minimum surface and air temperatures for paving of open-graded mixes.

TABLE OF CONTENTS

Project Objectives	iii
Acknowledgments	iv
Executive Summary	v
List of Tables	xvi
List of Figures	xviii
List of Abbreviations.....	xxiii
Conversion Factors	xxiv
1 Introduction	1
1.1 Background.....	1
1.2 Project Objectives.....	1
1.3 Structure and Content of this Report	3
1.4 Measurement Units.....	3
2 HVS Test Track Design and Construction.....	5
2.1 Selection of Open-Graded Mixes for Evaluation	5
2.2 Mix Designs.....	7
2.2.1 Caltrans 3/8 Inch (9.5 mm) Mix: Mix A	8
2.2.2 #4P (4.75 mm) Mix: Mixes B and C	9
2.2.3 Georgia 1/2 Inch Mix: Mix D.....	10
2.2.4 Binder Types and Contents	11
2.2.5 Mix Additives.....	12
2.3 Test Track Design.....	13
2.4 Test Track Construction	15
2.4.1 Paving Day 1, Monday, August 1, 2011: Mix D.....	15
2.4.2 Paving Day 2, Monday, October 24, 2011: Mixes A and B.....	16
2.4.3 Paving Day 3, Friday, October 28, 2011, Mix C.....	17
2.4.4 As-Built Air-Void Contents and Layer Thicknesses.....	17
3 Testing Program	19
3.1 Introduction	19
3.2 Material Description	19
3.3 HVS Testing Program	19
3.3.1 Objective	19
3.3.2 Test Section Layouts	19
3.3.3 HVS Test Protocols.....	20
3.3.4 Test Plan and Schedule.....	22
3.3.5 Rutting HVS Testing Program	23
3.3.6 Moisture Damage HVS Testing Program.....	24
3.3.7 Instrumentation and Data Collection Plan.....	26
3.4 Microstructure Change in Asphalt-Bound Layers Under HVS Trafficking.....	28
3.4.1 Objectives.....	28
3.4.2 Study Procedure	28
3.4.3 X-Ray CT Image Acquisition and Processing.....	32
3.4.4 Experiment Program.....	37
3.5 Surface Texture and Noise Testing on the HVS Test Track.....	37
3.5.1 Objectives.....	39
3.5.2 Testing Equipment	39
3.5.3 Test Procedures	40
3.5.4 Testing Program	44
3.6 Laboratory Testing	47

	3.6.1	Objective	47
	3.6.2	Testing Program	47
	3.6.3	Testing Procedures	48
	3.6.4	Specimen Preparation	48
3.7		Permeability and Clogging Evaluation	49
	3.7.1	Objectives and Methodology	49
	3.7.2	Measurement Locations	50
	3.7.3	Procedure for Permeability Measurements	52
	3.7.4	Procedure for Evaluating Runoff-Related Clogging	55
	3.7.5	Procedure for Evaluating Rutting-Related Clogging	60
4		Surface Texture and Noise Testing Results	61
4.1		Surface Texture and Noise Testing on HVS Test Tracks	61
	4.1.1	Dynamic Friction Tester Results	61
	4.1.2	Circular Texture Meter Results	63
	4.1.3	Laser Texture Scanner Results	66
	4.1.4	Outflow Meter Test Results	69
	4.1.5	Caltrans Portable Skid Tester Test Results	71
	4.1.6	Tire/Pavement Noise Measured by the OBSI Vehicle	73
	4.1.7	Summary of Surface Texture and Noise Measurements on HVS Test Track	79
4.2		Laboratory Test Results	81
5		Moisture Damage Susceptibility Test Results	85
5.1		Section 652HC: The First Pilot Test	85
	5.1.1	Temperature	85
	5.1.2	Permanent Deformation	87
	5.1.3	Visual Evaluation	87
	5.1.4	Summary of Test Results	88
5.2		HVS Test Results for Section 662HC: The Second Pilot Test	88
	5.2.1	Temperature	89
	5.2.2	Permanent Deformation	91
	5.2.3	Visual Damage	92
	5.2.4	Summary of Test Results	93
5.3		Summary of HVS Testing for Moisture Susceptibility	94
6		Permeability and Clogging Evaluation Results	95
6.1		Material Characteristics	95
6.2		Correlation of Permeability Results Measured by ASTM and NCAT Methods	95
6.3		Permeability Before HVS Trafficking	97
6.4		Rutting and Airborne Dust-Related Clogging	98
	6.4.1	Visual Indication	98
	6.4.2	Effect of Rutting on Permeability	99
	6.4.3	Effect of Airborne Dust on Permeability Reduction	101
	6.4.4	Change in Air-Void Content and Distribution	102
	6.4.5	Summary of Rutting-Related Clogging Test Results	103
6.5		Runoff-Related Clogging	104
6.6		Summary of Permeability and Clogging Evaluation Results	106
7		Rutting Performance	109
7.1		HVS Testing Results	109
	7.1.1	Temperature	109
	7.1.2	Visual Observation	110
	7.1.3	Permanent Deformation	112
7.2		Hamburg Wheel-Track Testing Results	114
	7.2.1	Material Characteristics of Specimens	114

	7.2.2	Visual Observations	115
	7.2.3	Test Results	116
7.3		Shear Stiffness Test Results	117
	7.3.1	Material Characteristics of Specimens	117
	7.3.2	Shear Stiffness of Different OGFC Mixes	117
7.4		Summary of Rutting Test Results.....	118
8		Microstructure Changes Under HVS Trafficking.....	119
	8.1	Densification of Asphalt Bound Layers	119
	8.2	Decomposition of Surface Downward Rut.....	121
	8.3	Aggregate Movement Caused by HVS Trafficking	122
	8.4	Summary of Results	126
9		Mix Durability	127
	9.1	Material Characteristics of Specimens	127
	9.2	Test Results	127
10		Summary, Observations, and Recommendations.....	129
	10.1	Summary.....	129
	10.2	Observations	129
	10.3	Recommendations	131
		References	134
		Appendix: Test Track Layout.....	137

LIST OF TABLES

Table 2.1: Summary of Characteristics of Mixes Selected for HVS Test Track	6
Table 2.2: OGFC Mixes Planned for Construction at ATIRC	7
Table 2.3: Aggregate Gradation Summary for 3/8 in. (9.5 mm) NMAS (Percent Passing).....	8
Table 2.4: Aggregate Gradation Summary for #4P (4.75 mm) NMAS (Percent Passing)	9
Table 2.5: Aggregate Gradation Summary for Mix D, 1/2 in.(12.5 mm) NMAS (Percent Passing).....	11
Table 2.6: Planned and Actual Binder Types and Binder Contents	12
Table 2.7: Planned and Actual HVS Test Track Design.....	14
Table 2.8: HVS Test Track Design and Layout	14
Table 2.9: Average and Standard Deviation of Measured Air-Void Contents of Each Test Cell.....	17
Table 2.10: Measured Density for Each Aggregate Bin Material	18
Table 2.11: Calculated Density and Air-Void Content for Coarse Aggregates	18
Table 3.1: HVS Testing Experiment Matrix	20
Table 3.2: Dates and Duration of HVS Testing of OGFC Sections	22
Table 3.3: Summary of HVS Loading Program for Rutting Tests.....	24
Table 3.4: Summary of HVS Loading Program for Moisture Damage Tests	26
Table 3.5: List of Tests for Surface Texture and Tire/Pavement Noise Evaluation.....	40
Table 3.6: Particle Gradations (Percent Passing) Used for Rainfall Simulation	58
Table 4.1: Dynamic Friction Values Measured at 20 km/h for Different Mixes	62
Table 4.2: Comparison of Dynamic Friction at 20 km/h of Different Mixes Against the Control	62
Table 4.3: Statistical Test on Effect of Binder Type on Dynamic Friction Measured by DFT	62
Table 4.4 Results of CTM-Measure MPD Values for Different Mixes	64
Table 4.5: Comparison of Initial CTM-Measured MPD for Experiment Mixes Against Control Mix	64
Table 4.6: Statistical Test on the Effect of Binder Type on CTM-Measured MPD Value	64
Table 4.7: Initial LTS-Measured MPD Values for the Different Mixes	66
Table 4.8: Comparison LTS-Measured MPD Values for the Different Mixes Versus the Control Mix	67
Table 4.9: Statistical Test on Effect of Binder Type on Initial LTS-Measured MPD.....	68
Table 4.10: Results of the OFT Values for Different Mixes.....	70
Table 4.11: Comparison of the Measured Outflow Time Values for Different Mixes Versus the Control	70
Table 4.12: Statistical Testing on the Effect of Binder Type on Initial Outflow Time.....	71
Table 4.13: COF Values Measured by California Portable Skid Tester (CST) for Different Mixes	71
Table 4.14: Comparison of COF Values Measured by CST for Different Mixes Against the Control	71
Table 4.15: Statistical Test on the Effect of Binder Type on Initial COF Measured by CST.....	72

Table 4.16 Mean and Standard Deviation of OBSI on Each Section for Each Frequency	74
Table 4.17: Summary of Surface Texture and Noise Measurements on Untrafficked Surfaces of Different OGFC Mixes Relative to Control Mix	80
Table 6.1: Measured Air-Void Content of Cores Used for X-Ray CT Imaging	95
Table 6.2: Statistics of Permeability for Different OGFC Mixes before HVS Trafficking	98
Table 7.1: Rutting Life of Test Sections	113
Table 7.2: Comparison of Rutting Life for Different Wheel Types.....	114
Table 7.3: Air-Void Contents of HWTT Specimens.....	115
Table 7.4: Summary of Characteristics of the HWTT Rut Accumulation Curves.....	116
Table 7.5: Air-Void Contents of Shear Stiffness Testing Specimens	117
Table 7.6: Summary of Rutting and Shear Stiffness for Different OGFC Mixes Relative to the Control Mix (Caltrans 3/8 inch Mix with PG 76-22PM Binder).....	118
Table 8.1: Downward Rut Caused by Air Void Reduction from X-Ray CT Images (mm).....	121
Table 8.2: Calculated Contributions of Shear, Densification, and Unbound Layer-Related Rutting to the Total Surface Rutting for OGFC and HMA Layers	122
Table 9.1: Percent Air-Void Content and Percent Weight Loss of Cantabro Test Specimens	127
Table 10.1: Summary of Performances of New OGFC Mixes Relative to the Control Mix	133

LIST OF FIGURES

Figure 2.1: Aggregate gradations from the laboratory evaluation report. [2]	7
Figure 2.2: Summary of design (“lab report”), as-built (“measured”), and specification (“operating limits”) gradations for the 3/8 in. (9.5 mm) aggregate gradation, Mix A.	9
Figure 2.3: Summary of design (“lab report”), as-built (“measured”), and specification (“operating limits”) gradations for the #4P (4.75 mm) aggregate gradation, mixes B and C.	10
Figure 2.4: Summary of design (“lab report”), revised (“design”), and specification (“operating limits”) gradations for the 1/2 in. (12.5 mm) mix, Mix D.	11
Figure 2.5: Aerial photo of the UC Davis ATIRC facility showing the test track locations and rough dimensions.	14
Figure 2.6: Scarring caused by crusted mix (Cell B1, #4P mix with PG 76-22PM).	16
Figure 3.1: Schematic and description of HVS test section layouts.	21
Figure 3.2: Schematic of an HVS test section and stations, thermocouple tree locations, and coordinate system.	21
Figure 3.3: Definition of maximum total rut (MTR).	23
Figure 3.4: Flooding method for the first HVS moisture damage test (Section 652HC).	25
Figure 3.5: Heater used for heating water and the wax dam used to pond the water for Section 662HC.	25
Figure 3.6: A “thermocouple tree” consisting of five Type-K thermocouples wrapped on a plastic dowel.	27
Figure 3.7: The laser profilometer.	27
Figure 3.8: The general procedure followed for x-ray CT image data collection.	31
Figure 3.9: Distributions of air voids in the block extracted from Section 655HB (#4P mix with PG 76-22PM binder) from two perspectives.	32
Figure 3.10: Segmented air voids in an asphalt concrete block taken from Section 655HB (#4P mix with PG 76-22PM binder) from two perspectives (colored volumes are air-voids).	34
Figure 3.11: Asphalt concrete blocks processed for rut calculations: (a) processed x-ray CT image (side view of the asphalt block) and (b) particle movement in deformed blocks.	35
Figure 3.12: Asphalt concrete block surface rutting profile located on the measured total surface rutting profile for Section 655HB (#4P mix with PG 76-22PM binder).	36
Figure 3.13: Cumulative distributions of the vertical deformations on the asphalt blocks to identify the contributions of the HMA and OGFC layers to total asphalt surface rutting, Section 655HB.	36
Figure 3.14: Section 653HB after 2,000 load repetitions with the asphalt concrete block at Station 5.	37
Figure 3.15: Pavement texture wavelength and the corresponding effects of surface characteristics [15].	38
Figure 3.16 Schematic plot of the effects of microtexture and macrotexture on pavement friction [16].	39

Figure 3.17: Dynamic Friction Tester.....	40
Figure 3.18: Circular Texture Meter.....	41
Figure 3.19: Laser Texture Scanner and an example of surface texture profile it measured (Section 655HB, #4P mix with PG 76-22PM binder).....	42
Figure 3.20: Outflow Meter.....	43
Figure 3.21: California Portable Skid Tester (CST) used to measured surface skid resistance following California Test (CT) 342.....	43
Figure 3.22: The UCPRC On-board Sound Intensity (OBSI) measurement vehicle.....	44
Figure 3.23: Locations of DFT, CTM, and OTF measurements for HVS rutting sections tested with dual wheels (i.e., Sections 651HB to 659HB).....	46
Figure 3.24: Locations of DFT, CTM, and OTF measurements for HVS rutting sections tested with NGWBT (i.e., Sections 661HB to 669HB).....	46
Figure 3.25: Preparation of ingot mold specimens for laboratory evaluation, including surface texture measurements and shear stiffness testing.....	49
Figure 3.26: Rainfall simulation locations.....	51
Figure 3.27: Spreading of passing #400 dust on the downslope wheelpath using a #200 sieve.....	52
Figure 3.28: NCAT field permeameter: (a) four cylindrical tiers with different diameters; (b) permeameter with bottom two tiers used in the field in this study.....	53
Figure 3.29: Permeameters used with the ASTM C1701 test method in this study.....	54
Figure 3.30: Photos of steps for evaluation of clogging susceptibility due to drainage of run-off using simulated rainfall.....	57
Figure 3.31: Rainfall simulation apparatus: schematic and actual device.....	59
Figure 3.32: Distribution of air voids in asphalt sample 1-655 (#4P mix with PG 76-22PM binder) from two perspectives.....	60
Figure 4.1: Dynamic friction measured by DFT at 20 km/h and 60 km/h for different mixes.....	62
Figure 4.2: Progression of dynamic friction measured with the DFT versus load repetitions for the different mixes at the beginning of HVS trafficking.....	63
Figure 4.3: Initial MPD values measured by CTM for the different mixes.....	65
Figure 4.4: The progression of CTM-measured MPD versus load repetitions for the different mixes.....	66
Figure 4.5: Initial LTS-measured MPD values for the different mixes.....	67
Figure 4.6: Relationship between MPD values measured by CTM and by LTS.....	68
Figure 4.7: The progression of LTS-measured MPD values versus repetition for the different mixes.....	69
Figure 4.8: Initial outflow time measured by OTF for the different mixes.....	70
Figure 4.9: Initial coefficient of friction values measured by the California Skid Tester for the different mixes.....	72

Figure 4.10: Initial and terminal COF values in the wheelpath for the different mixes.....	73
Figure 4.11: Overall sound intensities measured at 35 mph for the different mixes.....	76
Figure 4.12: 1/3 octave band noise content for the four mixes.	77
Figure 4.13: Relationship between surface macrotexture and sound intensity at 800 Hz.....	77
Figure 4.14: Relationship between permeability and sound intensity at (a) 1,000 Hz, (b) 1,250 Hz, and (c) 1,600 Hz.	79
Figure 4.15: Surface friction as measured by the CST and DFT on untrafficked surfaces.....	80
Figure 4.16: Mean profile depth measured by CTM and LTS on untrafficked surfaces.	81
Figure 4.17: Coefficients of friction measured on ingot specimens using the DFT.....	82
Figure 4.18: Mean profile depths measured on ingot specimens by both CTM and LTS.....	82
Figure 4.19: Outflow time on ingot specimens measured by the OTF.	83
Figure 5.1: Average hourly temperatures for Section 652HC.....	86
Figure 5.2: Average daily temperatures during HVS testing for Section 652HC.....	86
Figure 5.3: Accumulation of maximum total rut with load repetition for Section 652HC.	87
Figure 5.4: Photos of HVS Test Section 652HC after HVS trafficking showing cracking and subgrade rutting but no moisture damage in the OGFC surface layer.	88
Figure 5.5: Average hourly temperatures for Section 662HC.....	89
Figure 5.6: Average daily temperatures during HVS testing for Section 662HC.....	90
Figure 5.7: Average hourly water temperatures during HVS testing for Section 662HC grouped by HVS and heater status.....	91
Figure 5.8: Accumulation of maximum total rut with load repetitions for Section 662HC.....	92
Figure 5.9: Photos of HVS Test Section 662HC after HVS trafficking showing no sign of moisture damage in the OGFC surface layer other than that caused by the removal of Ecoflex sealant while taking permeability measurements.	93
Figure 6.1: Correlation between the permeability values measured by the ASTM and NCAT methods with standard 12 in. (300 mm) and modified 6 in. (150 mm) cylinder sizes.	96
Figure 6.2: Permeability for different OGFC mixes before HVS trafficking.	97
Figure 6.3: Surface photos of two sections previously tested with the HVS showing different residual permeability during a 0.17 in. (4.3 mm) rain.....	98
Figure 6.4: Variation of normalized residual permeability measured with the NCAT method with a normalized number of load repetitions for each test section.	100
Figure 6.5: Variation of normalized residual permeability measured with the NCAT method with average maximum total rut for each test section.....	100

Figure 6.6: Percent reduction in permeability for the different OGFC mixes after HVS trafficking, which led to approximately 0.5 in. of average maximum total rut.....	101
Figure 6.7: Comparison of percent reductions in permeability measured by both the NCAT and ASTM methods under different conditions with respect to airborne dust application.	102
Figure 6.8: Air-void content distributions of three asphalt cores before and after rutting tests, depth = 0 for the OGFC surface.	103
Figure 6.9: Air-void content distributions of cores before and after rainfall simulations with <38 micron particle gradation (depth = 0 for the surface OGFC layer).....	105
Figure 6.10: Air-void content distributions of cores before and after rainfall simulations with <600 micron particle gradation (depth = 0 mm is the surface of the OGFC layer).	106
Figure 7.1: Hourly average temperatures while trafficking for Section 657HB (dual wheel, #4P mix with PG 64-16 binder).	109
Figure 7.2: Surface photos of Sections 651HB and 661HB (Georgia 1/2 inch mix with PG 58-34PM binder, Cell D) after HVS trafficking.	110
Figure 7.3: Surface photos of Sections 653HB and 663HB (Caltrans 3/8 inch mix with PG 76-22PM binder, Cell A) after HVS trafficking.	110
Figure 7.4: Surface photos of Sections 655HB and 665HB (#4P mix with PG 76-22PM binder, Cell B1) after HVS trafficking.	111
Figure 7.5: Surface photos of Sections 657HB and 667HB (#4P mix with PG 76-22PM binder, Cell B2) after HVS trafficking.	111
Figure 7.6: Surface photos of Sections 659HB and 669HB (#4P mix with PG 64-16 binder, Cell C) after HVS trafficking.	111
Figure 7.7: Accumulation of total rut for the HVS sections tested under dual-wheel traffic.....	112
Figure 7.8: Accumulation of total rut for the HVS sections tested under next generation wide base tire (NGWBT) traffic.	113
Figure 7.9: Examples of specimens of each OGFC mix after HWTT testing.....	115
Figure 7.10: Comparison of rut accumulation in HWTT results for the different mixes; the results plotted are the average of four replicates except for the Georgia mix, which had only two replicates.	116
Figure 7.11: Shear stiffness of different OGFC mixes tested at 131°F (55°C) under different loading frequencies.....	117
Figure 8.1: Reductions in air-void content caused by HVS trafficking (a) in the wheelpath area and (b) in the hump area (b).	120

Figure 8.2: Rutting distributions caused by air void reductions in (a) Section 653HB (Caltrans 3/8 inch mix with PG 76-22PM binder), (b) Section 655HB (#4P mix with PG 76-22PM binder), and (c) Section 657HB (#4P mix with PG 64-16 binder)..... 121

Figure 8.3: Displacement vectors for one 0.8 in. (20 mm) segment of each of the asphalt concrete blocks (front view): (a) Section 653HB (Caltrans 3/8 inch mix with PG 76-22PM binder), (b) Section 655HB (#4P mix with PG 76-22PM binder), and (c) Section 657HB (#4P mix with PG 64-16 binder). 124

Figure 8.4: Cumulative distribution functions of the vertical particle displacements..... 125

Figure 9.1: Examples of residual specimens after Cantabro testing of the different OGFC mixes. 128

Figure A.1: HVS section layout on the north outer track for OGAC study. 137

Figure A.2: HVS section layout on the west outer track for OGAC study. 138

LIST OF ABBREVIATIONS

AASHTO	American Association of State Highway and Transport Officials
ASTM	American Society for Testing and Materials
Caltrans	California Department of Transportation
COF	Coefficient of Friction
CST	California Portable Skid Tester
CTM	Circular Texture Meter
DFT	Dynamic Friction Tester
DGAC	Dense-graded asphalt concrete
FHWA	Federal Highway Administration
HMA-O	Open-graded hot-mix asphalt
HVS	Heavy Vehicle Simulator
HWTT	Hamburg Wheel-Tracking Test
MPD	Mean profile depth
NCAT	National Center for Asphalt Technology
NGWBT	Next generation wide-base tire
OBC	Optimum Binder Content
OBSI	On-board sound intensity
OGFC	Open-graded friction course
OTF	Outflow Meter
PPRC	Partnered Pavement Research Center
RHMA-O	Open-graded rubberized hot-mix asphalt
RHMA-O-HB	High-binder rubberized open-graded hot-mix asphalt
SPE	Strategic Plan Element
SST	Simple Shear Tester (Superpave)
TSS	Total Suspended Solid concentration
UCDMC	University of California, Davis, Medical Center
UCPRC	University of California Pavement Research Center
X-ray CT imaging	X-ray computerized tomography imaging

CONVERSION FACTORS

SI* (MODERN METRIC) CONVERSION FACTORS				
Symbol	Convert From	Convert To	Symbol	Conversion
LENGTH				
mm	millimeters	inches	in	mm x 0.039
m	meters	feet	ft	m x 3.28
km	kilometers	mile	mile	km x 1.609
AREA				
mm ²	square millimeters	square inches	in ²	mm ² x 0.0016
m ²	square meters	square feet	ft ²	m ² x 10.764
VOLUME				
m ³	cubic meters	cubic feet	ft ³	m ³ x 35.314
kg/m ³	kilograms/cubic meter	pounds/cubic feet	lb/ft ³	kg/m ³ x 0.062
L	liters	gallons	gal	L x 0.264
L/m ²	liters/square meter	gallons/square yard	gal/yd ²	L/m ² x 0.221
MASS				
kg	kilograms	pounds	lb	kg x 2.202
TEMPERATURE (exact degrees)				
C	Celsius	Fahrenheit	F	°C x 1.8 + 32
FORCE and PRESSURE or STRESS				
N	newtons	poundforce	lbf	N x 0.225
kPa	kilopascals	poundforce/square inch	lbf/in ²	kPa x 0.145
<p><small>*SI is the symbol for the International System of Units. Appropriate rounding should be made to comply with Section 4 of ASTM E380. (Revised March 2003)</small></p>				

1 INTRODUCTION

1.1 Background

The University of California Pavement Research Center (UCPRC) has been investigating quieter pavement technologies since 2005 by performing extensive field, laboratory, and modeling studies. The initial investigations were first carried out under the direction of the California Department of Transportation (Caltrans) Quieter Pavement Research (QPR) Task Group, and later by the Caltrans Office of Pavement. The goal of this quieter pavement research program is to help reduce tire/pavement and roadside noise by producing results required to develop specifications, guidelines, standardized laboratory and field test methods, and other information needed for quieter pavement research to be incorporated into standard Caltrans practice. This work has considered existing asphalt and concrete pavement surface types, and the development and/or evaluation of new types of asphalt and concrete surfaces.

In Caltrans Standard Specifications, open-graded friction courses (OGFC) include open-graded hot-mix asphalt (HMA-O), open-graded rubberized hot-mix asphalt (RHMA-O) and high-binder rubberized open-graded hot-mix asphalt (RHMA-O-HB). A previous UCPRC noise research project on asphalt pavements identified several new OGFC mix types from studies by other agencies in the U.S. and Europe, and developed several new mix designs based on the recommendations from the first two years of available noise data on flexible pavements [1]. In a separate laboratory testing study completed in 2009 and published in 2010 [2], the durability and acoustical properties of these new OGFC mix designs were evaluated.

In order to further evaluate those new mixes, a follow-up project included construction of a Heavy Vehicle Simulator (HVS) test track at the UCPRC research site on the UC Davis campus to obtain additional information regarding the construction and performance of the new open-graded mixes recommended by the laboratory evaluation [2]. The construction, HVS and other testing, and related laboratory evaluation of the materials placed on the test track are the subject of this report; they were performed as part of Partnered Pavement Research Center Strategic Plan Element (PPRC SPE) 3.21. The results include evaluation of constructability, surface texture, tire/pavement noise, moisture damage susceptibility, permeability, clogging susceptibility, durability, and rutting performance. A current typical Caltrans OGFC mix per 2006 Caltrans Standard Specification [3] was included as the control for comparison with the results from the new mixes.

1.2 Project Objectives

The goal of the UCPRC work is to support the Caltrans Quieter Pavement Research Program in the development of specifications, guidelines, and standardized laboratory and field test methods that will result in quieter pavements. The following are the objectives of PPRC SPE 3.21, "Implementation of New Quieter Pavement Research":

- Accelerated pavement testing with the Heavy Vehicle Simulator and other field and laboratory testing to estimate the performance of asphalt mixes identified in PPRC SPE 4.20, “Laboratory Evaluation of Durability and Noise Properties of Asphalt Surface Mixes”;
- Monitoring of surface characteristics on projects that use technologies for quieter rigid and flexible pavements through the construction process and the service life.

This report presents the results of the first task. The second task is the subject of another report regarding new concrete pavement surface technologies [4].

To address the first objective, the HVS and related field and laboratory testing programs were developed to answer the following questions about the selected OGFC mixes:

- **Will these OGFC mixes be quieter than the control mix as measured with on-board sound intensity (OBSI) in the field?** This was answered by running the OBSI test vehicle at reduced speed over the test tracks after construction.
- **Will the texture benefits of these OGFC mixes last in the field relative to the control mix?** This was answered by monitoring the surface texture change of OGFC mixes during HVS testing.
- **Will these OGFC mixes be more susceptible to moisture damage in the field than the control mix?** An attempt was made to answer the question by applying HVS loading with water heated to around 25°C ponded on the surface. Structural failure of the pavement occurred before moisture damage was observed in the OGFC layer.
- **Will the voids in these OGFC mixes be more prone to clogging than the control mix in the field?** This was answered differently depending on the clogging mechanism:
 - Clogging due to compression of voids caused by rutting was evaluated by monitoring the permeability in the wheelpath during HVS testing.
 - Clogging due to material deposited on the pavement surface being carried into the voids by rainfall was evaluated by rainfall simulation and use of x-ray computerized tomography (CT) scans to examine the air-void content and distribution before and after clogging simulation.
 - Clogging due to airborne dust deposition on the surface being pushed into the voids by traffic was evaluated by spreading dry dust on pavement surface before and during HVS testing along the wheelpath and monitoring the permeability during HVS testing.
- **Will these OGFC mixes rut more in the field than the control mix?** This was answered by applying HVS loading and measuring rutting with the pavement surface heated to 122°F (50°C) under dry conditions. The OGFC layer thickness change was separated from the total deformation to determine the rutting in the OGFC layer.

- **Will these mixes have better laboratory rutting performance than the control mix?** This was answered by performing Hamburg Wheel-Track Testing in the laboratory.
- **How durable are these OGFC mixes compared to the control mix?** This was answered by performing Cantabro tests, which provide an evaluation of the mechanical durability of the mix and the resistance to mix disintegration or raveling under traffic.

1.3 Structure and Content of this Report

The results of this project are organized in this report as follows:

- Chapter 2 describes the HVS test track design, construction, as-built materials, and structure.
- Chapter 3 presents the experimental plan for the HVS tests and laboratory evaluation, and the testing methods for CT scans of microstructure changes, surface texture, tire/pavement noise, permeability and clogging.
- Chapter 4 presents surface texture measurements from the HVS test track and in the laboratory, friction testing results, and noise measurements taken on the HVS test track.
- Chapter 5 details HVS test results related to moisture susceptibility performance.
- Chapter 6 presents the results and findings from the permeability and clogging evaluation on the test track, including clogging caused by simulated rain that contains suspended solids, from rutting, and from airborne dust.
- Chapter 7 documents the HVS and laboratory test results related to rutting performance.
- Chapter 8 presents open-graded layer microstructure changes caused by HVS trafficking
- Chapter 9 documents the laboratory durability test results for the open-graded mixes.
- Chapter 10 provides a summary, conclusions, and recommendations based on this study.

1.4 Measurement Units

Caltrans has recently returned to the use of US standard measurement units. The data acquisition systems and databases for the HVS test tracks and laboratory testing were set up for metric units 20 years ago, which continue to be used for measurement to avoid dual units in the same databases. In this report, both US and metric units are shown.

2 HVS TEST TRACK DESIGN AND CONSTRUCTION

The mix types used for this project were based on earlier laboratory work performed by UCPRC, and were to be studied on a test track designed specifically for this evaluation. The track, which was built at the Advanced Transportation Infrastructure Research Center (ATIRC) facility west of the UC Davis campus, was to be used for an investigation of constructability, for accelerated pavement testing with the Heavy Vehicle Simulator (HVS), clogging and moisture susceptibility testing, and for noise and skid testing. Materials for laboratory testing were also taken from the test-track construction site.

2.1 Selection of Open-Graded Mixes for Evaluation

A comprehensive review of national and international experience with OGFC mixtures and subsequent laboratory testing on several mixes at the UCPRC recommended further evaluation of three mix types in either field or HVS test sections [2]. These three mix types had been shown to have good overall laboratory performance in terms of sound absorption, which is correlated with tire/pavement noise, and for other performance-related properties determined with other laboratory tests:

- OGFC mixes with #4 (4.75 mm) nominal maximum aggregate size (NMAS), containing either an asphalt rubber or polymer-modified binder (referred to in this report as *#4 mixes*). Two #4 mixes were developed and were designated #4 and #4P due to small differences in aggregate gradation requirements. Compared with current Caltrans OGFC mix types, the smaller maximum aggregate size was expected to permit paving in thinner lifts, and to reduce noise by maintaining relatively high permeability but with reduced positive texture.
- Georgia OGFC mix with 1/2 inch (12.5 mm) NMAS (hereafter referred to as *Georgia 1/2 inch mix*).
- European double-layer porous asphalt (DLPA) mix, which uses an OGFC mix with a 5/16 inch (8 mm) NMAS as the upper layer and an OGFC mix with 5/8 inch (16 mm) NMAS as the lower layer.

Based on these recommendations and the limited space available on the HVS test track, a decision was made to construct HVS test sections using the #4 mixes and the 1/2 inch Georgia mix, as well as a standard Caltrans OGFC mix that would serve as the control. Table 2.1 lists the selected mixes. The European DLPA mixes were not selected for further testing due to limited space and the expected greater cost and construction difficulty compared to the other mixes.

Table 2.1: Summary of Characteristics of Mixes Selected for HVS Test Track

No.	Mix Type	Binder Type	Nominal Maximum Aggregate Size (NMAS)		Lab Report [2] ID Label
			Sieve Size	Opening (mm)	
1	Control	Asphalt rubber	3/8 inch	9.50	AR95
2	#4 mix	Asphalt rubber	#4	4.75	AR475
3	#4P ¹ mix	Asphalt rubber	#4P ¹	4.75	AR475P ¹
4	#4 mix	PG 76-22PM	#4	4.75	P475
5	Georgia mix ²	PG 76-22PM	1/2 inch	12.50	G125

¹: The “P” in AR475P and in #4P signifies “plus,” which represents a coarser gradation compared to the #4 mix but with the same NMAS.

²: Georgia 1/2 inch open-graded friction course mix contains lime-treated aggregates (1.4 percent by dry weight of aggregate) and mineral fibers (0.4 percent by total weight of mix).

Figure 2.1 shows the target aggregate gradations of the five mixes listed in Table 2.1 and those used in the earlier laboratory study.

Several local asphalt plants near Davis and in other parts of Northern California area had difficulty producing the required gradations with their current crushing and sorting set-ups. For example, operators of alluvial deposit quarries in the Central Valley were unable to produce either #4 or #4P NMAS gradations. Alluvial mining operations in southern California who were approached had similar difficulties producing these gradations with their current set-ups. Both of these alluvial quarry operators said that they could meet the gradation if they changed some parts of their operations; however, they could not do that for a reasonable cost to produce the small test sections for this study.

Two hard rock mines in the San Francisco Bay Area were able to produce the #4 NMAS gradation, but with difficulty: it required material losses of up to 50 percent to obtain the gradation. Similarly, with some material loss, the #4P NMAS gradation could also be produced. It was determined that to produce the #4 NMAS gradation for commercial production would require significant changes in the mining and grading processes, which would only be warranted if a sufficiently large market for these materials were to be created.

As the date for test track construction neared, Syar Industries was approached and agreed to produce the mixes using its hard rock basalt material from Lake Herman. Syar was selected because of its proximity to the construction site as well as its ability to produce the experimental mixes, which are listed in Table 2.2.

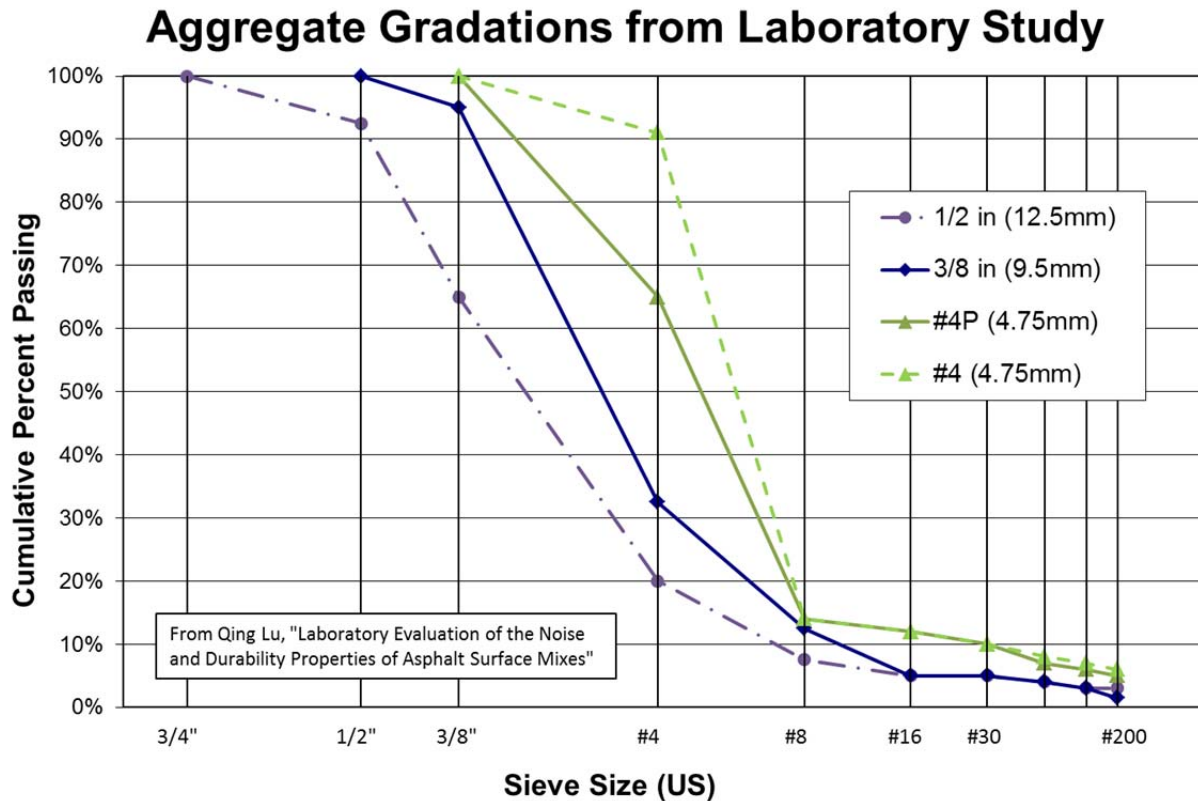


Figure 2.1: Aggregate gradations from the laboratory evaluation report. [2]

Table 2.2: OGFC Mixes Planned for Construction at ATIRC

Mix ID	Mix Type	Aggregate NMA5	Binder Type	Notes
A	Caltrans 3/8 inch mix (Control)	3/8 inch (9.5 mm)	Asphalt rubber	
B	#4P mix	#4P sieve (4.75 mm)	Asphalt rubber	
C	#4P mix	#4P sieve (4.75 mm)	Polymer-modified	
D	Georgia 1/2 inch mix	1/2 inch (12.5 mm)	Polymer-modified	No lime treatment or mineral filler

2.2 Mix Designs

Mix designs for the selected open-graded aggregate mix types are discussed below. Mix A, the Caltrans standard mix using the 2006 standard specifications [3] is covered in Section 2.2.1; Mixes B and C, with the #4P gradation are covered in Section 2.2.2; and Mix D, the Georgia mix with the 1/2 inch (12.5 mm) gradation that differs from the Caltrans 1/2 inch (12.5 mm) open gradation, is discussed in Section 2.2.3. Section 2.2.4 reviews the binder types and contents for the four mixes. Finally, Section 2.2.5 discusses mix additives considered during this study.

The aggregate gradation for each mix is discussed, including the limits of the proposed gradation, the operating and contract compliance ranges, the gradation used for the laboratory study, the proposed gradation for the test tracks, and the results of ignition oven testing for the as-built aggregate gradation following AASHTO T 30 (although without correction for aggregate burn-off). Following those is a review of the planned and final constructed binder types and binder contents, with constructed binder contents determined from ignition oven testing, again without any correction to the binder content.

2.2.1 Caltrans 3/8 Inch (9.5 mm) Mix: Mix A

Mix A, a Caltrans mix that follows the standard specification of 2006 [3], was included in the study as a control. An aggregate gradation summary for Mix A appears Table 2.3.

Table 2.3: Aggregate Gradation Summary for 3/8 in. (9.5 mm) NMAS (Percent Passing)

Sieve Sizes	Limits of Proposed Gradation	Operating Range	Contract Compliance	Laboratory Gradation	Target Construction Gradation	Measured Construction Gradation *
1/2 inch	–	100	100	100	100	100
3/8 inch	–	90 – 100	88 – 100	95	100	100
No. 4	29 – 36	X ± 4	X ± 7	33	30	27
No. 8	7 – 18	X ± 4	X ± 5	13	8	7
No. 16	–	0 – 10	0 – 12	5	6	5
No. 200	–	0 – 3	0 – 4	1.5	1.7	3.3

*from uncorrected ignition oven results.

Figure 2.2 presents the operating limits of the proposed gradation, the gradation used during the earlier laboratory study [2], the target gradation for this study, and the measured gradation from samples taken the day of construction and burned with an ignition oven according to AASHTO T 30, with no corrections made to the gradation results.

3/8 inch Aggregate Gradation

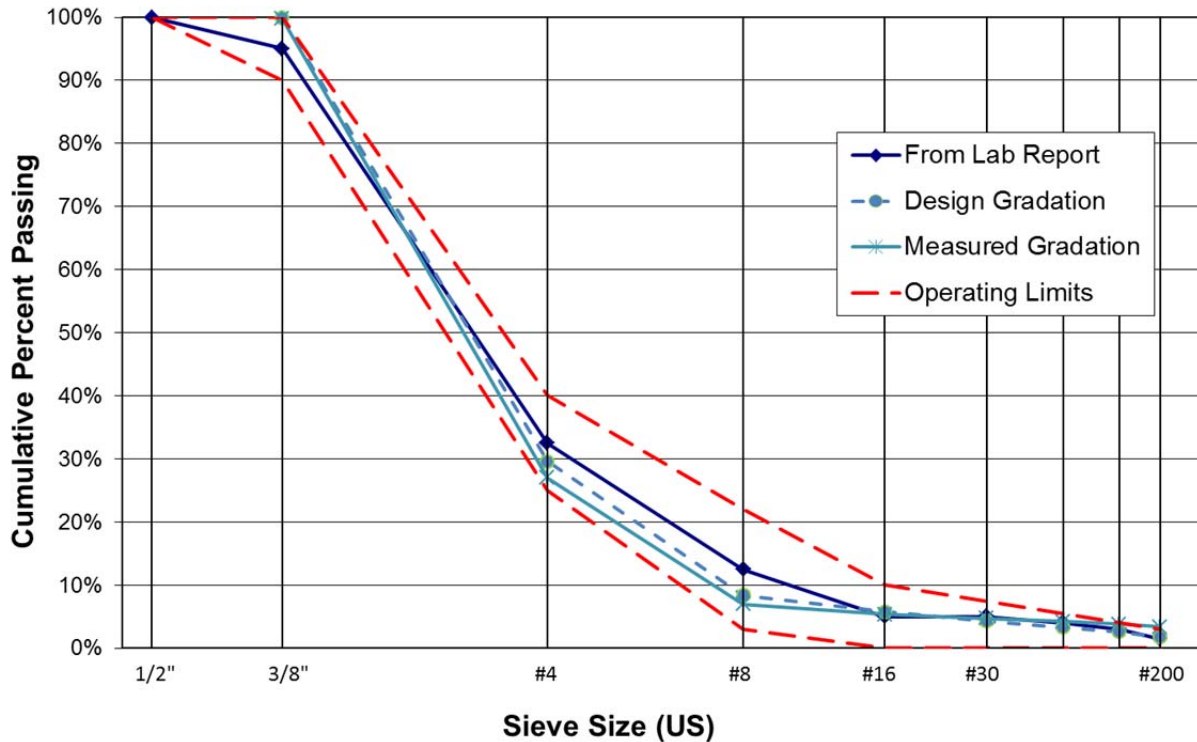


Figure 2.2: Summary of design (“lab report”), as-built (“measured”), and specification (“operating limits”) gradations for the 3/8 in. (9.5 mm) aggregate gradation, Mix A.

2.2.2 #4P (4.75 mm) Mix: Mixes B and C

An aggregate gradation summary for mixes B and C appears in Table 2.4. The proposed gradation limits, operating range, and contract compliance values were generated based on the target gradation and limits to the Caltrans 3/8 inch open-graded mix. The measured construction gradation is based on samples taken from both mixes.

Table 2.4: Aggregate Gradation Summary for #4P (4.75 mm) NMAAS (Percent Passing)

Sieve Sizes	Limits of Proposed Gradation	Operating Range	Contract Compliance	Laboratory Gradation	Target Construction Gradation	Measured Construction Gradation*
3/8 inch	—	100	100	100	100	100
No. 4	62 – 68	X ± 4	X ± 6	65	65	63
No. 8	11 – 17	X ± 4	X ± 6	14	14	15
No. 30	—	0 – 15	0 – 19	10	5	6
No. 200	—	0 – 7	0 – 9	5.0	2.2	3.5

*from uncorrected ignition oven results.

Figure 2.3 presents the operating limits of the proposed gradation, the gradation used during the earlier laboratory study, the design gradation for this study, and the measured gradation from samples taken the day of construction and burned with an ignition oven.

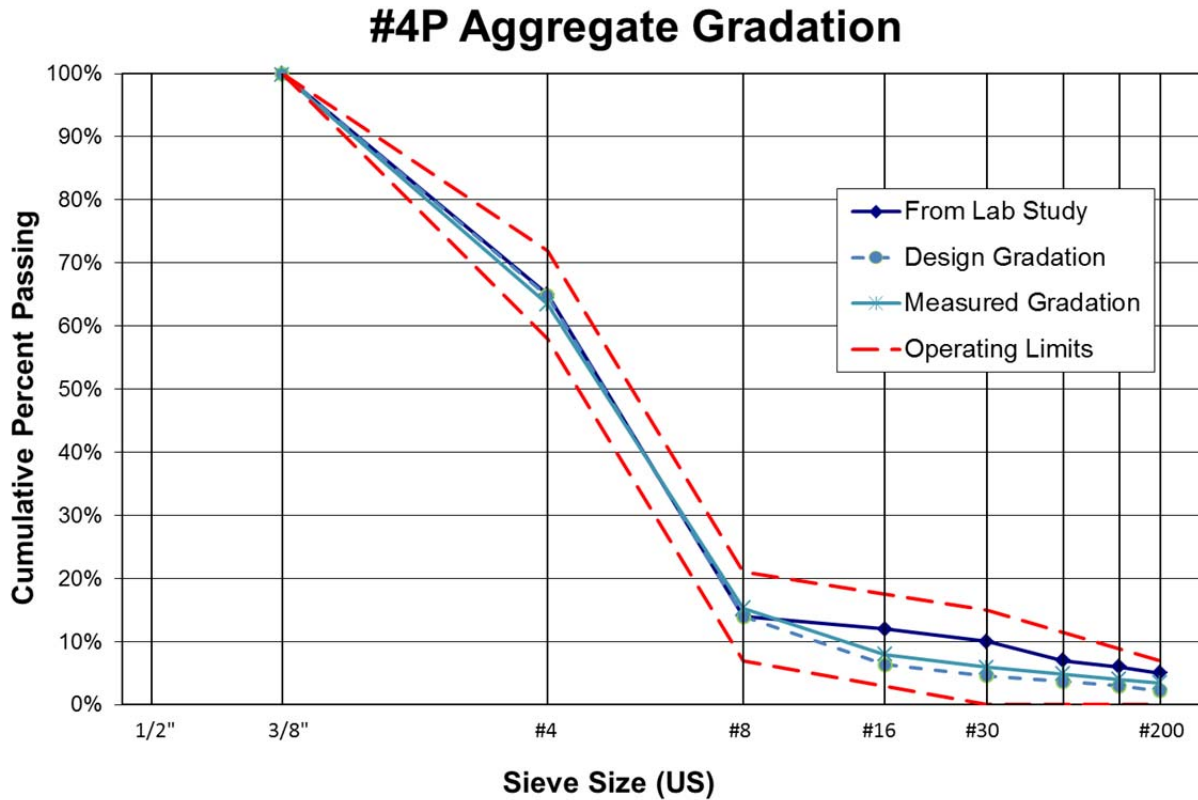


Figure 2.3: Summary of design (“lab report”), as-built (“measured”), and specification (“operating limits”) gradations for the #4P (4.75 mm) aggregate gradation, mixes B and C.

2.2.3 Georgia 1/2 Inch Mix: Mix D

An aggregate gradation summary for Mix D appears in Table 2.5, with a graphical presentation in Figure 2.4. According to Georgia specifications, the aggregate for the Georgia mix should be lime-treated, with 1.4 percent lime by weight of aggregate—and the mix contains 0.4 percent mineral fiber by weight of total mix. However, because of inexperience at the plant with either of these materials, and difficulties introducing fibers at the plant, a decision was made just before construction to forgo incorporating these additives into the mix. No samples were tested to measure the gradation as constructed because of other construction problems.

Table 2.5: Aggregate Gradation Summary for Mix D, 1/2 in.(12.5 mm) NMA (Percent Passing)

Sieve Sizes	Limits of Proposed Gradation	Operating Range	Contract Compliance	Laboratory Gradation	Target Construction Gradation
3/4 inch	–	100	100	100	100
1/2 inch	90 – 95	X ± 5	X ± 7	93	95
3/8 inch	62 – 68	X ± 5	X ± 7	65	63
No. 4	18 – 22	X ± 4	X ± 6	20	18
No. 8	6 – 9	X ± 3	X ± 6	8	6
No. 200	–	2 – 4	0 – 6	3.0	1.7

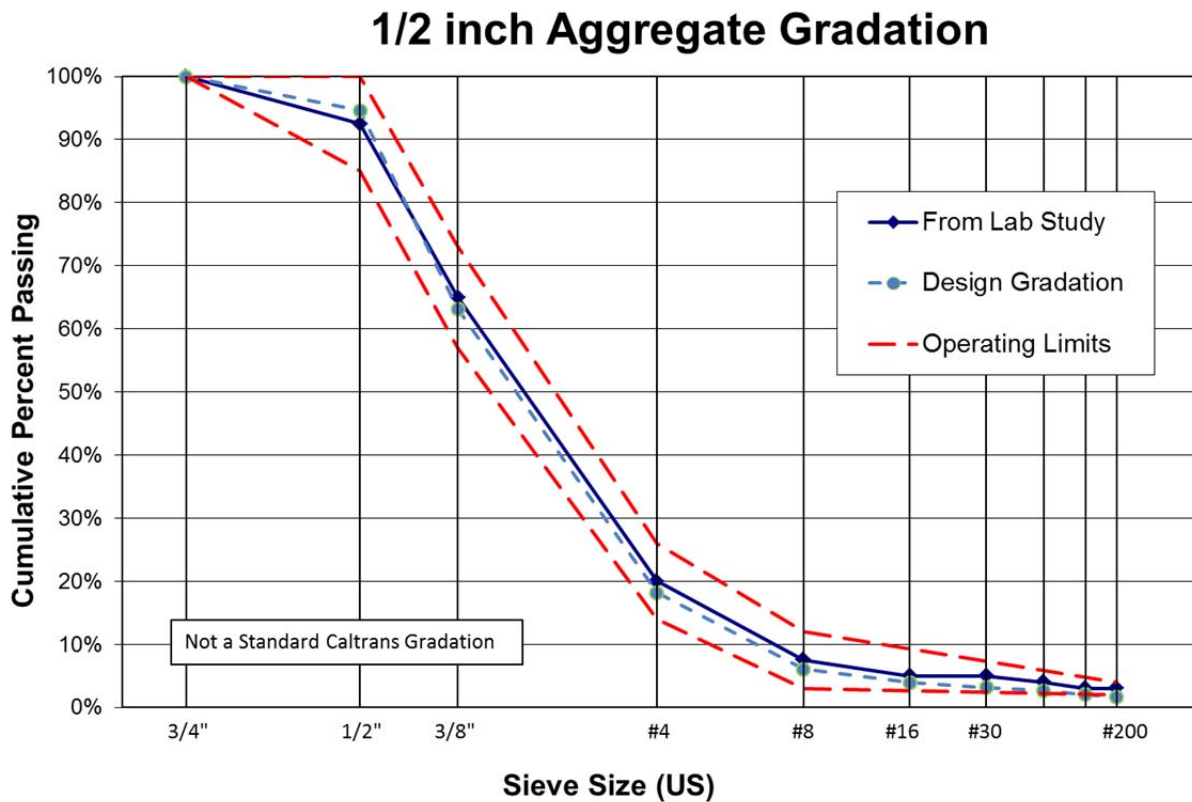


Figure 2.4: Summary of design (“lab report”), revised (“design”), and specification (“operating limits”) gradations for the 1/2 in. (12.5 mm) mix, Mix D.

2.2.4 Binder Types and Contents

Mix designs conformed to California Test 368 (2003) [5] to determine the optimum binder content (OBC) of the rubberized hot-mix asphalt, Type O (RHMA-O), except that the base binder used was PG 64-10 instead of AR4000. Following the mix design procedure, the OBC calculated was multiplied by 1.2 to determine the binder content with asphalt rubber-modified binder.

Table 2.6 shows the binder type and binder content proposed in the initial mix designs for the four mixes, as well as the ones that were actually used in construction. As the table shows, the initial mix designs proposed an asphalt rubber and a polymer-modified binder; however last-minute difficulties in procuring the proposed binder types (see Section 2.4.1) led to changes in both the binder type and binder content of the mixes that were eventually constructed, as is shown in the table. Another late decision was to include Evotherm™ warm mix additive because of low temperatures anticipated on the days of construction. The Georgia Department of Transportation (GDOT) normally specifies a PG 70-22 binder for the Georgia mix, however that was unavailable when the mix was produced for the test sections. A decision was made to proceed in order to measure the permeability obtained for this gradation, understanding that other types of performance of the mix would not be to the standards expected of the GDOT specifications.

Table 2.6: Planned and Actual Binder Types and Binder Contents

Mix ID	Mix Type	Planned Mix Design		Actual Mix Design		Measured Binder Content (% DWA [*])
		Binder Type	Binder Content (% DWA [*])	Binder Type	Measured Binder Content (% DWA [*])	
A	Caltrans 3/8 inch	Asphalt rubber	7.0	PG 76-22PM	5.9	7.8
B	#4P	Asphalt rubber	8.4	PG 76-22PM	6.5	7.6
C	#4P	PG 58-34PM	7.0	PG 64-16	6.5	6.7
D	Georgia 1/2 inch	PG 58-34PM	6.1	PG 58-34PM	6.1	**

*: DWA = dry weight of aggregates; using uncorrected ignition oven results

** not measured

Loose mix collected during the construction of mixes A, B, and C was used to conduct draindown tests according to AASHTO T 305 at a single temperature. Two replicate samples of each mix type were subjected to an elevated temperature of 290°F (143°C) for one hour. None of the mixes exhibited any binder draindown. It should be noted that because the test specifies the use of recently mixed samples, it is debatable whether this material should have been used. However, due to problems associated with excessive binder draindown during the delivery of Mix D (see Section 2.4.1), the test was conducted after construction to confirm that the binder content was not excessive.

2.2.5 Mix Additives

Several mix additives were considered for this construction. These included mineral fibers and lime treatment (both specified for the Georgia mix), and warm mix additives (which have become popular for reducing production and placement costs).

Mineral Fibers

Mineral fibers are specified by the GDOT for the Georgia open-graded friction course 1/2 inch mix (0.4 percent by total weight of mix). According to GDOT experience [6], the fibers allow the use of very coarse gradations, such as the one for a Georgia 1/2 inch mix that has at least 91 percent of the aggregates retaining on sieve #8 (2.36 mm opening). The fibers also allow more binder to be used in the mix while limiting excessive binder draindown. As noted previously, it was found just before construction that fibers could not be added to this mix at the plant, and the expected drain down occurred. Also as noted, the main purpose of placing this mix despite the difficulties was to measure permeability as placed and after HVS loading.

Warm Mix Additive

Difficulty constructing Mix D with the soft PG 58-34PM binder (see Section 2.4.1) led to the use of warm-mix technologies in mixes A, B, and C. Evotherm, the product used, was added to the mixes to make them more workable given the 90 minute truck haul between the plant and the project site and the low temperature expected when paving in late October.

2.3 Test Track Design

Figure 2.5 presents an aerial view of the ATIRC facility, and shows the location of various test tracks used for this study. The HVS test sections for this study were planned to be constructed as surface layers on top of the existing pavements on the Outside North Track (ONT), the Outside West Track (OWT), and a 360 ft long by 16.4 ft wide lane in the southwest part of the 49 ft wide Inside North Track (INT). The ONT and OWT tracks each had two lanes. Among the three tracks used, a total of five cells were available for evaluating the performance of the different OGFC mix/structure combinations under HVS testing. Since only four mixes were selected, an additional cell was designed for evaluating the effect of OGFC thickness on performance. A description of the initial HVS test track design is shown in Table 2.7.

A layout of the test cells is listed in Table 2.8. The design of test track allowed evaluation of the following effects:

- Mix type: Cells A, B2, C, and D each had a different OGFC mix, with the corresponding typical layer thickness or design thickness for the given mix.
- OGFC layer thickness: Cells B1 and B2 had the same #4P mix but different OGFC layer thicknesses.
- Binder type: Cells B2 and C had the same OGFC layer thickness and aggregate gradation and type but different binders.

Table 2.7: Planned and Actual HVS Test Track Design

Cell	Mix Label	Planned Mix Type	Actual Mix Type	Design OGFC Thickness
A	A	Caltrans 3/8 inch mix with asphalt rubber binder	Caltrans 3/8 inch mix with polymer-modified binder	0.08 ft (25 mm)
B1	B	#4P mix with asphalt rubber binder	#4P mix with polymer-modified binder	0.08 ft (25 mm)
B2	B	#4P mix with asphalt rubber binder	#4P mix with polymer-modified binder	0.05 ft (15 mm)
C	C	#4P mix with polymer-modified binder	#4P mix with conventional binder	0.05 ft (15 mm)
D	D	Georgia 1/2 inch mix with polymer-modified binder	Georgia 1/2 inch mix with polymer-modified binder	0.15 ft (45 mm)



Figure 2.5: Aerial photo of the UC Davis ATIRC facility showing the test track locations and rough dimensions. The Outside North Track, Outside West Track, and a 360 ft long-by-16.4 ft wide area at the south part of Inside North Track were used for OGFC testing.

Table 2.8: HVS Test Track Design and Layout

Cell No.	Mix ID	Layer Thickness	Track	Lane
A	A	0.08 ft (25 mm)	Outside West Track (OWT)	Northbound (NB)
B1	B	0.08 ft (25 mm)	Outside West Track (OWT)	Southbound (SB)
B2	B	0.05 ft (15 mm)	Outside North Track (ONT)	Westbound (WB)
C	C	0.05 ft (15 mm)	Outside North Track (ONT)	Eastbound (EB)
D	D	0.15 ft (45 mm)	Inside North Track (INT)	Southwest corner

2.4 Test Track Construction

2.4.1 Paving Day 1, Monday, August 1, 2011: Mix D

The weather was warm and clear. The first of the Georgia 1/2 inch mix arrived at approximately 10:30 a.m. By 11 a.m., three transfer trucks had arrived with all 60 tons of the mix. The air temperature at the start of paving was 66°F (19°C) and the pavement surface temperature was 59°F (15°C).

As unloading proceeded, it was found that the first load could not be completely discharged. Twenty-five to 35 percent (by visual estimate) of the mix stuck to the truck bed due to binder draindown, which prevented the second load, the transfer load, from being quickly discharged.

The draindown was likely caused by excess binder in the mix, which normally would be taken up by the fibers that were eliminated at the last minute. In addition, the combination of a long haul time and the use of the tarps, which were used for the long haul distance to retain heat, may have contributed to the draindown. Another contributor to the problem may have been excessive binder in the mix, although the amount of draindown made measurement of binder content from sampling impossible.

Using material that could be salvaged, construction of Cell D continued, but its total constructed length was shortened from 360 ft (110 m) to 164 ft (50 m).

The mixing temperature for the Georgia 1/2 inch mix, Mix D, was approximately 320°F (160°C) as reported by the plant operator. Initial mix temperatures taken on site in the truck and in the paver hopper measured between 266°F (130°C) and 284°F (140°C). The mix cooled quickly after lay down. The mat temperature dropped by over 54°F (30°C) in five minutes and approximately 90°F (50°C) within 10 minutes. These drops in temperature were likely affected by the ground temperature. Although the weather was sunny with moderate air temperatures, the pavement surface did not receive much sunlight before paving started.

Based on these binder issues, a decision was made to find a stiffer polymer-modified binder for the remaining mixes. Paramount Petroleum was contacted regarding the use of PG 76-22PM (polymer-modified binder) and Telfer Oil was contacted regarding the use of warm-mix additives. Both companies were willing to supply the requested materials, which were unavailable at the time of the Georgia mix construction. The remaining UCPRC mix designs were re-run to account for these changes, with a resulting binder content reduction of about 0.5 percent for the #4P mixes, mixes B and C.

2.4.2 Paving Day 2, Monday, October 24, 2011: Mixes A and B

As on the first day of paving, the weather was warm and clear. The test cells with revised mixes A (Caltrans 3/8 inch mix, now with polymer-modified binder) and B (#4P mix, now with polymer-modified binder) were paved. Air temperature at the start of paving was 62°F (17°C) and the pavement surface temperature was 55°F (13°C). Insufficient aggregate was available to pave Mix C (#4P mix, now with unmodified binder) on this day.

At the paving site, the #4P mix with polymer-modified binder first arrived around 11 a.m., and the Caltrans 3/8 inch mix with polymer-modified binder arrived at approximately 1:30 p.m. These mixes contained the PG 76-22PM binder supplied by Paramount Petroleum and the warm mix additive Evotherm supplied by Telfer Oil.

As seen in Figure 2.6, there were difficulties with spreading and compacting the two mixes, due to the crusting of the mix in the truck and the cooling of the thin lift. The scarred mat was caused by chunks of crusted material being dragged by the paver.



Figure 2.6: Scarring caused by crusted mix (Cell B1, #4P mix with PG 76-22PM).

The mixing temperature for the mixes (i.e., the Caltrans 3/8 inch mix and the two #4P mixes) with the warm mix additive was approximately 295°F (146°C), as reported by the plant operator. Initial mix temperatures taken from the paver hopper measured between 248°F (120°C) and 302°F (150°C). As with Mix D, these mixes cooled quickly after laydown. The mat temperature dropped more than 54°F (30°C) in five minutes.

2.4.3 Paving Day 3, Friday, October 28, 2011, Mix C

Test Cell C with revised Mix C (#4P mix with unmodified binder) was constructed on Friday, October 28, 2011 in the late afternoon, under the best conditions of all the paving days for this project: sunny and warm with no wind. The air temperature at the start of paving was 86°F (30°C) and the pavement surface temperature was 97°F (36°C). No problems were encountered during paving.

2.4.4 As-Built Air-Void Contents and Layer Thicknesses

To determine the as-built air-void contents and thicknesses, eight cores were taken from each test cell adjacent to the HVS test sections. The OGFC layer was separated from the underlying pavement by cutting. Bulk specific gravity tests were conducted on the OGFC specimens according to AASHTO T 331. Maximum specific gravity tests were conducted on loose mix sampled during construction by the mixing plant according to AASHTO T 209. Table 2.9 shows the layer thicknesses and air-void contents measured from the cores.

Table 2.9: Average and Standard Deviation of Measured Air-Void Contents of Each Test Cell

Test Cell	Mix ID	Mix Type	Design Thickness (ft)	Layer Thickness (ft)		Air Void (%)	
				Average	Std. Dev.	Average	Std. Dev.
A	A	Caltrans 3/8 inch mix w/ PG 76-22PM	0.08	0.06	0.01	26.7	3.0
B1	B	#4P mix w/ PG 76-22PM	0.08	0.06	0.01	27.8	2.5
B2	B	#4P mix w/ PG 76-22PM	0.05	0.07	0.02	25.8	2.5
C	C	#4P mix w/ PG 64-16	0.05	0.05	0.01	29.5	1.4
D	D	Georgia 1/2 inch mix w/ PG 58-34PM	0.15	0.15	0.01	21.0	0.97

The as-built thicknesses show that the thickness was difficult to control during construction. The thickness differences among the four cells were relatively small. This made it impractical to evaluate the effect of OGFC layer thickness on performance, and cells B1 and B2 became replicates. The constructed air voids in the mixture approached 30 percent for the 3/8 inch and #4P mixes, while the air voids were closer to 20 percent for the Georgia mix.

The as-built air-void contents were higher than expected. To double check, the aggregate bulk density was measured according to AASHTO T 19, Standard Method of Test for Bulk Density (“Unit Weight”) and Voids in

Aggregate, and AASHTO T 85, Specific Gravity and Absorption of Coarse Aggregate. Coarse aggregate bulk specific gravity tests were conducted on bin samples, with the results shown in Table 2.10. Materials from the bins were combined according to the batching regime used by the plant, with the results shown in Table 2.11. It can be seen that the voids in the coarse aggregate (VCA_{DRC}) were greater than 40 percent, and therefore air-void contents above 25 percent were considered reasonable.

Table 2.10: Measured Density for Each Aggregate Bin Material

Materials	Bulk Specific Gravity, Dry	Bulk Specific Gravity, SSD	Average Bulk Density (lb/ft ³) [kg/m ³]
Bin 1: 3/8 inch crushed	2.64	2.72	0.095 [1.52]
Bin 2: 1/4 inch x dust	2.63	2.70	0.094 [1.51]
Bin 3: 1/4 inch x #10	2.62	2.71	0.091 [1.46]

Table 2.11: Calculated Density and Air-Void Content for Coarse Aggregates

NMAS	Bin 1: 3/8 in. Crushed	Bin 2: 1/4 in. x Dust	Bin 3: 1/4 in. x #10	Bulk Specific Gravity, Dry	Dry Bulk Density (lb/ft ³) [kg/m ³]	VCA_{DRC} Void Content (%)
3/8 inch	90%	10%	0%	2.64	0.095 [1.52]	42.18
#4P (4.75 mm)	24%	15%	61%	2.63	0.092 [1.48]	43.48

3 TESTING PROGRAM

This chapter presents details of the various tests conducted in this study, and includes the objectives, procedure, schedule, and location for each test.

3.1 Introduction

The HVS tests and the related laboratory testing programs were developed to answer the questions about the selected OGFC mixes shown in Chapter 1.

3.2 Material Description

The binder type and binder contents of the materials used in the test track are shown in Table 2.7; the as-built aggregate gradations are listed in Table 2.3, Table 2.4, and Table 2.5 respectively; and the as-built air-void contents are listed in Table 2.9.

3.3 HVS Testing Program

3.3.1 Objective

The main objective of HVS testing was to evaluate the rutting performance of selected OGFC mixes in different test sections. The UCPRC also investigated the feasibility of using HVS testing to evaluate the moisture damage susceptibility of the different OGFC mixes.

During HVS testing, the OGFC layer underwent significant permanent deformation, providing an opportunity to study whether the benefits of the OGFC layer would be affected by rutting. Specifically, the effects of rutting on surface texture and permeability were monitored during the rutting tests. These studies are described in Sections 3.5 and 3.7.

HVS testing also provided an opportunity to study how the microstructure of the asphalt-bound layers (including the OGFC and underlying HMA layers) changed under the action of HVS trafficking. That part of the study is described in Section 3.4.

3.3.2 Test Section Layouts

A total of five test cells were constructed at the ATIRC facility. A schematic of the layout of the HVS test cells along with a description of the mixes appears in Figure 3.1. Four HVS test sections were planned for each test cell in order to form a full factorial of the following two factors:

- Tire type: standard dual-wheel truck tires and next generation wide base tires (NGWBT)
- Testing condition: dry testing for rutting performance and wet testing for moisture damage susceptibility

Moisture damage testing was cancelled after two sections (652HC and 662HC) because it was found that HVS trafficking could not induce moisture damage in the OGFC layer before structural failure.

Each test cell was at least 260 ft (80 m) long, and each HVS test section was 26.2 ft (8 m) long. Placements of the test sections within the test cells were based on the outflow time measured by the outflow meter (see Sections 3.5.2 and 3.5.3 for a description of that testing). Specifically, HVS test sections were sited within each test cell at a location where the outflow time was representative of the readings taken for that test cell. The exact location of the test sections are shown in the Appendix. The HVS test section designations are listed in Table 3.1.

Table 3.1: HVS Testing Experiment Matrix

Test Cell	Wet Moisture Tests		Dry Rutting Tests	
	Dual Wheel	NGWBT ³	Dual Wheel	NGWBT ³
Cell A: Caltrans 3/8 inch mix w/ PG 76-22PM	652HC	662HC ¹	653HB	663HB
Cell B1: #4P mix w/ PG 76-22PM	654HC ²	664HC ²	655HB	665HB
Cell B2: Same mix as Cell B1	658HC ²	668HC ²	659HB	669HB
Cell C: #4P mix w/ PG 64-16	656HC ²	666HC ²	657HB	667HB
Cell D: Georgia 1/2 inch mix w/ PG 58-34PM	650HC ²	660HC ²	651HB	661HB

¹: Section 662HC was tested with dual wheels instead of NGWBT.

²: A strikethrough (—) indicates a section where testing was cancelled.

³ Next Generation Wide Base Tire

3.3.3 HVS Test Protocols

The Heavy Vehicle Simulator (HVS) test section layout, test setup, trafficking, and measurements followed standard University of California Pavement Research Center (UCPRC) protocols [7]. Figure 3.2 shows a schematic of an HVS rutting test section, along with the stationing and coordinate system. The protocol for moisture testing was the same except for the section width, which was 3.3 ft (1.0 m), to allow HVS wheels to wander in the transverse direction (i.e., the y-direction) defined in Figure 3.2. Stations were placed at 1.6 ft (0.5 m) increments.

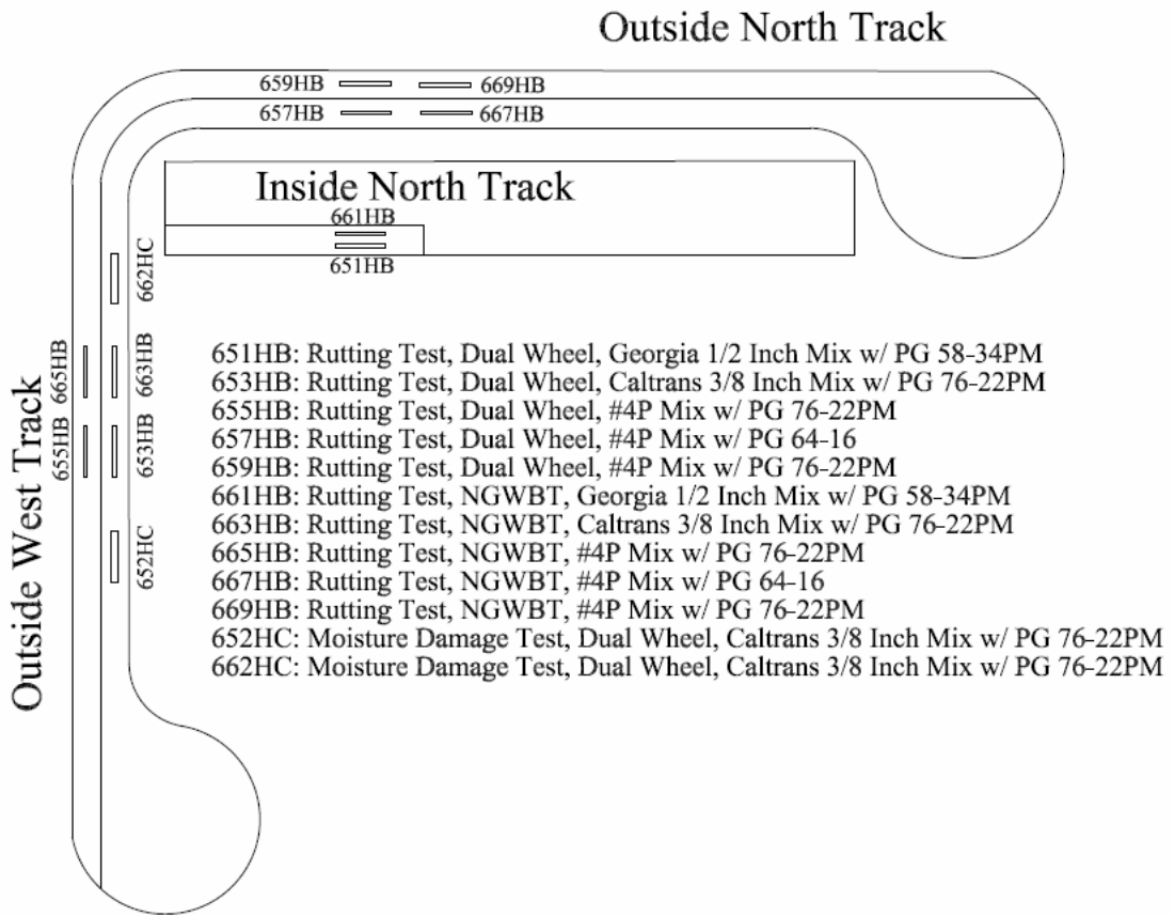


Figure 3.1: Schematic and description of HVS test section layouts.

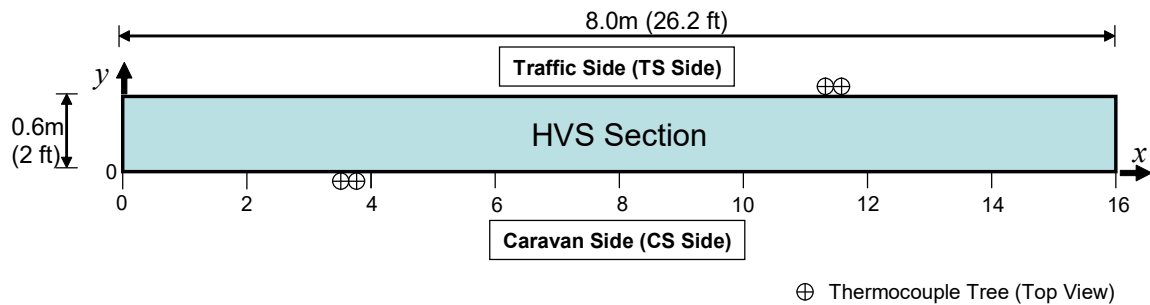


Figure 3.2: Schematic of an HVS test section and stations, thermocouple tree locations, and coordinate system. The z-axis points upward following the right-hand convention with zero at the pavement surface.

3.3.4 Test Plan and Schedule

To evaluate the rutting performance of the different OGFC mixes, HVS trafficking was applied with the pavement heated to 122°F (50°C) and without transverse wander to speed up rut accumulation. Rut accumulation was not accelerated by overloading unless the accumulated surface rut had not reached 0.5 in. (12.5 mm) by 200,000 repetitions.

To evaluate moisture damage susceptibility, HVS trafficking was applied at reduced load levels; this was done to avoid causing structural damage. Unlike the HVS rutting testing, transverse wander was allowed and resulted in an overall traffic area width of 3.28 ft (1.0 m). A perforated PVC pipe was used to spray water onto the pavement surface during HVS testing.

Table 3.2 shows when HVS testing of OGFC sections was performed. The testing sequence did not follow the section numbering order because at least one open lane was required between the outside north track (ONT) and the outside west track (OWT).

Note: Test section names contain a number and one of two designations, either HB or HC. HB indicates testing by UCPRC HVS-B or HVS-C, respectively.

Table 3.2: Dates and Duration of HVS Testing of OGFC Sections

Testing Type	Section	Start Date	End Date	Duration (days)	2012				
					Jan	Feb	Mar	Apr	May
Rutting tests with dual wheels	651HB	Jan. 15, 2012	Feb. 16, 2012	32	X	X			
	653HB	Apr. 16, 2012	Apr. 20, 2012	5				X	
	655HB	Apr. 20, 2012	Apr. 25, 2012	6				X	
	657HB	Apr. 26, 2012	May, 7, 2012	12				X	X
	659HB	Mar. 22, 2012	Mar. 30, 2012	9			X		
Rutting tests with NGWBT	661HB	May 8, 2012	May 11, 2012	4					X
	663HB	Apr. 6, 2012	Apr. 12, 2012	6				X	
	665HB	Apr. 4, 2012	Apr. 5, 2012	2				X	
	667HB	Mar. 23, 2012	Mar. 25, 2012	3			X		
	669HB	Mar. 4, 2012	Mar. 10, 2012	7			X		
Moisture testing	652HC	Jan. 25, 2012	Feb. 14, 2012	21	X	X			
	662HC	Feb. 22, 2012	Mar. 26, 2012	34		X	X		

3.3.5 Rutting HVS Testing Program

Test Section Failure Criteria

The rutting test failure criterion was determined to be when the *average maximum total rut* (AMTR) measured between Stations 3 and 13 reached 0.5 in. (12.5 mm). The definition of *maximum total rut* (MTR) is shown in Figure 3.3. When a pavement reached rutting failure, HVS trafficking was stopped.

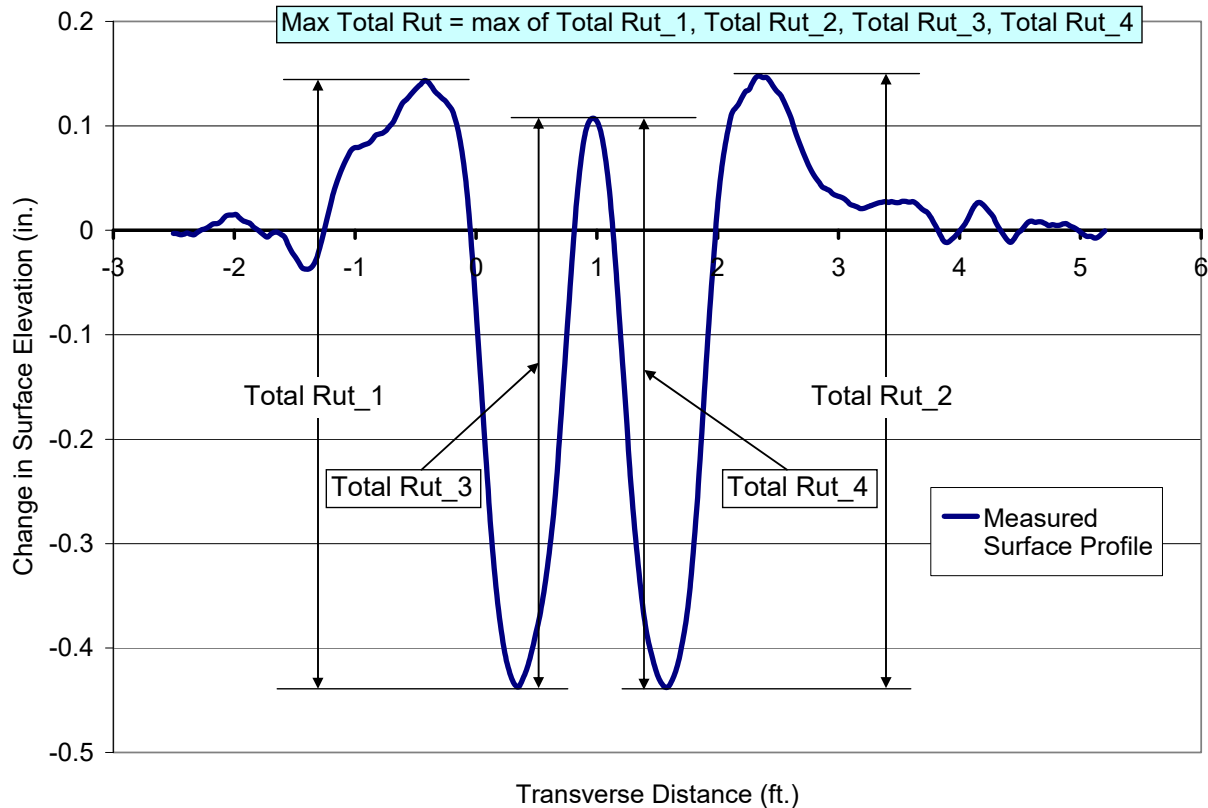


Figure 3.3: Definition of maximum total rut (MTR).

Environmental Conditions

All testing was carried out with an environmental chamber that enclosed the HVS and the test section and allowed the pavement temperature to be controlled. For the rutting tests, the pavement temperature at 2 in. (50 mm) depth was maintained at 122°F (50°C)±3°F. This testing did not include introduction of water onto the pavement.

Loading Program

The HVS loading program for each section is summarized in Table 3.3. Trafficking was applied in a channelized, unidirectional mode using either dual-wheel truck tires (Firestone FS507 Radial, 11R22.5 14PR) or NGWBT (Goodyear C394 SST, 445/50R22.5) inflated to 102 psi (703 kPa) under load of 9 kips (40 kN).

(Note: an HVS load is applied on half of an axle.) For HVS sections that did not fail in rutting after 200,000 load repetitions, tire pressure was increased to 112 psi (772 kPa). Trafficking was stopped after a total of 300,000 load repetitions regardless of whether or not the section reached rutting failure. Load was checked with a portable weigh-in-motion pad at the beginning and end of each test and after each load change.

Table 3.3: Summary of HVS Loading Program for Rutting Tests

Phase No.	Wheel Load kips (kN)	Tire Pressure psi (kpa)	Transverse Wander	Loading Direction	Total Repetitions Applied
1	9 (40)	102 (703)	No	Unidirectional	Up to 200,000
2*	9 (40)	112 (772)	No	Unidirectional	Up to 300,000

*: Necessary only if pavement did not reach rutting failure in 200,000 load repetitions.

3.3.6 Moisture Damage HVS Testing Program

Test Section Failure Criteria

The failure criterion for moisture damage testing was defined as when the OGFC layer showed clear signs of raveling unrelated to structural failure.

Environmental Conditions

Pavement temperatures were not controlled during this testing. Ambient temperatures ranged from 34°F (1°C) to 95°F (35°C) during the two HVS moisture damage tests. The test section was flooded with water sprayed from a perforated PVC pipe (Figure 3.4).

Water was allowed to flow at a rate that kept the level of the draining water flush with the pavement surface during HVS trafficking. The actual flow rate varied between 50 and 100 gal/hour even though the water table in the water tank was maintained at a constant level using a device that automatically shut off the faucet when the water table reached a certain level. The flooding method is shown in Figure 3.4.

At the conclusion of the first moisture test, it was discovered that the test section showed extensive unbound layer rutting and HMA layer cracking but no signs of moisture damage in the OGFC layer. A decision was then made to continue the testing program with a reduced load and more aggressive flooding. For the next test, the HVS load was reduced to 4.5 kips (20 kN) from 9 kips (40 kN), and the water from the tank was heated to approximately 77°F (25°C)—using two Ariston GL 4 heaters connected in serial—before it flowed into the spraying pipe (see Figure 3.5a). The heated water was also ponded by using a wax dam parallel to the HVS test section (see Figure 3.5b). The wax dam was built by sawing a shallow one inch wide trench down to the top of the underlying HMA layer and filling the trench with melted wax.



(a) Water tank



(b) Auto shut-off device to maintain constant water head



(c) Water sprayed onto pavement with perforated PVC pipe

Figure 3.4: Flooding method for the first HVS moisture damage test (Section 652HC).



(a) Water heater



(b) Ponding of water with a wax dam parallel to the test section at the down slope side

Figure 3.5: Heater used for heating water and the wax dam used to pond the water for Section 662HC.

Loading Program

The HVS loading program for each section is summarized in Table 3.4. Trafficking was applied with wander in bidirectional mode using dual-wheel truck tires (GeoStar, 11R22.5 14PR) inflated to 102 psi (703 kPa). As noted, the initial HVS load was 9.0 kips (40 kN) for the first moisture damage test section (652HC) and reduced by half to 4.5 kips (20 kN) to avoid inducing structural damage in the second test (on Section 662HC). Note that HVS load was applied on half of an axle.

Table 3.4: Summary of HVS Loading Program for Moisture Damage Tests

Section	Wheel Load kips (kN)	Tire Pressure psi (kpa)	Transverse Wander	Water Temperature	Loading Direction	Total Repetitions Applied
652HC	9.0 (40)	102 (703)	3.28 ft (1.0 m)	Not heated	Bidirectional	178,200
662HC	4.5 (20)			Heated		447,500

3.3.7 Instrumentation and Data Collection Plan

The rutting evaluation employed two types of instruments:

- Thermocouples: for measuring pavement and ambient temperatures
- Laser profilometer: for measuring transverse surface profiles to allow tracking of profile changes

Intervals between measurements, in terms of load repetitions, were selected to enable adequate characterization of the pavement as rutting developed.

Thermocouples

In this project, pavement and air temperatures (both inside and outside the temperature chamber) were measured with Type-K thermocouples. Individual thermocouples measured the air temperature, and five bundled thermocouples, forming a “thermocouple tree” (Figure 3.6), measured pavement temperatures at multiple depths at each location. The locations of thermocouple trees are shown in Figure 3.2. Note that two sets of thermocouples were used: one for manual measurements using a thermometer and the other for automatic measurements using the HVS data acquisition (DAQ) system.



Figure 3.6: A “thermocouple tree” consisting of five Type-K thermocouples wrapped on a plastic dowel.

Laser Profilometer

A laser profilometer (Figure 3.7) was used to measure the transverse surface profile of the test section at every station, i.e., from Station 0 to Station 16. The permanent change in surface profile is defined as the difference between the initial surface profile and the surface profile after HVS trafficking. Therefore, using the change in surface profile at each station, the maximum total rut was determined for each station, as illustrated in Figure 3.3. Laser profilometer measurements were taken at the following load repetitions: 0, 250, 500, 1,000, 2,000, 5,000, 10,000, and once a day afterward.



Figure 3.7: The laser profilometer.

3.4 Microstructure Change in Asphalt-Bound Layers Under HVS Trafficking

HVS trafficking causes permanent deformation in the different layers of the pavement. Understanding how the microstructure of asphalt-bound layers changes under HVS trafficking can help identify the rutting and clogging mechanisms of asphalt-bound layers.

3.4.1 Objectives

The following were the main objectives of this portion of the study:

- Use x-ray CT imaging to identify changes in the microstructure of the OGFC and HMA layers caused by HVS trafficking
- Gather insight into the mechanisms of rutting to support the development of improved mix and structural designs of OGFC layers
- Provide data to support the development and understanding of laboratory tests for OGFC design.

This study also provided experimental data for the continued development of advanced mechanistic modeling of multilayered flexible pavement structures.

3.4.2 Study Procedure

In this study, the procedure developed by Coleri et al. [8] was used to evaluate microstructure changes using x-ray CT imaging. The steps outlined below correspond with the photographs displayed in Figure 3.8.

1. After construction of the OGFC layer on top of the dense-graded layers (Figure 3.8a), square blocks measuring approximately 6.7 in. (approximately 170 mm) by 6.7 in. were sawn and removed from HVS test sections (Figure 3.8b) that had both the OGFC layer and the underlying HMA layer. One block was sawn from every test section. To enable monitoring of lateral shear flow, the blocks selected came from locations where one half lay in the wheelpath and the other was outside of the wheelpath.
2. The blocks were delivered to the University of California Davis Medical Center (UCDMC), where x-ray CT images of them were acquired (Figure 3.8c).
3. The x-ray CT images were processed to obtain the aggregate, air-void (Figure 3.8d), and mastic distributions within the asphalt blocks.
4. Extended cuts created during sawing of the blocks, due to the circular shape of the concrete saw, were filled with an emulsion-sand mixture to avoid localized failures (Figure 3.8e).
5. The scanned blocks were re-installed into their original positions with fast-setting epoxy (Figure 3.8f and Figure 3.8g).

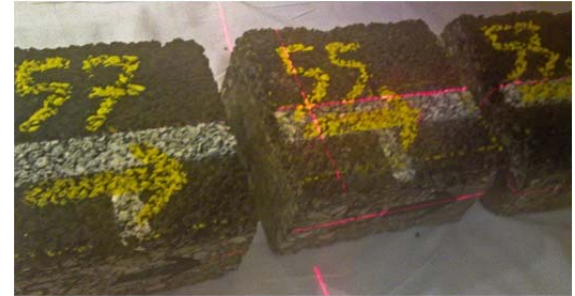
6. After HVS testing was completed on the test sections containing the blocks (Figure 3.8h), the blocks, now with accumulated permanent deformation, were again removed and returned to UCDMD to obtain post-testing images (Figure 3.8i).
7. The post-testing images were then processed to determine the post-testing distributions of the aggregate, mastic, and air-void phases.
8. By comparing the before and after test images, it was possible to determine changes in air-void distributions and permanent particle movement attributable to HVS trafficking. These results were used to evaluate the rutting failure mechanisms of the study's multilayered asphalt pavement systems.



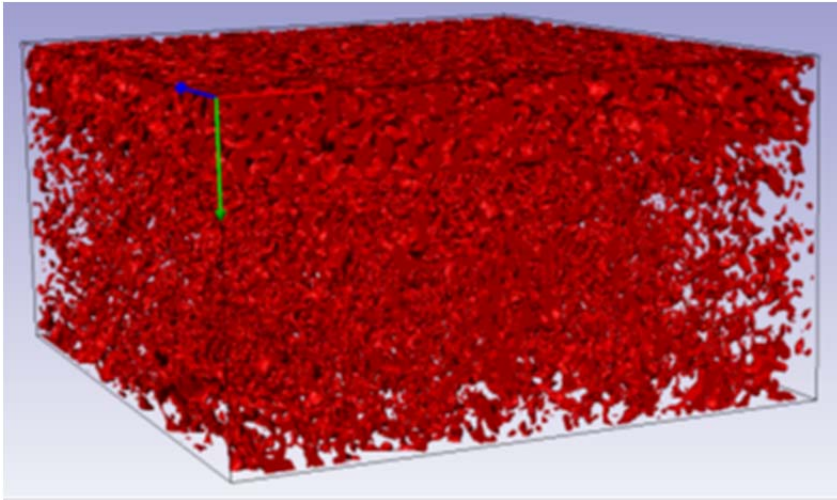
(a) Construction of OGFC



(b) Sawing of blocks



(c) Blocks delivered for x-ray CT imaging



(d) Processed x-ray CT images showing distribution of air voids within the asphalt concrete blocks



(e) Extended cuts in test sections refilled with emulsion-sand mixture



(f)



(g)

Replacement of blocks in the HVS test section



(h) HVS testing of sections containing scanned blocks



(i) Removal of scanned blocks for post-test scanning

Figure 3.8: The general procedure followed for x-ray CT image data collection.

3.4.3 X-Ray CT Image Acquisition and Processing

The X-ray CT scanner at UCDCMC was used to obtain a three-dimensional spatial distribution of the attenuation coefficients of the scanned materials. Three-dimensional images of the specimen were generated by combining a series of two-dimensional images. In this study, horizontal planar images were acquired at 1 mm intervals while the resolution for the other two dimensions was 0.58 mm. Each pixel in an x-ray CT image represented an intensity value related to the density and atomic number of the material at that particular point. The intensity for any given pixel in an image was represented by a value between 0 and 255. Because aggregates are denser than both mastic and air voids, they occupied the highest portion of the intensity scale. Air voids, which have the lowest density of the three, appeared at the lowest intensity portion of the scale, and the mastic's intensity appeared between the other two because of its intermediate density.

Identification of Air Voids

A software program named *Simpleware* [9] was used to identify the air voids in the CT images based on their measured intensity. Once the air voids were identified, it became possible to calculate air-void content based on the three-dimensional CT images. The actual air-void content for each block was also determined using the standard CoreLok method [10]. The maximum specific gravity of each two-layer asphalt block was the weighted average of the maximum specific gravities of both layers using volume as the weight. The upper limit for the air void intensity range was determined by matching the calculated and measured air-void contents for each whole block. Figure 3.9 shows the distribution of air voids for the Section 655HB (#4P mix with PG 76-22PM binder). The developed three-dimensional images were processed further to obtain the distribution of air voids with depth.

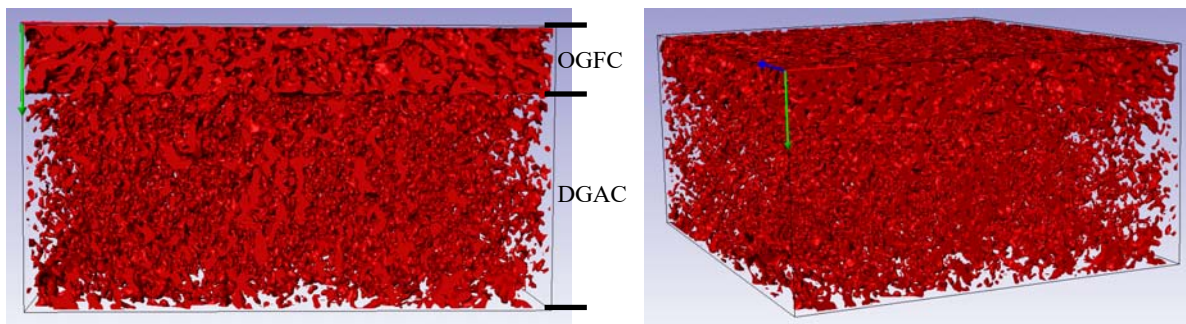


Figure 3.9: Distributions of air voids in the block extracted from Section 655HB (#4P mix with PG 76-22PM binder) from two perspectives. (Note: actual width of this block is 167 mm.)

Tracking Particle Movements

In this study, a tracking algorithm of the software program *Imaris* (Version 7.2) [11] was used to determine the permanent particle movement caused by HVS trafficking. The procedure developed by Coleri et al. [8] was used to create an aggregate domain in asphalt concrete blocks. The “spot object” feature of *Imaris*, which had proven to be the most effective method for particle tracking in asphalt concrete blocks [8], was used to determine the particle movement. Displacement vectors developed by particle tracking were quantified to evaluate the shear and densification response of the pavement structures.

The spot tracking algorithm of *Imaris* was used to determine the displacement field in the two-layered asphalt concrete blocks. Adjacent voxels (*Note: a voxel is a volume element representing a value on a regular grid in three-dimensional space*) with close intensity values were combined to form spots in the x-ray CT images made before and after trafficking. Coordinates for each spot in the pre- and post-trafficking asphalt concrete blocks were determined and used for displacement vector development. The resolution of the CT images was not expected to affect the particle tracking because spot intensity does not change during testing. However, since the particle tracking algorithm excludes pre-testing spots that cannot be matched in the post-testing image, higher CT image resolution results in more displacement vectors. It should be noted that higher CT image resolution can only be achieved by reducing the dimensions of a block.

Spots that were furthest from the HVS load (at the bottom of the block) were assumed to be stationary after HVS trafficking [8]. These spots were used as reference points to match the before and after trafficking images. It should be noted that no significant differences between the displacement fields were observed when different spots (furthest from the HVS load) were used for reference. This suggests that movement of the spots that are furthest from the HVS load were negligible and that they can be used as reference points for particle tracking.

Determination of Vertical Air-Void Content Profile

In order to determine the variation of air-void content in the vertical direction, asphalt concrete blocks were first divided into 0.07 in. (1.76 mm) thick slices in the vertical direction. Volumetric air-void content for each slice was calculated with *Simpleware* [9] for each slice. As an example, Figure 3.10 shows the segmented air-void content distribution before HVS trafficking for the asphalt concrete block from Section 655HB (#4P mix with PG 76-22PM binder). Segmented images allow the determination of the variation of air-void content with depth. In order to determine the change in air-void content with HVS trafficking, air-void content distributions, similar to Figure 3.10, for both the before and after trafficking images were developed. After-trafficking air-void content distributions were subtracted from the before-trafficking distributions to calculate the reduction in air-void content distributions caused by HVS trafficking.

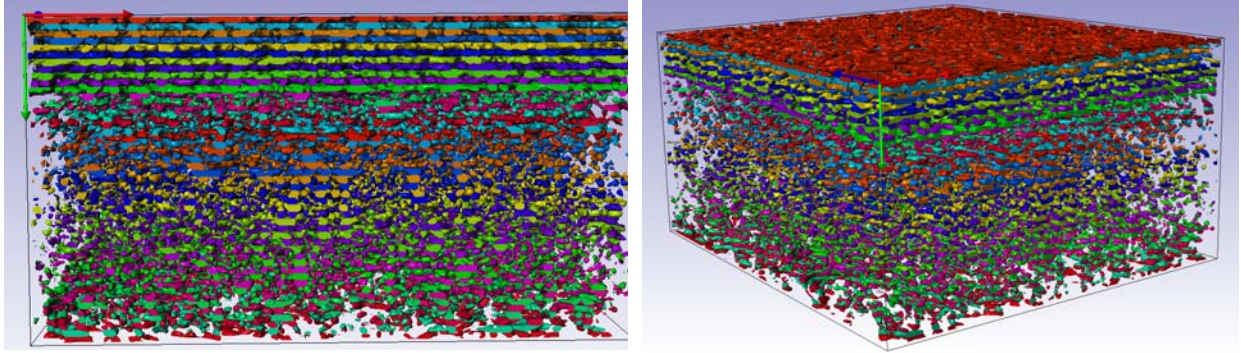


Figure 3.10: Segmented air voids in an asphalt concrete block taken from Section 655HB (#4P mix with PG 76-22PM binder) from two perspectives (colored volumes are air-voids). (Note: width of this block is 167 mm.)

In this study, the three-dimensional images of the blocks were divided into two sub-blocks: one corresponding to under the wheelpath and another corresponding to the remainder, which was outside of the wheelpath. The reduction in air-void content caused by HVS trafficking was determined for each of the sub-blocks.

Determination of Densification in Asphalt-Bound Layers

Assuming that horizontal permanent strains were negligible, the reduction in air-void content (i.e., densification) would be approximately equal to the vertical permanent strain. The downward rut caused by air void reduction for each slice could in turn be calculated by multiplying the air-void content reduction by the slice thickness [i.e., 0.07 in. (1.76 mm)]. The total densification-related rut for a given asphalt-bound layer could then be calculated as the sum of the downward rut for all the slices for that layer.

Decomposition of Surface Downward Rut

The contributions by shear, densification, and rutting in the unbound layers to the total surface downward rut were calculated for all the test sections using the x-ray CT block images taken before and after HVS testing, and the profilometer data taken on top of the asphalt concrete blocks. Calculations were made by taking the following steps:

1. Create x-ray CT images of the asphalt concrete block taken before and after HVS trafficking (Figure 3.11a). These three-dimensional images are referred to as “virtual blocks.”
2. Use the particle tracking algorithm of *Imaris* (Version 7.2) software to determine the deformation on the surface of the virtual blocks (Figure 3.11b). (The procedure for particle tracking is described in the section “Tracking Particle Movements” on page 33.)

3. Place the virtual asphalt concrete block on the surface rutting profile measured by the laser profilometer and determine the percentage contribution of asphalt layer rut to total surface rut by dividing the average under-tire asphalt rut by the average under-tire total surface rut (Figure 3.12).
4. Determine the percentage contributions of the OGFC and HMA layers to total asphalt rutting by dividing the OGFC and HMA vertical displacement distributions by the total surface rutting distribution (Figure 3.13).
5. Calculate the densification-related rut on the wheelpath by following the procedure given in the previous section, “Determination of Densification in Asphalt-Bound Layers” on page 34.
6. Subtract densification-related rut for the HMA layer from the total HMA rut to get the shear-related rut for the HMA layer.
7. Subtract the calculated rut of the unbound layers, the rut of the HMA layer, and the OGFC densification-related rut from the total surface rut to determine OGFC shear related rut.

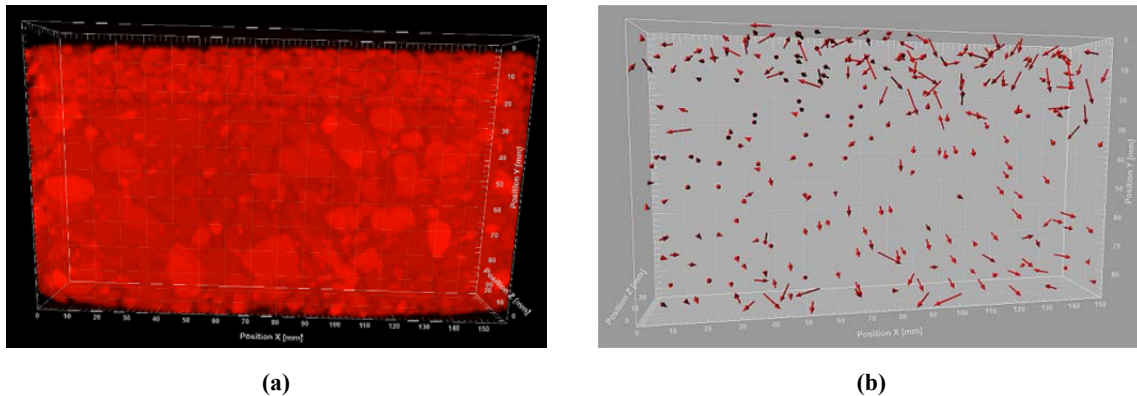


Figure 3.11: Asphalt concrete blocks processed for rut calculations: (a) processed x-ray CT image (side view of the asphalt block) and (b) particle movement in deformed blocks.

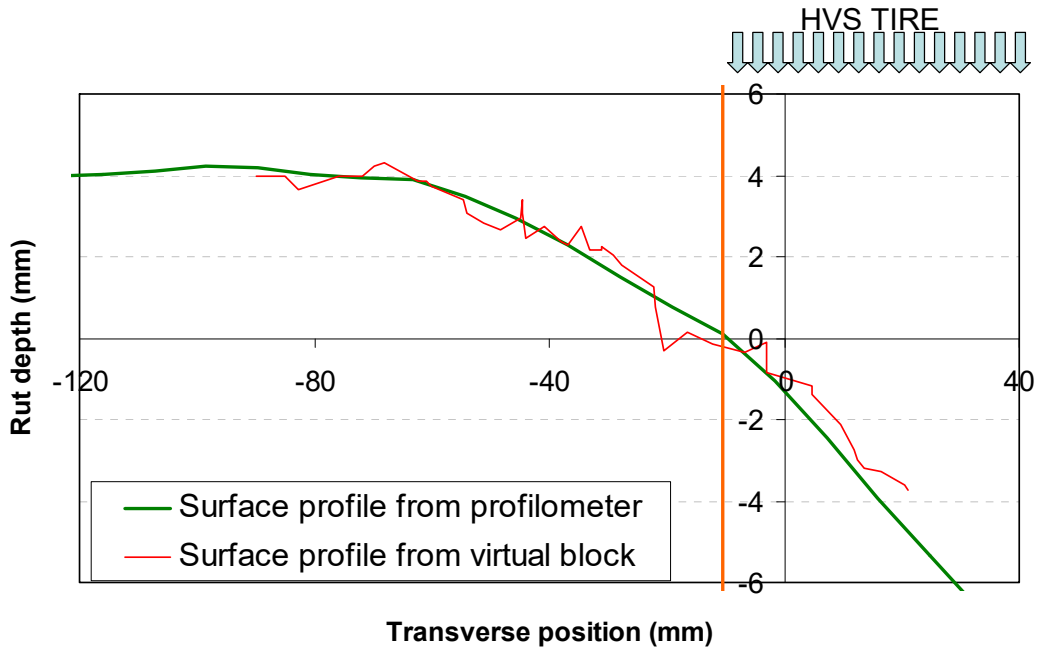


Figure 3.12: Asphalt concrete block surface rutting profile located on the measured total surface rutting profile for Section 655HB (#4P mix with PG 76-22PM binder).

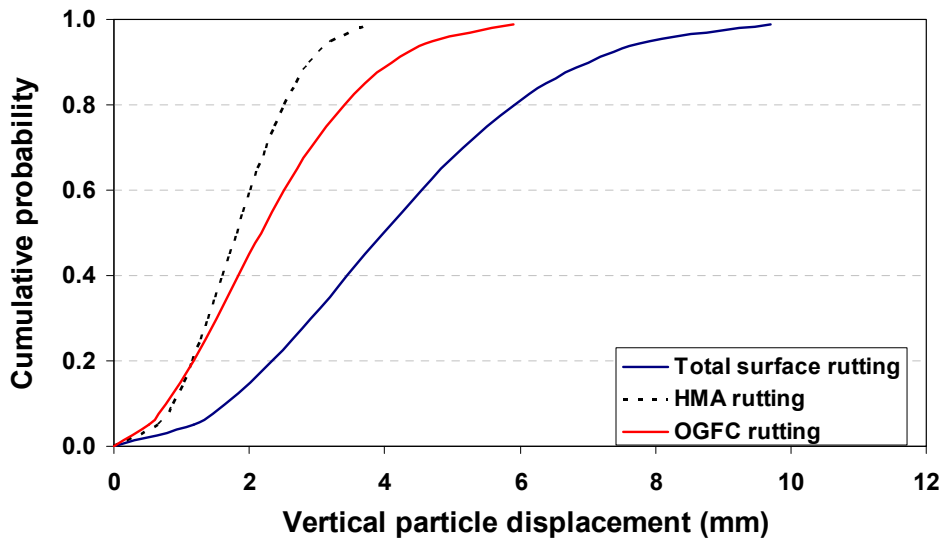


Figure 3.13: Cumulative distributions of the vertical deformations on the asphalt blocks to identify the contributions of the HMA and OGFC layers to total asphalt surface rutting, Section 655HB.
 (Note: Deformation distributions for cumulative probability larger than 0.5 are used for calculating the contributions of OGFC and HMA layers to total asphalt rutting.)

3.4.4 Experiment Program

Three HVS sections were selected for this study with each representing a different OGFC mix: 653HB (Caltrans 3/8 inch mix with PG 76-22PM binder), 655HB (#4P mix with PG 76-22PM binder), and 657HB (#4P mix with PG 64-16 binder).

One asphalt concrete block was obtained for each of the three selected HVS sections at the upslope side of the section (see Figure 3.14).



Figure 3.14: Section 653HB after 2,000 load repetitions with the asphalt concrete block at Station 5.

3.5 Surface Texture and Noise Testing on the HVS Test Track

Traffic safety is an ongoing first priority for state highway agencies, and friction measurements as indications of skid resistance have become an essential part of pavement management systems [12]. The friction-related properties of a pavement depend on its surface texture characteristics, which are known as macrotexture and microtexture [13].

According to the American Society for Testing and Materials (ASTM) [14], surface asperities less than 0.02 in. (0.5 mm) in height are classified as microtexture, while asperities greater than 0.02 in. (0.5 mm) are considered to be macrotexture. Figure 3.15 shows the different categories of pavement texture and their corresponding effects on surface characteristics. The figure indicates that microtexture affects wet pavement friction and tire wear while macrotexture affects wet pavement friction, exterior noise, in-vehicle noise, and splash and spray.

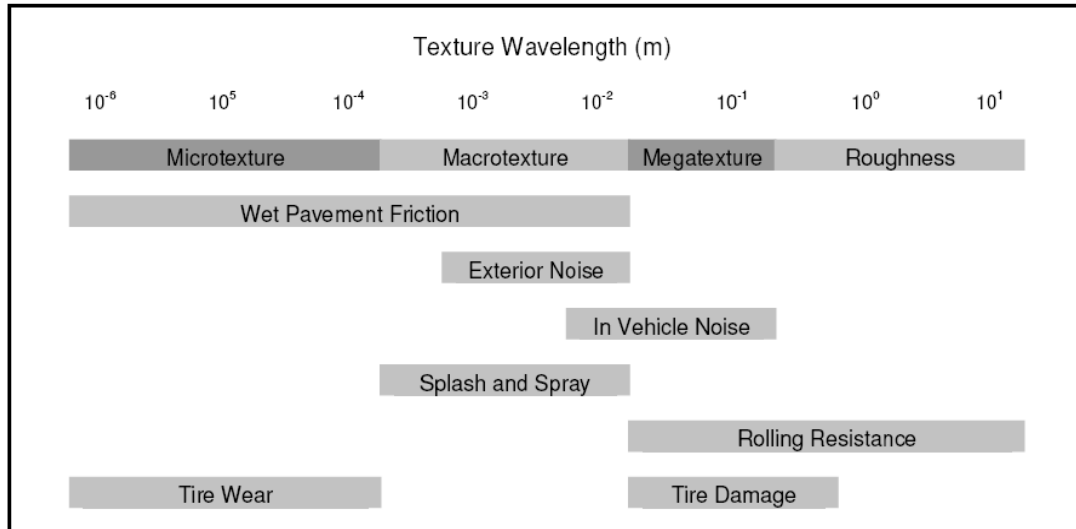


Figure 3.15: Pavement texture wavelength and the corresponding effects of surface characteristics [15].

Skid Resistance

A change of skid resistance with vehicle speed depends on both microtexture and macrottexture [16]. Microtexture defines the magnitude of skid resistance, and macrottexture controls the slope of skid resistance reduction as speed increases. Moreover, macrottexture affects the skid resistance of pavements at high speeds by reducing the friction-speed gradient and facilitating the drainage of water. Macrottexture has little effect on friction level at low speeds. Microtexture dominates and defines the level of friction at low speeds, as shown in Figure 3.16.

Tire/Pavement Noise

The mechanisms of tire/pavement noise generation and propagation are complex. Some mechanisms generate sound, and others enhance or amplify sound generated by other mechanisms. Positive pavement macrottexture (protrusions above the surface the tire rides on) causes vibration of the tire, and is the major cause of low frequency tire/pavement noise (<1,000 Hz) [17]. This mechanism can be referred to as the *tire vibration mechanism*. As a wheel turns, the grooves and passages of the tire tread in contact with the surface are compressed and distorted. The air trapped in these passages is compressed and pumped in and out, causing aerodynamically generated sound. This mechanism is responsible for high frequency noise (>1,000 Hz) and can be called the *air pumping mechanism*. Open-graded mixes damp the air vibrations inside their surface pores and cause a major reduction in the air pumping portion of tire/pavement noise [18].

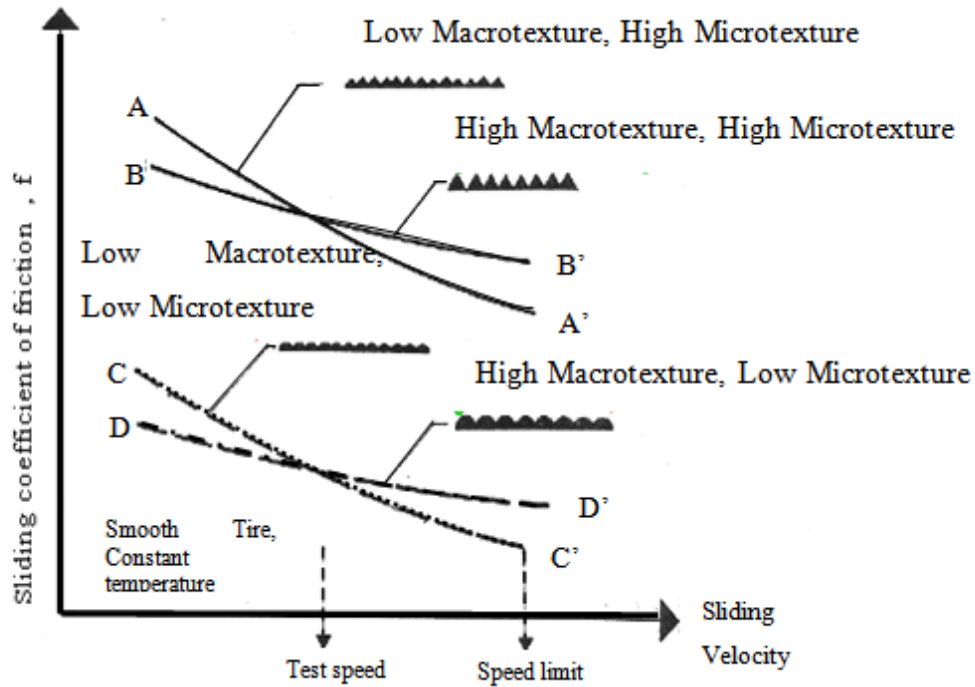


Figure 3.16 Schematic plot of the effects of microtexture and macrotexture on pavement friction [16].

3.5.1 Objectives

Surface texture measurements were taken so that the micro- and macrotextures of different OGFC mixes could be compared with those of the control mix (Caltrans 3/8 inch mix). In addition, the levels of noise generated by the tire/pavement interaction of different OGFC mixes were also compared against the level of the control mix.

3.5.2 Testing Equipment

There is no standard test procedure for measuring pavement friction during mix design, and the tests conducted in this study for surface texture and tire/pavement noise evaluation are shown in Table 3.5. As indicated in Figure 3.16, surface friction or skid resistance is a function of both micro- and macrotexture. Texture drainage of a pavement surface is highly correlated with the MPD of the surface except when it is highly porous. Tire/pavement noise is related to macrotexture, as indicated by Figure 3.15.

Table 3.5: List of Tests for Surface Texture and Tire/Pavement Noise Evaluation

Measurement	Standard	Equipment
Friction	ASTM E1911-09ae1	Dynamic Friction Tester (DFT)
Skid resistance	California Test 342	California Portable Skid Tester (CST)
Macrotexture	ASTM E2157-09	Circular Texture Meter (CTM)
Macrotexture	N/A	Laser Texture Scanner (LTS)
Texture drainage	ASTM E2380/E2380M-09	Outflow Meter (OTF)
Tire/pavement noise	AASHTO TP-76-09	UCPRC OBSI Vehicle (OBSI)

3.5.3 Test Procedures

A short description of the procedures followed in this study are presented below for each of the test methods used.

Dynamic Friction Tester

The DFT (Figure 3.17) consists of a horizontal spinning disk fitted with three spring-loaded rubber sliders that contact the paved surface as the disk's rotational speed decreases due to the friction generated between the sliders and the paved surface. A water supply unit delivers water to the paved surface being tested. The torque generated by the slider forces measured during the spin down is then used to calculate friction as a function of speed [14]. This test method measures paved surface frictional properties as a function of speed. In this study, DFT measurements were taken at 20 and 60 km/h spinning speed. The friction value at 20 km/h is an indication of microtexture [15].

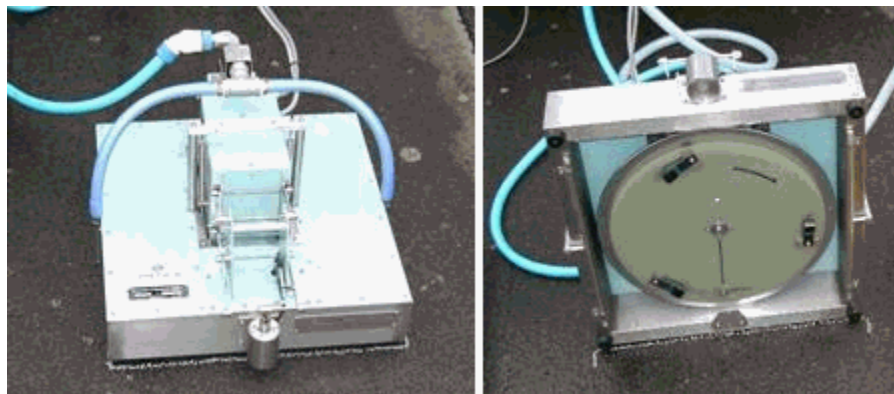


Figure 3.17: Dynamic Friction Tester.
(Courtesy of Penn State, Larson Institute).

Circular Texture Meter

The Circular Texture Meter (CTM) (Figure 3.18) is used to obtain and analyze pavement macrotexture profiles. The CTM consists of a charge coupled device (CCD) laser displacement sensor mounted on an arm that rotates. The CCD sensor follows a circular track with a diameter of 11.2 in. (284 mm). The CTM is designed to measure the same circular track measured by DFT. The MPD is calculated for each of the 4.4 in. (111.5 mm) long one-eighth arc segments. The calculated MPD values for all eight segments are averaged and presented as MPD for the surface tested [19, 20].

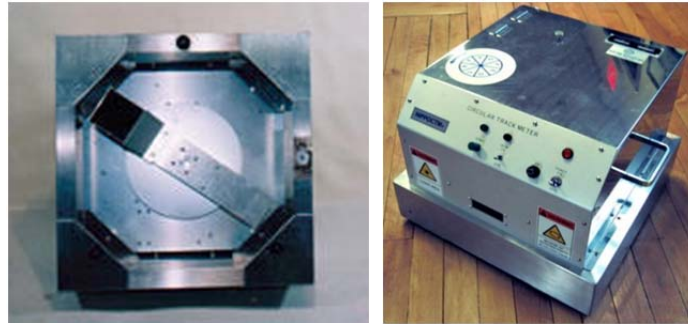


Figure 3.18: Circular Texture Meter.

Laser Texture Scanner

The Laser Texture Scanner (LTS) (Figure 3.19) measures pavement surface macrotexture. Unlike the circular tracks measured by CTM, the LTS measures the surface profile of an area 3 inches wide by 4 inch long. Manufactured by Ames Engineering, the LTS has laser dot size of approximately 0.050 mm, a vertical sample resolution of 0.015 mm, and a horizontal sample spacing of 0.015 mm [21]. In this study, the LTS was used to measure the MPD of surface of each pavement section subjected to HVS testing.

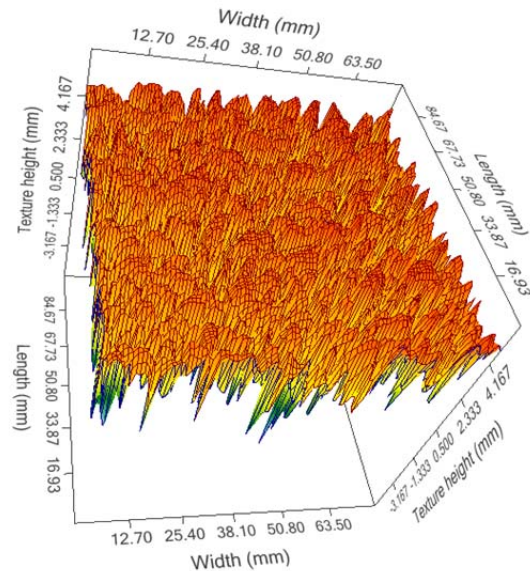


Figure 3.19: Laser Texture Scanner and an example of surface texture profile it measured (Section 655HB, #4P mix with PG 76-22PM binder). (Photo of LTS courtesy of Ames Engineering, Inc.)

Outflow Meter

The Outflow Meter (OTF) (see Figure 3.20:) is a device that measures the rate at which a known quantity of water, under gravitational pull, escapes through voids in the pavement texture of the structure being tested. The time required for this to complete is referred to as *outflow time*. Use of the OTF provides a measure of a pavement's ability to relieve pressure from the face of vehicular tires, and thus an indication the potential for hydroplaning under wet conditions [14]. The reciprocal of the outflow time is highly correlated with MPD except when a surface is highly porous. The OTF can also be used to detect surface wear and predict correction measures [22].

California Portable Skid Tester

Operation of the California Portable Skid Tester (CST) (Figure 3.21) involves spinning a rubber-tired wheel to a speed of 80 km/h (50 mph) while it is off the ground, then lowering it to the pavement and noting the distance the wheel travels against the resistance of a spring before stopping. The device measures the coefficient of friction values of bituminous and portland cement concrete pavements and bridge decks. During testing the device is attached to the rear of a suitable stationary vehicle. Glycerin is used to wet the full circumference of the test tire before each test. The CST operates initially with a slip ratio of one since the test wheel is rotating but the test carriage is not moving relative to the pavement. Once the wheel is in contact with the pavement the slip ratio changes to zero since there is no braking effort applied to the wheel. In addition, the test is not conducted at a constant speed as there is no further energy applied to the wheel once it touches the ground [23].



Figure 3.20: Outflow Meter.
(Courtesy of KLARUW Systems.)



Figure 3.21: California Portable Skid Tester (CST) used to measured surface skid resistance following California Test (CT) 342.

UCPRC On-Board Sound Intensity Measurement Vehicle

Tire/pavement noise measurements were performed using the UCPRC's OBSI measurement vehicle (Figure 3.22). The vehicle is a Ford Escape with a rear-mounted laser profilometer and the OBSI measurement device installed on the right rear wheel. In the figure, the steel box on the back of the vehicle is the inertial laser profilometer, which measures the pavement elevation profiles on both wheel tracks. The surface texture, expressed as MPD, is also measured in the right wheel track. The OBSI measurement equipment was developed in California by Paul Donovan of Illingworth & Rodkin, Inc.



Figure 3.22: The UCPRC On-board Sound Intensity (OBSI) measurement vehicle.

In this study, data was gathered on each test cell at 35 mph (56 km/h). The speed was limited because of the short length of the test track.

3.5.4 Testing Program

Before HVS testing began, the outflow time for each test cell was measured every 8.2 ft (2.5 m) in the longitudinal direction and every 3.3 ft (1.0 m) in the transverse direction. This process allowed the creation of maps that were then used to determine a location on each HVS test section where the outflow time was representative of the corresponding test cell.

Once HVS test section locations were determined (see Figure 3.1), the surface texture of each test section was characterized using DFT, CTM, OTF, LTS, and CST. Measurements were taken before, during, and after HVS trafficking, except for the CST which could not fit under the HVS for measurements during trafficking. When and where measurements were taken are described below.

DFT, CTM, OTF, and LTS Measurements

Once HVS trafficking began, measurements were taken after one day of trafficking—typically at only 500 repetitions because of the intense profilometer data collection schedule—and again after another 5,000 load repetitions. After that, measurements were scheduled for Mondays and Fridays, with the number of load repetitions increasing by about 10,000 every day (including weekends).

Note: DFT measurements were stopped once surface rut increased significantly and the surface become too rough for the device to work properly. This typically occurred between approximately 2,000 to 5,000 load repetitions.

The measurement locations for the varied devices depended on the number of wheelpaths of each HVS test section. For rutting tests with dual wheels, measurements were taken at Stations 4, 8, and 12 for both wheelpaths, and at two untrafficked locations at Station 8 (see Figure 3.23). Measurements on the untrafficked areas were used to determine whether nontraffic-related factors affected the readings. Figure 3.24 shows the measurement locations for sections tested with the NGWBT. Measurement locations of the two moisture susceptibility test sections with a wandering traffic pattern, i.e., Sections 652HB and 662HB, were similar to those shown in Figure 3.24, except that those test sections were 3.3 ft (1.0 m) wide and the wheelpath covered the test sections' entire width.

California Portable Skid Tester (CST)

CST testing was performed once on all the planned test sections before HVS testing began, and included the moisture testing sections that were eventually cancelled. Testing was done on each section at stations 5 and 9. Per typical Caltrans practice, six measurements were taken at each location.

After HVS testing, CST measurements were taken again on the 10 HVS rutting test sections. Testing was performed along the HVS wheelpaths on stations 5 and 9, as well as on the untrafficked area at Station 8 where the other measurements had been taken. Measurements on the untrafficked surface were expected to be comparable to the values measured before HVS trafficking.

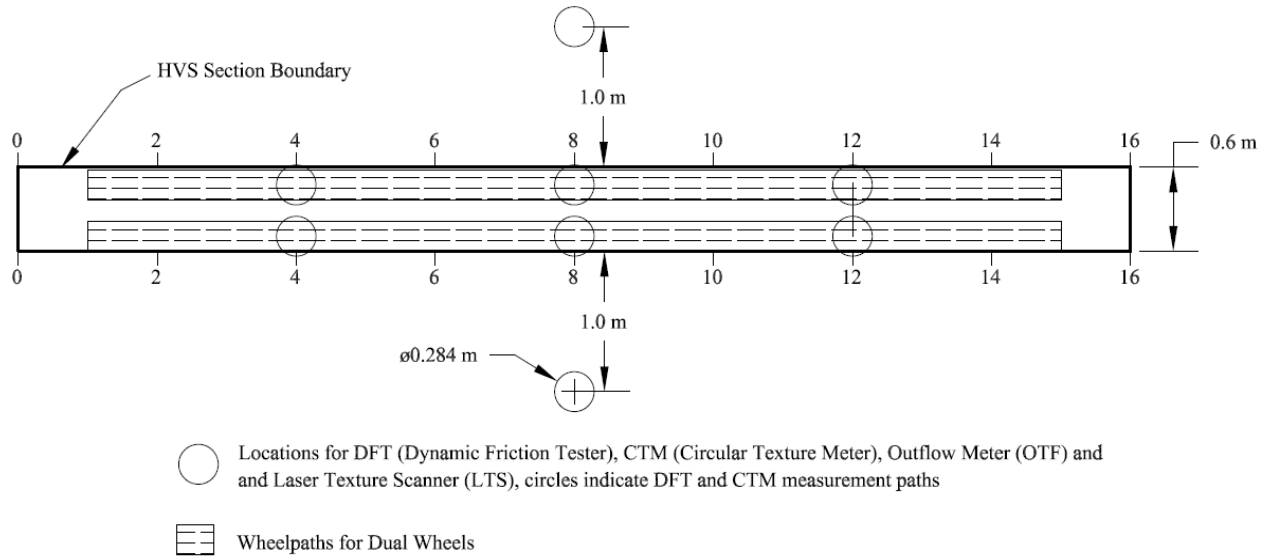


Figure 3.23: Locations of DFT, CTM, and OTF measurements for HVS rutting sections tested with dual wheels (i.e., Sections 651HB to 659HB).

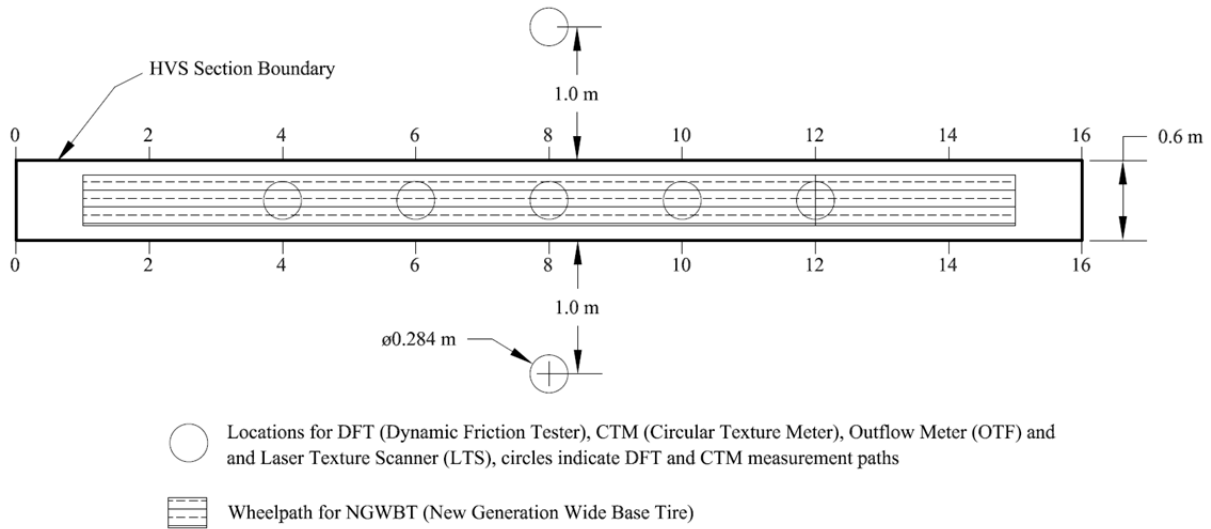


Figure 3.24: Locations of DFT, CTM, and OTF measurements for HVS rutting sections tested with NGWBT (i.e., Sections 661HB to 669HB).

3.6 Laboratory Testing

3.6.1 Objective

The objective of laboratory testing was to compare the relative performance of the mixes under laboratory conditions and to correlate those results with the relative performance of the mixes under HVS testing. The laboratory tests were conducted on plant-produced loose mix collected the day of construction.

3.6.2 Testing Program

To evaluate the rutting performance and durability of these new mixes in the laboratory, three tests common to open-graded mix design and mix quality control were conducted on cores prepared from loose mix sampled during construction:

- AASHTO T 324: Standard Method of Test for Hamburg Wheel-Track Testing (HWTT) of Compacted Hot Mix Asphalt (HMA). This test is used to evaluate the rutting performance of different HMA mixes.
- ASTM D7064: Standard Practice for Open-graded Friction Course (OGFC) Mix Design (referred to in this report as the Cantabro test). The Cantabro test is used to evaluate the durability of different OGFC mixes.
- AASHTO T 320-07 (2011): Standard Method of Test for Determining the Permanent Shear Strain and Stiffness of Asphalt Mixtures Using the Superpave Shear Tester (SST). In particular, the shear stiffnesses of different OGFC mixes were determined at 55°C under different loading frequencies.

All three tests were conducted on all the mixes with two exceptions: the Cantabro test and the shear stiffness test were not performed on the Georgia 3/8 inch mix because specimens were unavailable. Eight specimens were used in the HWTT for each of the mixes, and six specimens were used for the Cantabro testing.

The HWTT was conducted with specimens immersed in a 122°F (50°C) water bath, while Cantabro tests were conducted at room temperature.

In addition, surface texture measurements were taken on ingot specimens compacted on the day of construction using loose mix sampled from the supply trucks. These characteristics were tested:

- Dynamic friction, as measured by DFT
- Mean profile depth, as measured by both CTM and LTS, and
- Outflow time, as measured by outflow meter

A total of four ingot specimens were prepared for each of the OGFC mixes, except the Georgia 1/2 inch mix (for which there were no specimens because of difficulties with mix construction).

3.6.3 Testing Procedures

Each Hamburg Wheel-Tracking Test (HWTT) uses two 6 in. (150 mm) diameter cores loaded under a steel wheel. The specimens are submerged in water at a temperature of 122°F (50°C). The device runs two tests side-by-side so that four cores are used at once to produce two sets of test results. The test provides an evaluation of mix stability and the resistance to permanent deformation under saturated conditions.

The Cantabro test subjects a single 4 in. (100 mm) core to continued tumbling action within a rotating steel cylinder chamber. This test provides an evaluation of the durability of the mix and its resistance to disintegration or raveling. The test provides a lower boundary for the amount of binder to be included in the mix.

Procedures for surface texture measurements on ingot specimens are described in Section 3.5.3. For each ingot, surface texture measurements were taken with the following sequence:

- CTM, DFT, and OTF: The surface of the ingot was divided into four quadrants. On each quadrant, CTM testing was repeated eight times, DFT was performed three times, and OTF was repeated five times. The average values from the repeated tests were used for analyses.
- LTS: The surface of the ingot was divided into a 3x3 grid and one measurement was taken on each grid. As these were not repeated measurements, each reading was treated as an independent sample.

One notable difference between the texture measurement procedures on the HVS test tracks and those in the laboratory was the wire-brushing of the ingot specimens to remove the binders coating the surface aggregates. This was done to the laboratory specimens to simulate the effect of the first one-to-two years of trafficking, which tends to expose aggregate surfaces.

3.6.4 Specimen Preparation

All laboratory specimens were prepared from loose mix sampled from the supply truck when the test sections were constructed. Loose mix for the HWTT and Cantabro tests were stored and reheated for later compaction. The loose mixes were stored in closed pails in a temperature-controlled room at 68°F (20°C). The loose mixes were reheated to 295°F (145°C) for compaction using the Superpave gyratory compactor. Specimens were compacted to bulk densities similar to those measured from field cores, approximately 27 percent air-void content.

Compacted specimens for the HWTT were 2.5 inches (63.5 mm) high with a diameter of 6 inches; the compacted Cantabro specimens were also 2.5 inches high but with a diameter of 4 inches (100 mm). To maintain a consistent level of compaction effort, specimens were compacted according to the number of gyrations, not using height control. In other words, by using gyration control, the amount of loose mix was adjusted to produce a specimen with both the target height and density.

The number of required gyrations was determined by observing when the aggregate reached a consistent interlock, which was considered to have been achieved after three consecutive gyrations without a change in height. For the three different mixes in this study, 65 gyrations were used for compaction.

Ingot specimens were prepared on the day of construction. The ingots were 1.5 inches (38 mm) thick, 20 inches (505 mm) wide, and 23 inches (575 mm) long. Figure 3.25 shows the compaction using rolling wheel compactor and the finished ingot specimen with the mold still attached. Once surface texture measurements were obtained, 6 inch (150 mm) diameter cores were taken from the ingot specimens and used for determining shear stiffness at 131°F (55°C). The amount of loose mix used and the number of rolling passes were the same for each ingot. The target was to obtain approximately 20 percent air-void content.



(a) Compaction using rolling wheel



(b) Finished ingot specimen in the mold

Figure 3.25: Preparation of ingot mold specimens for laboratory evaluation, including surface texture measurements and shear stiffness testing.

3.7 Permeability and Clogging Evaluation

3.7.1 Objectives and Methodology

One of the main benefits of OGFC is its ability to reduce tire splash or spray in wet weather. This ability requires that an OGFC mix have permeability adequate to allow efficient runoff drainage. The first objective of this part of the study was to compare the permeabilities of the selected OGFC mixes right after construction, and to determine how they compared to the control mix (Caltrans 3/8 inch mix). This was achieved by measuring the permeability on each HVS test section before trafficking was applied.

OGFC mixes provide good drainage because of their high air-void contents, and it is critical for the voids to remain open for that capability to be maintained. Consequently, the second objective of this portion of the study was to evaluate the clogging susceptibility of the different OGFC mixes compared to the control mix.

Clogging in OGFC refers to the loss of voids that in turn causes decreased permeability of the layer. Clogging can occur if the voids fill with particles, if they close due to permanent deformation (i.e., rutting), or both. In this study, three different possible mechanisms that can cause clogging were evaluated: (1) clogging due to drainage of runoff that contains suspended solids that fill the voids (runoff-related clogging); (2) clogging due to loss of air voids caused by rutting under HVS trafficking (rutting-related clogging); and (3) clogging due to deposition of airborne dust particles in the voids (airborne dust-related clogging). Several earlier studies sought to evaluate the impact of particles in runoff-related clogging [22-23], but no research has been published on rutting-related or airborne dust-related clogging.

In this study of runoff-related clogging, simulated rainfall with a known concentration of suspended solids was used to generate runoff. The runoff was drained over designated areas for a certain duration. X-ray CT images taken on cores sampled from the drainage before and after the simulated rain were then used to study the change in air-void content and its distribution, and to determine the extent of clogging caused by the runoff drainage.

Rutting-related clogging was studied by measuring permeability on the rutted surface during HVS testing. For some sections tested with dual wheels, fine dust was spread on one of the two wheelpaths to simulate the effect of airborne dust on clogging. This was determined by comparing the difference in measured permeability between the two wheelpaths.

The rutting-related clogging was further studied using x-ray CT images taken of the same cores before and after HVS trafficking. Since all of these cores were taken from HVS sections tested with dual wheels and from the wheelpath that was spread with dust, the clogging was attributed to airborne dust as well.

3.7.2 Measurement Locations

This section describes the different types of measurements taken for permeability and clogging evaluation, and their locations.

Permeability Measurements

Figure 3.1 shows the location of the HVS test sections. For sections tested with dual wheels, permeability was measured on both wheelpaths at Stations 4, 8, and 12. For sections tested with the NGWBT, permeability was measured at Stations 4, 6, 8, 10, and 12 along the centerline of the single wheelpath. Three permeability measurements were made at each location and the average was used for analysis.

Rain Simulation

Figure 3.26 shows the locations of the rainfall simulations with respect to the HVS test track and types of open-graded pavement material. As can be seen, rainfall simulations were performed on three mixes: the control mix and the two #4P mixes. Two rainfall simulations were performed on each test section: one simulation using water containing particles less than 38 microns (the <38 micron gradation listed in Table 3.6) and the other using particles up to 600 microns (the <600 micron gradation listed in Table 3.6).

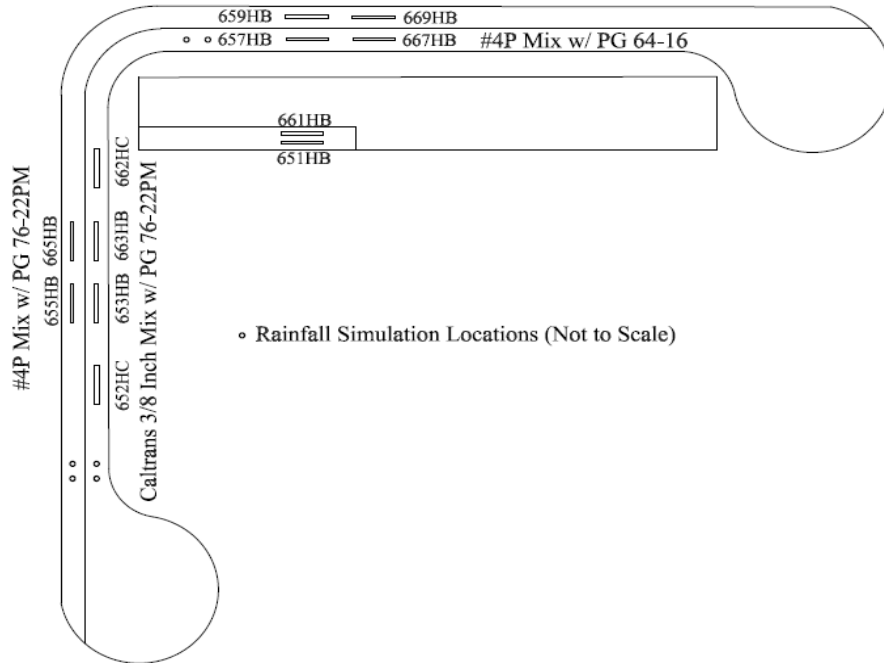


Figure 3.26: Rainfall simulation locations.

Dust Application

In order to study the effect of dry dust on clogging of the OGFC layer, dry dust particles were applied over three of the HVS test sections that were trafficked with dual wheels. For this experiment, 100 grams of particles passing the #400 sieve (sieve opening 1.5×10^{-6} in. [38 micron]) were applied on the downslope wheelpath at two different times: once at the beginning of HVS testing and again after the development of about 0.25 in. (6.3 mm) of average maximum total rut. The estimated 200 gram mass was calculated based on the HVS wheelpath surface area and an assumed average rainfall of 15 inches per year for 15 years. In addition, it was assumed that the total suspended solid (TSS) concentration of highway runoff is equal to 140 mg/L and that only 10 percent of the particles found in the TSS can pass the #400 sieve [24]. This 200 gram mass was applied uniformly using a #200 sieve.



(a) Spreading the dust using a #200 sieve



(b) Test section with dust spread on the down-slope wheelpath

Figure 3.27: Spreading of passing #400 dust on the downslope wheelpath using a #200 sieve.

Dust was applied on Sections 653HB (Caltrans 3/8 inch mix with PG 76-22PM binder), 655HB (#4P mix with PG 76-22PM binder), and 657HB (#4P mix with PG 64-16 binder) following the procedure described above. It was also applied on Section 659HB (#4P mix with PG 76-22PM binder), again following the same procedure, except that the total 200 grams of dust was applied at the beginning of the HVS test.

Sampling of Cores for X-Ray CT Imaging

One core was taken at the downslope wheelpath at Station 13 for Sections 653HB, 655HB, and 657HB respectively to study the clogging susceptibility of the three OGFC mixes due to rutting. Since dust was also spread on these locations, the clogging could also be attributed to deposition of airborne dust in the air voids. Each core was removed before the start of HVS trafficking, subjected to x-ray CT imaging, replaced and secured at its original location, subjected to HVS trafficking, and then removed for another round of x-ray CT imaging.

3.7.3 Procedure for Permeability Measurements

Permeability was measured using the recently developed ASTM C1701 (Standard Test Method for Infiltration Rate of In Place Pervious Concrete) and a permeameter developed by the National Center for Asphalt Technology (NCAT). Brief descriptions of both test methods are presented below. Additional details about the permeability measurements under field conditions can be found in Reference [25].

NCAT Permeability Test Method

A photograph of the NCAT permeameter used during field measurement is shown in Figure 3.28. The permeameter is comprised of four tiers of plastic cylinders of different diameters. For pavements with high permeability, the bottom two tiers are sufficient and the top two tiers can be added when permeability is low and/or a longer time is needed to complete the test.

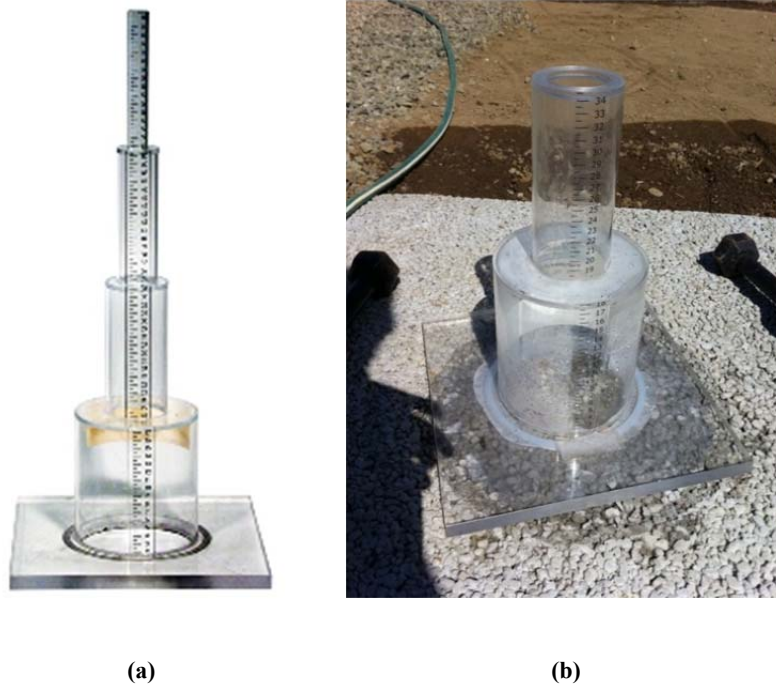


Figure 3.28: NCAT field permeameter: (a) four cylindrical tiers with different diameters; (b) permeameter with bottom two tiers used in the field in this study.

The NCAT permeability test is a falling head method in which permeability is measured by recording the time required for water to fall the height of the permeameter. The coefficient of permeability, K , which is also known as *saturated hydraulic conductivity*, is calculated using the following relationship:

$$K_s = \frac{al}{At} \ln\left(\frac{h_1}{h_2}\right)$$

where:

K_s = saturated hydraulic conductivity, cm/s

a = inside cross-sectional area of inlet standpipe, cm²

l = thickness of the permeable porous asphalt or pervious concrete pavement, cm

A = cross-sectional area of tested pavement, cm²

t = average elapsed time of water flow between timing marks ($t_1 - t_2$), s

h_1 = hydraulic head on pavement at time t_1 , cm

h_2 = hydraulic head on specimen at time t_2 , cm

When measuring permeability under field conditions, leakage between the pavement surface and the base of the permeameter must be prevented. The NCAT method specifies the use of plumbing putty to prevent water leakage and states that a test must be terminated if leakage is detected. However, earlier field measurements verified that plumbing putty did not adequately prevent water leakage [26]. Therefore, a silicone rubber called Ecoflex 5 (by Smooth-On[®]) was applied to the bottom to the permeameater to better seal it to the pavement and prevent leaking.

ASTM C1701 Test Method

The ASTM C1701 test method requires the use of a hollow cylinder with a 12 in. (300 mm) inner diameter that is at least 2.0 in. (50 mm) tall. However, the standard-sized cylinder was too large to fit inside the individual wheelpaths created by the dual wheels. The cylinder diameter was therefore reduced to 6 in. (150 mm). The two cylinders with different diameters used in this study are shown in Figure 3.29. The ASTM 1701C permeability test was performed based on the constant head method.



(a). Standard-sized (12 in.) cylinder



(b) Modified (6 in.) cylinder

Figure 3.29: Permeameters used with the ASTM C1701 test method in this study. Photos show sealing of the base using Ecoflex 5 silicone rubber.

The test procedure was as follows:

1. Secure the permeameter to the pavement with sealant, in this case Ecoflex 5 silicone rubber.
2. Wait 3 to 5 minutes for the Ecoflex to dry.
3. Fill the permeameter with about 5 kg of water and check for any obvious water leakage; if no water leakage is observed, continue performing the actual permeability measurement.
4. Pour about 18 kg of water into the ring at a rate sufficient to maintain a head between the two marked lines at a distance of 10 and 15 mm from the bottom respectively, until all 18 kg of water has been used.
5. Begin keeping time as soon as water impacts the pervious pavement surface, and stop when free water is no longer present on the pervious surface. Record the elapsed time t duration.
6. Calculate the infiltration rate (a.k.a. *coefficient of permeability* or *hydraulic conductivity*) by using the following formula:

$$I = \frac{KM}{D^2t}$$

where:

I = infiltration rate, mm/h

M = mass of infiltrated water, kg

D = inner diameter of infiltration ring, mm

t = time required for measured amount of water to infiltrate the pavement, s, and

K = constant factor, 4,583,666,000 in SI units.

3.7.4 Procedure for Evaluating Runoff-Related Clogging

The steps used for evaluation of clogging susceptibility due to drainage of runoff using rainfall simulation are listed below and illustrated with photographs in Figure 3.30. In short, the process involved x-ray CT imaging of cores before and after they were subjected to drainage from simulated rainfall.

1. Using epoxy, seal impermeable paper over the core specimen area in order to prevent air from penetrating the core samples (Figure 3.30a).
2. Initiate air-cooled coring while vacuuming dust (Figure 3.30b).
3. Remove the cored sample along with the impermeable paper (Figure 3.30c). (Attachment of the paper is noted in “Obtaining Pavement Core Samples” on page 58.)
4. Peel off the impermeable paper (Figure 3.30d) and conduct x-ray CT imaging (Figure 3.30e).
5. Process x-ray CT images to determine the distributions of air-voids in the asphalt cores (Figure 3.30f).
6. Put the core back into the pavement for rainfall simulation:
 - a. Tape the top part of the core hole to avoid any exposure to fast-setting epoxy before putting the core back (Figure 3.30g).
 - b. Apply epoxy to the bottom half of the core (Figure 3.30h).
 - c. Replace the core in its original location and fill the upper portion of the open-graded pavement with large sand particles (Figure 3.30i).
7. Initiate rainfall simulation over the newly replaced core using a water solution with a known TSS concentration (Figure 3.30j).
8. After the rainfall simulation is completed, wait 24 hours for the core area to dry.
9. Re-core the specimens by repeating steps 1 through 5 (Figure 3.30k).
10. Scan the re-cored samples (Figure 3.30l).
11. Compare the air-void distributions of the core samples before and after the rainfall simulation to evaluate possible particle-related clogging.

Additional details relating to pavement sample coring, preparation of simulated rainfall solution, a description of simulated rainfall apparatus, rainfall simulation test locations, and the x-ray CT image processing associated with this aspect of clogging evaluation are presented next.



(a)



(b)

Air-cooled coring



(c)

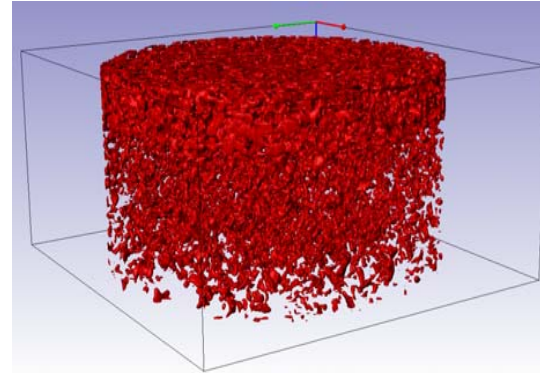


(d)

Extracted core and removal of impermeable paper



(e) X-ray CT imaging



(f) Processed x-ray CT images showing distribution of air voids within an asphalt concrete block



(g)

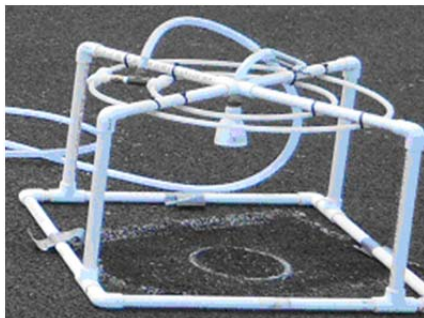


(h)

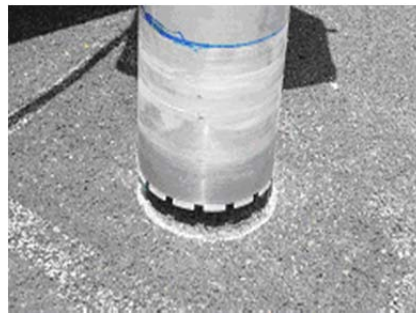
Replacement of core in the HVS test section



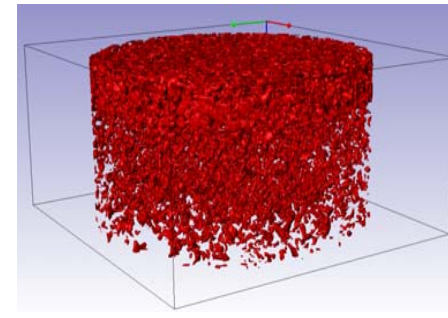
(i)



(j) Rainfall simulation



(k) Removal of cores for post-test scanning



(l) Post-test image processing

Figure 3.30: Photos of steps for evaluation of clogging susceptibility due to drainage of run-off using simulated rainfall.

Obtaining Pavement Core Samples

Air-cooled coring was used to avoid contaminating the cores with the water/sediment slurry associated with water-cooled coring. In addition, to further reduce the possibility of the cooling air blowing residues from the core and the drill bit through the voids in the sample, a nonpermeable paper patch was glued to the pavement surface over the cored area. A detailed description of the procedure for replacing the cores using epoxy can be found in Reference [8].

Preparation of Water Containing Suspended Solids

Dust was obtained by processing granite aggregates that came from the Graniterock Company quarry at Aromas, California. All particles larger than 600 microns (retained on sieve #30) were discarded. The dust was separated using the following sieves: #30, #50, #100, #200, and #400. These smaller particle size ranges were used since they were assumed to be the cause of the clogging of the voids. Two particle-size distributions were prepared for the rainfall simulations (see Table 3.6): one containing only particles passing the #400 (the <38 micron gradation), and the other containing particles passing between the #30 and #400 sieves (the <600 micron gradation). The total amount of dust used was 28 grams for the <38 micron gradation and 56 grams for the <600 micron gradation, respectively.

Table 3.6: Particle Gradations (Percent Passing) Used for Rainfall Simulation

Sieve Size U.S. (metric)	<38 micron	<600 micron
#30 (600 micron)		100
#50 (300 micron)		76.7
#100 (150 micron)		53.4
#200 (75 micron)		30
#400 (38 micron)	100	15
Total amount	28 grams	56 grams

Dust particles from each gradation were mixed with 200 L of water to create a solution with specified total suspended solid (TSS) concentration. During first set of rainfall simulations using <38 micron particles, the TSS concentration was set to be 140 mg/L based on the typical California statewide highway runoff characterization study [27]. The runoff volume was estimated by using the simulated rainfall surface area and the total annual rainfall of 15 in. for 15 years' duration. After the first set of simulations, it was observed that minimal clogging was induced by the simulated rainfall. The TSS concentration was then increased to 280 mg/L for the <600 micron particles; 280 mg/L corresponds to the upper bound of TSS concentrations that were measured on certain California highways [27].

Rainfall Simulation Apparatus

The rainfall simulation apparatus is shown in Figure 3.31. The apparatus is comprised of a tank with 1,000 L capacity equipped with a mixer motor and a paddle mixer, a submersible pump, and a shower head placed on top of the pavement. The shower head discharged runoff over the core samples at a constant rate of about 0.3 L/min.

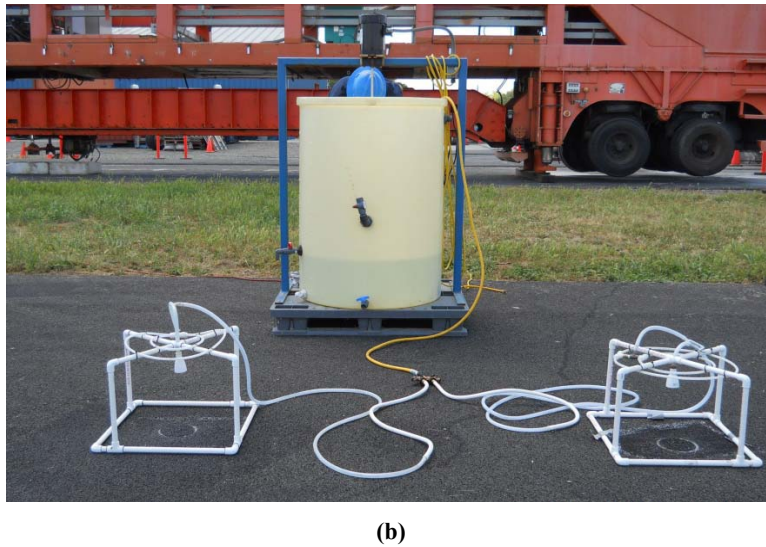
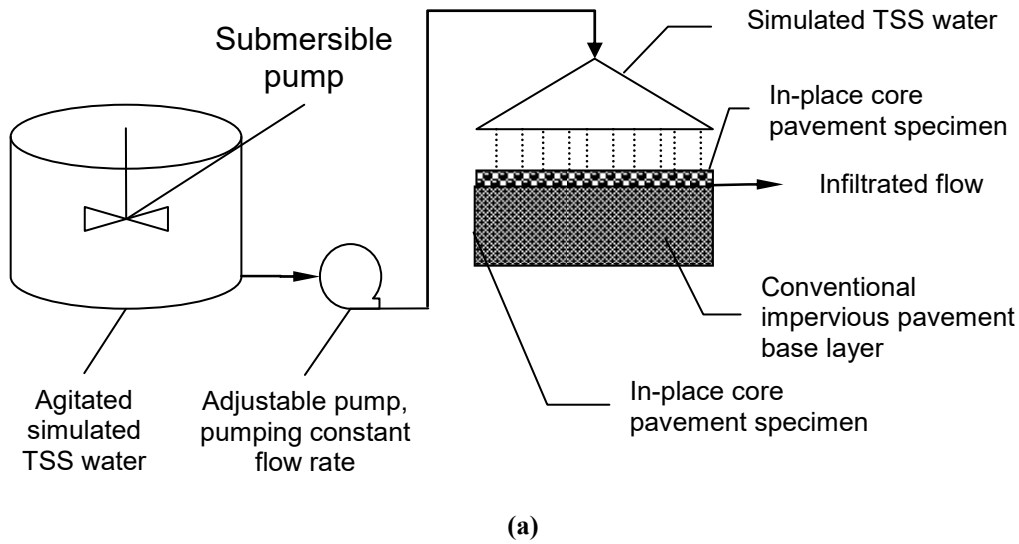


Figure 3.31: Rainfall simulation apparatus: schematic and actual device.

X-Ray CT Image Processing for Clogging Evaluation

The same technique described in Section 3.4.3 was used here to acquire and process x-ray CT images. Figure 3.32 illustrates an example of air void distributions, which in this case is Sample 1-655; this sample was taken from near Section 655HB before it was subjected to rainfall simulation.

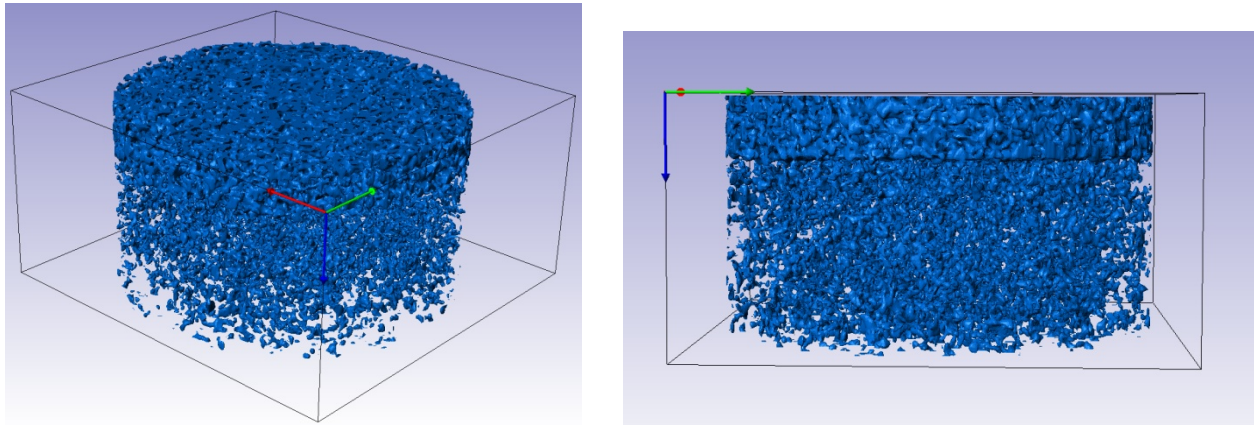


Figure 3.32: Distribution of air voids in asphalt sample 1-655 (#4P mix with PG 76-22PM binder) from two perspectives. Colored volumes represent air-voids. (Note: core diameter is 150 mm.)

The three-dimensional images developed were further processed to obtain the distribution of air voids with depth using the same procedure described in Section 3.4.3, except that in this case the specimens were cores rather than square blocks and the thickness of the slices was 2 mm (which differed from the thickness used with the blocks).

3.7.5 Procedure for Evaluating Rutting-Related Clogging

The focus of this test was to evaluate clogging caused by rutting under HVS operation. This evaluation was performed by comparing the differences in the vertical air-void content profiles based on the x-ray CT images of the cores taken just before and just after HVS trafficking. Sample coring, scanning, and image processing were the same as described in Section 3.7.4. Since the HVS test sections were enclosed in a temperature control chamber, there was no runoff drainage through these cores, and any difference in the vertical air-void content profiles before and after HVS trafficking could be considered due to pavement rutting. Since all of these cores were taken from HVS sections tested with dual wheels and in the wheelpath that was spread with dust, the clogging was attributed to airborne dust as well.

4 SURFACE TEXTURE AND NOISE TESTING RESULTS

This chapter presents the results of surface texture and noise measurements made on HVS test sections and friction measurements on ingots made from loose mix. Presentation of the results is laid out according to the measurement device used. For details of the surface texture and noise testing procedure and program, see Section 3.5.

4.1 Surface Texture and Noise Testing on HVS Test Tracks

4.1.1 *Dynamic Friction Tester Results*

The dynamic friction of the surface of each test section was measured with the Dynamic Friction Tester (DFT). As noted in Section 3.5, the dynamic friction value at a spinning speed of 20 km/h is an indicator of microtexture, so this value was selected as the basis for comparisons among the different mixes.

The Initial DFT

The initial dynamic friction values, those measured at 20 km/h before HVS trafficking, for the different mixes are listed in Table 4.1 and shown in Figure 4.1. The #4P mixes exhibited an initial average dynamic friction value of 0.52, which is close to the typical value for OGFC mixes reported by other researchers (0.51) [28]. Table 4.2 shows a comparison of the dynamic friction measured at 20 km/h among the different OGFC mixes and the control mix (Caltrans 3/8 inch mix with PG 76-22PM binder). The table indicates that the dynamic friction of all of the mixes were significantly higher than that of the control mix, and that the Georgia 1/2 inch mix with PG 58-34PM had the highest dynamic friction.

Figure 4.1 also includes the results measured at 60 km/h. Kobayashi [29] recommended a minimum DFT dynamic friction value of 0.50 for OGFC at 60 km/h, which was only met by the Georgia 1/2 inch mix with PG 58-34PM binder.

A statistical test, with the results shown in Table 4.3, indicates that binder type had no statistically significant effect on the dynamic friction of the two #4P mixes as measured by the DFT at 20 km/h.

Table 4.1: Dynamic Friction Values Measured at 20 km/h for Different Mixes

Mix Type	HVS Test Cell	DFT Value	Count	Std. Dev.
Caltrans 3/8 inch mix w/ PG 76-22PM	Cell A	0.45	59	0.050
#4P mix w/ PG 76-22PM	Cell B1	0.52	44	0.087
#4P mix w/ PG 76-22PM	Cell B2	0.53	15	0.029
#4P mix w/ PG 64-16	Cell C	0.51	37	0.053
Georgia 1/2 inch mix w/ PG 58-34PM	Cell D	0.63	54	0.042

Table 4.2: Comparison of Dynamic Friction at 20 km/h of Different Mixes Against the Control

Control Mix	Mix Type	Mean Difference	Std. Deviation of Difference	Statistically Significant?
Caltrans 3/8 inch mix w/ PG 76-22PM	#4P mix w/ PG 76-22PM	-0.07	0.012	Yes
	#4P mix w/ PG 64-16	-0.07	0.011	Yes
	Georgia 1/2 inch mix w/ PG 58-34PM	-0.19	0.0087	Yes

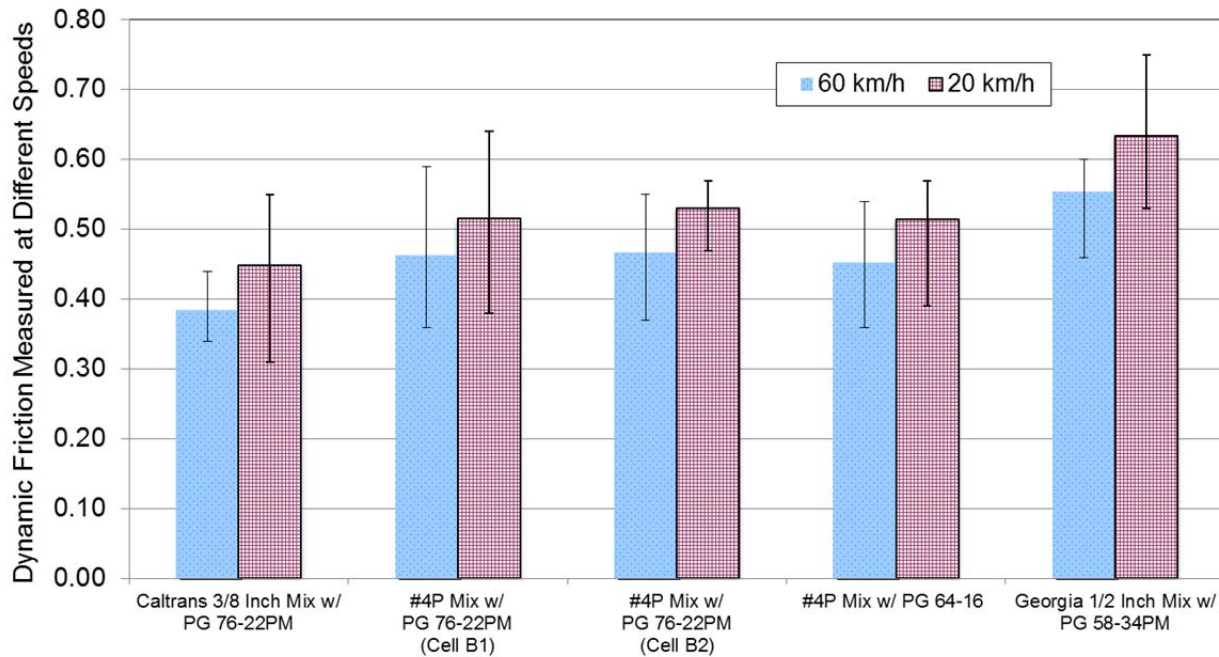


Figure 4.1: Dynamic friction measured by DFT at 20 km/h and 60 km/h for different mixes.

Table 4.3: Statistical Test on Effect of Binder Type on Dynamic Friction Measured by DFT

Mix Types	DFT Value	Count	Std. Dev.	P-value	Significant?
#4P mix w/ PG 64-16	0.51	37	0.053	0.27	No
#4P mix w/ PG 76-22PM (Cell B2)	0.53	15	0.029		

Variation of DFT Values with Load Repetition

In order to study the effect of HVS trafficking on dynamic friction values, the measured dynamic friction values were plotted against load repetitions for the different mixes (Figure 4.2). However, only a limited amount of data could be obtained because the surface rutting caused by HVS trafficking quickly made the surface too rough for the DFT to operate properly. Therefore, although Figure 4.2 shows initial decreases in dynamic friction values with increasing load repetitions, it is believed that the data is insufficient for any conclusive observations to be drawn.

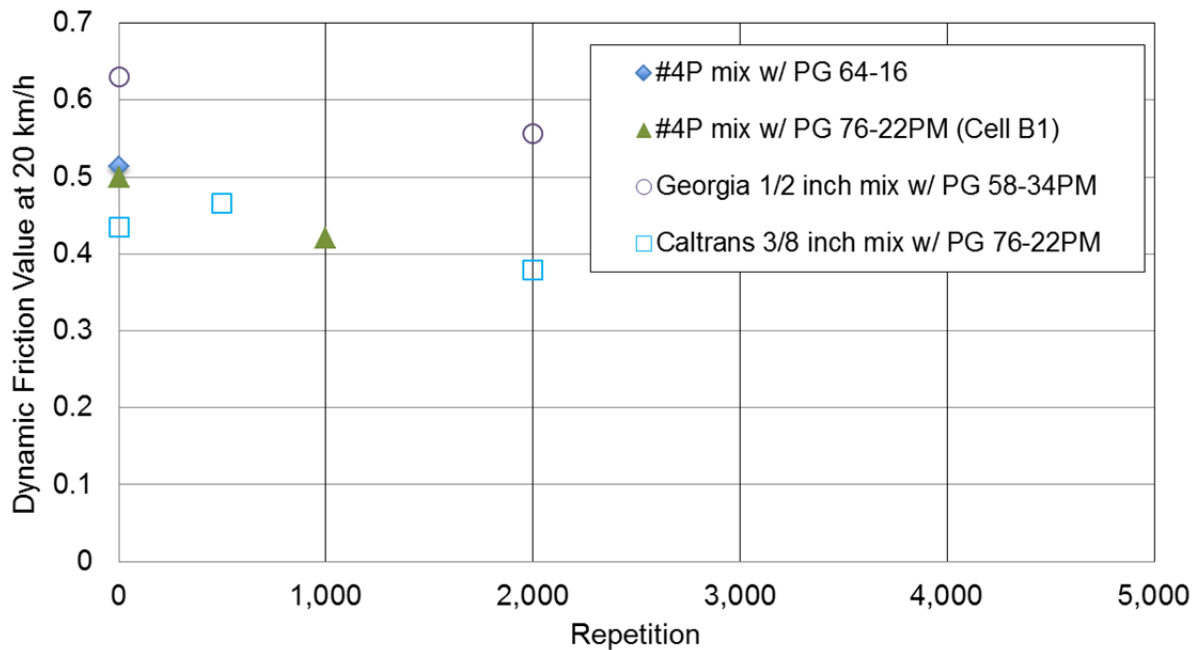


Figure 4.2: Progression of dynamic friction measured with the DFT versus load repetitions for the different mixes at the beginning of HVS trafficking.

4.1.2 Circular Texture Meter Results

The Circular Texture Meter (CTM) was one of the two instruments used in the study to measure the mean profile depth (MPD) of the surface of each section (the other method, which used the Laser Texture Scanner, is discussed next). Although HVS trafficking created a small amount of uplifted material between the treads of the tires moving in a channelized path on the pavement (e.g., Figure 7.4a), each MPD profile was thoroughly investigated and the effect of the tire tread impression was removed. The following section discusses the results of initial CTM measurements and their variation as a function of loading.

Initial MPD from CTM

The initial MPDs measured by the CTM for the different mixes are listed in Table 4.4 and plotted in Figure 4.3. Table 4.5 shows the results of a comparison of the MPDs measured for the different mix types against the control. It can be seen that all of the mixes had MPD values significantly lower than the control. The #4P mixes had roughly the same MPD, which was the lowest among all the mixes. The range of measured MPD values for newly constructed open-graded mixes in California is 0.8 mm to 1.6 mm [30]. It should be noted that aggregate size is not the only factor that determines MPD values: factors such as aggregate shape and gradation also play important roles.

Table 4.4 Results of CTM-Measure MPD Values for Different Mixes

Mix Type	MPD Value (mm)	Count	Std. Dev.
Caltrans 3/8 inch mix w/ PG 76-22PM	1.55	59	0.213
#4P mix w/ PG 76-22PM (Cell B1)	1.03	43	0.098
#4P mix w/ PG 76-22PM (Cell B2)	1.03	15	0.138
#4P mix w/ PG 64-16	1.04	38	0.128
Georgia 1/2 inch mix w/ PG 58-34PM	1.31	54	0.146

Table 4.5: Comparison of Initial CTM-Measured MPD for Experiment Mixes Against Control Mix

Control Mix	Mix Type	Mean Difference	Std. Deviation of Difference	Difference Significant?
Caltrans 3/8 inch mix w/ PG 76-22PM	Georgia 1/2 inch mix w/ PG 58-34PM	0.23	.034	Yes
	#4P mix w/ PG 76-22PM	0.51	.031	Yes
	#4P mix w/ PG 64-16	0.51	.035	Yes

Results of a statistical test, shown in Table 4.6, indicated that binder type did not have a statistically significant effect on the initial CTM-measured MPD for the two #4P mixes.

Table 4.6: Statistical Test on the Effect of Binder Type on CTM-Measured MPD Value

Mix Type	MPD Value (mm)	Count	Std. Dev.	P-value	Difference Significant?
#4P mix w/ PG 64-16	1.04	38	0.128	0.78	No
#4P mix w/ PG 76-22PM (Cell B2)	1.03	15	0.138		

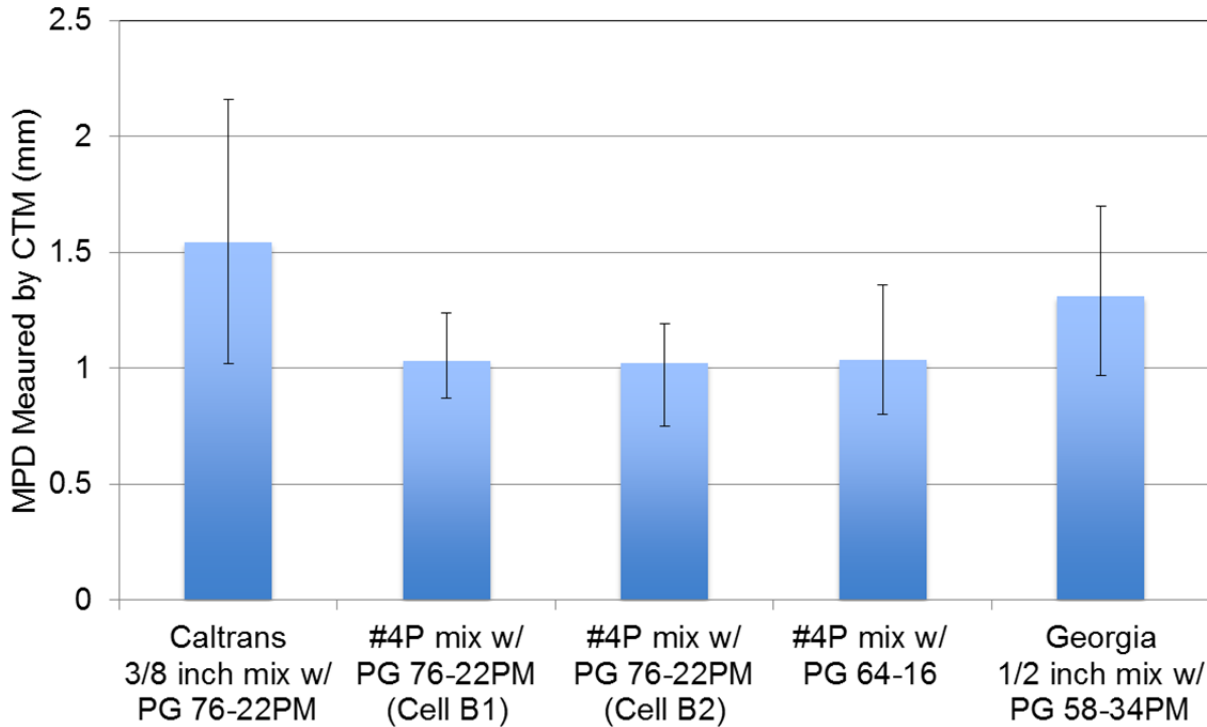


Figure 4.3: Initial MPD values measured by CTM for the different mixes.

Variation of MPD Measured by CTM with Load Repetitions

In order to study the effect of HVS trafficking on variation of the MPD values, the CTM-measured MPD values were plotted against load repetitions for each mix (Figure 4.4). Since the loading process continued until structural failure of the layer could be observed, the number of load repetitions for the mixes covered a wide range. The figure only shows the part of this testing where most of the mixes could handle the load.

Figure 4.4 indicates that all of the mixes were able to maintain their initial macrotexture over the course of loading. The Georgia 1/2 inch mix and #4P mixes exhibited a slight increase in MPD values of up to 0.5 mm. All of the mixes maintained an MPD greater than 0.5 mm, a macrotexture level that has been recommended by previous researchers to minimize the potential for hydroplaning [31].

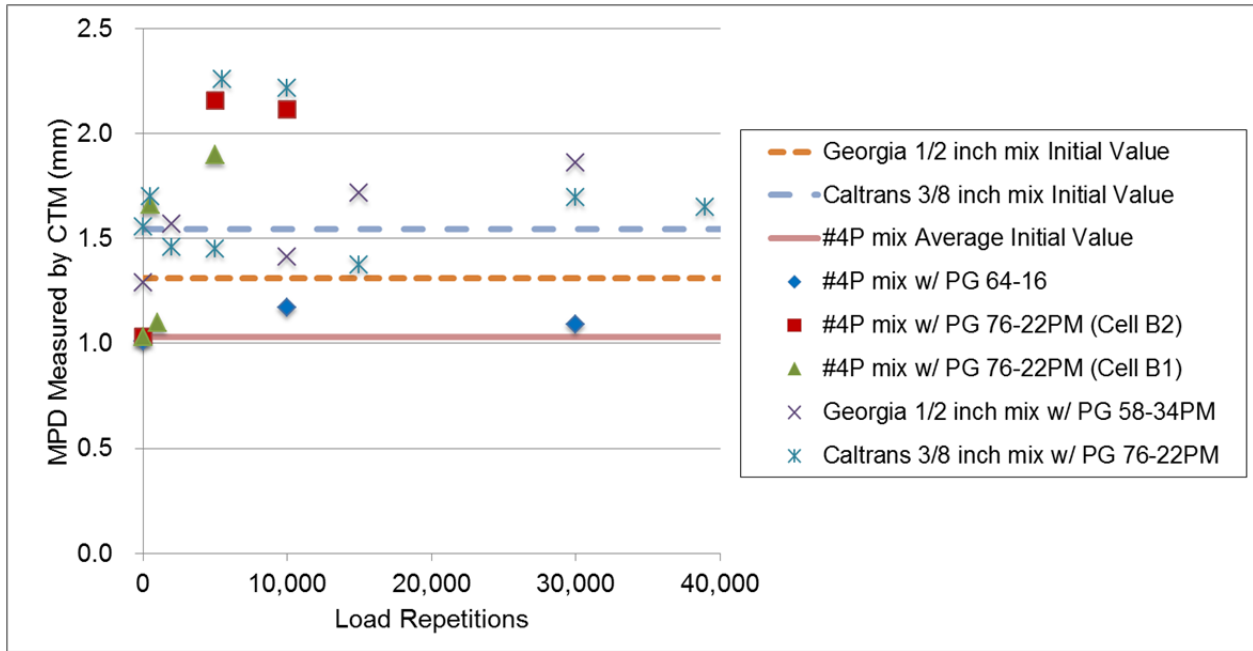


Figure 4.4: The progression of CTM-measured MPD versus load repetitions for the different mixes.

4.1.3 Laser Texture Scanner Results

The laser texture scanner (LTS) was also used to measure the initial MPD of the surface of each test track, and these values and their changes due to HVS trafficking are discussed below. As with the CTM-measured MPD values, the effect of HVS tire tread impression was removed from the measured LTS data.

Initial MPD Measured by LTS

The initial MPD values measured by the LTS for the different mixes are listed in Table 4.7 and plotted in Figure 4.5. Table 4.8 shows the results of the comparison between the MPD values measured by LTS for the different mixes against the control mix. The results indicate that all other mixes had statistically significant lower MPD values than the control mix. MPD measured by LTS and CTM showed the same trend even though their values did not match exactly.

Table 4.7: Initial LTS-Measured MPD Values for the Different Mixes

Mix Design	MPD Value (mm)	Count	Std. Dev.
Caltrans 3/8 inch mix w/ PG 76-22PM	1.779	64	0.424
#4P mix w/ PG 76-22PM (Cell B1)	1.105	34	0.127
#4P mix w/ PG 76-22PM (Cell B2)	1.156	49	0.197
#4P mix w/ PG 64-16	1.135	34	0.194
Georgia 1/2 inch mix w/ PG 58-34PM	1.471	57	0.246

Table 4.8: Comparison LTS-Measured MPD Values for the Different Mixes Versus the Control Mix

Control Mix	Mix Type	Mean Difference	Std. Deviation of Difference	Difference Significant?
Caltrans 3/8 inch mix w/ PG 76-22PM	#4P mix w/ PG 76-22PM	0.64	.056	Yes
	#4P mix w/ PG 64-16	0.67	.059	Yes
	Georgia 1/2 inch mix w/ PG 58-34PM	0.31	.062	Yes

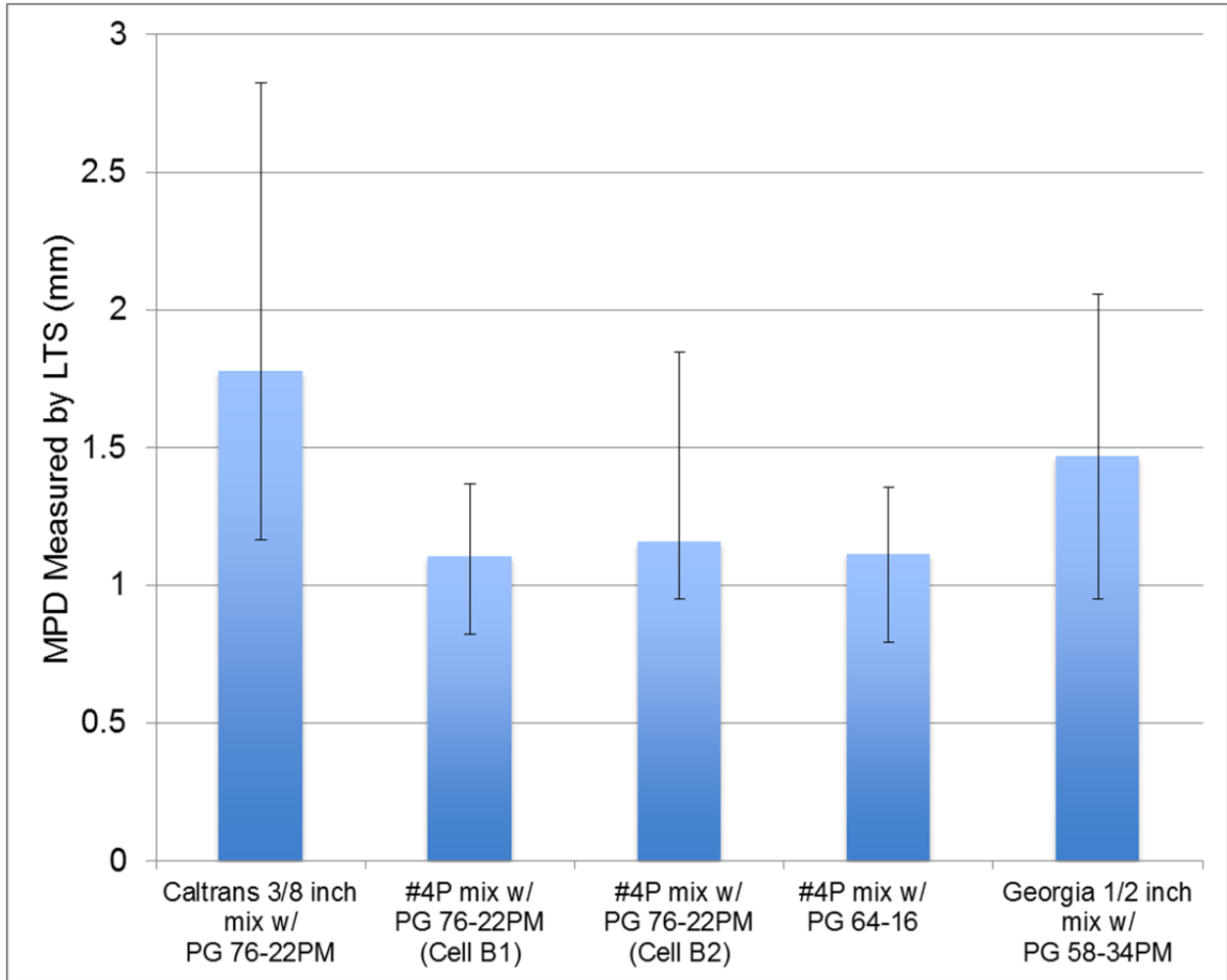


Figure 4.5: Initial LTS-measured MPD values for the different mixes.

A statistical test on the effect of binder type on LTS-measured MPD for the two #4P mixes is listed in Table 4.9; the results indicate that binder type had no statistically significant effect.

Table 4.9: Statistical Test on Effect of Binder Type on Initial LTS-Measured MPD

Mix Design	MPD Value (mm)	Count	Std. Dev.	P-Value	Difference Significant?
#4P mix w/ PG 64-16 (0.5 in.)	1.135	34	0.194	0.62	No
#4P mix w/ PG 76-22PM (0.5 in.)	1.156	49	0.197		

Figure 4.6 shows the relationship between MPD values measured by the CTM and the LTS. This figure indicates that MPD measured by the two devices perfectly correlated with an R-square of 0.99, with LTS-measured values slightly higher. This difference could be attributed to the texture measurement methods of the two devices: the CTM reports MPD values taken on a circular path, whereas the LTS reports MPD values calculated from parallel lines along the length of the test section.

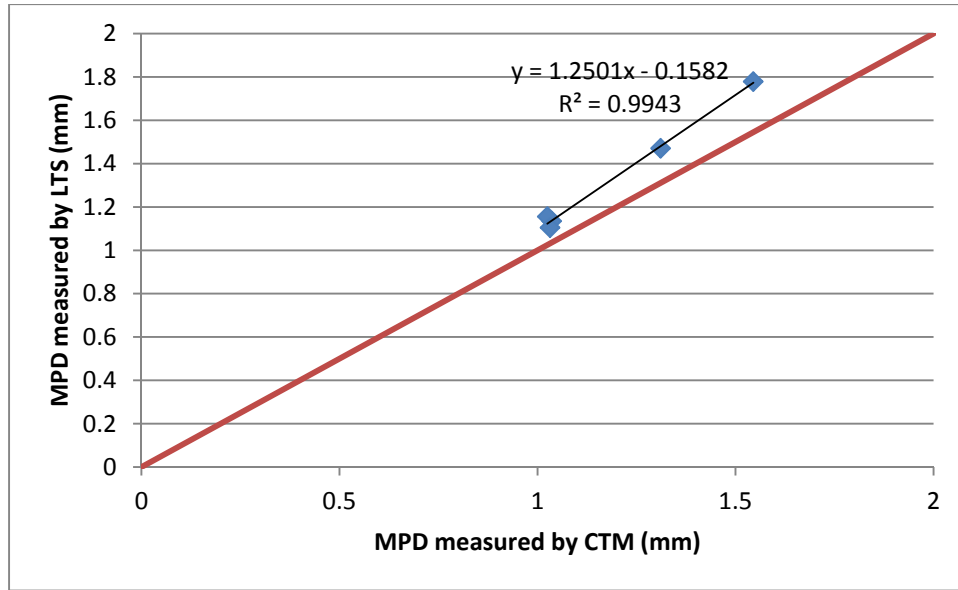


Figure 4.6: Relationship between MPD values measured by CTM and by LTS.

Variation of LTS-Measured MPD with Load Repetitions

In order to study the effect of HVS trafficking on MPD, the MPD values measured by the LTS were plotted against load repetitions for all the mixes (Figure 4.7). The figure only shows the load repetitions that most of the mixes could withstand.

Figure 4.7 indicates that all of the mixes were able to maintain their initial texture over the course of the loading, and maintained an MPD greater than 0.5 mm, a macrotexture level that has been recommended by previous researchers to minimize the potential for hydroplaning [31].

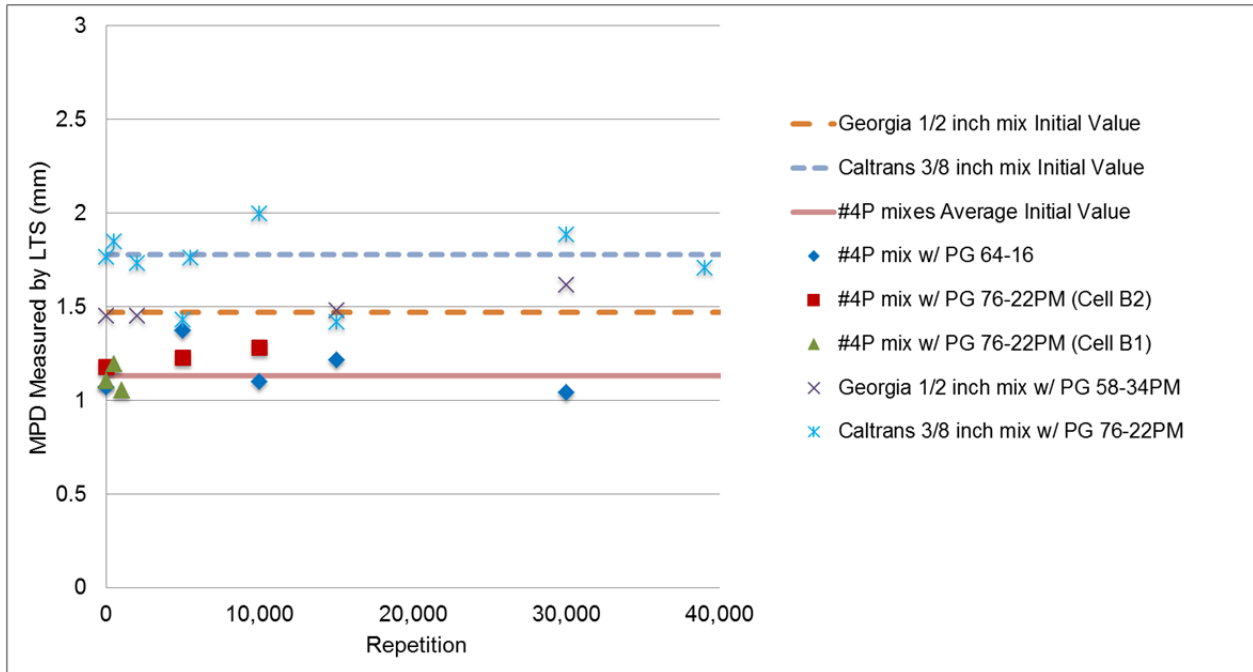


Figure 4.7: The progression of LTS-measured MPD values versus repetition for the different mixes.

4.1.4 Outflow Meter Test Results

The outflow meter (OTF) was used to measure the outflow time for the different OGFC surfaces. Each test track was measured before loading and intermittently after several thousand load repetitions. The following section discusses the results of the initial and later measurements using outflow time values as a function of loading. The results after HVS trafficking were heavily affected by impressions of the tire treads in the wheelpaths because the OTF does not require that its base be sealed. Therefore, the results are believed to be irrelevant to surface texture and are not reported here.

The Initial OTF Outflow Time

The outflow times measured by the OTF for the different mixes are listed in Table 4.10 and plotted in Figure 4.8.

Table 4.11 shows a comparison of the outflow time between the different mixes and the control mix. The results indicate that the Caltrans 3/8 inch mix had a statistically significant shorter outflow time than the two #4P mixes, but one not statistically different from the value for the Georgia 1/2 inch mix. Table 4.10 includes a column for calculated MPD values based on the measured outflow time using the following equation [32]:

$$MPD = 2.05817 - 1.3865 \times \text{LOG}(OFT) \quad R^2 = 0.75$$

The MPD values calculated based on OTF outflow times are in agreement with those measured by both the LTS and CTM in terms of their relative ranking, even though the exact values differed.

Table 4.10: Results of the OFT Values for Different Mixes

Mix Design	Outflow Time (sec)	MPD (mm)	Count	Std. Dev.
Caltrans 3/8 inch mix w/ PG 76-22PM	2.57	1.490	28	0.773
#4P mix w/ PG 76-22PM (Cell B1)	4.15	1.201	15	0.990
#4P mix w/ PG 76-22PM (Cell B2)	3.97	1.228	15	0.978
#4P mix w/ PG 64-16	4.04	1.217	15	0.976
Georgia 1/2 inch mix w/ PG 58-34PM	2.84	1.430	39	0.506

Table 4.11: Comparison of the Measured Outflow Time Values for Different Mixes Versus the Control

Control Mix	Mix Type	Mean Difference	Std. Deviation of Difference	Difference Significant?
Caltrans 3/8 inch mix w/ PG 76-22PM	#4P mix w/ PG 76-22PM	-1.49	0.23	Yes
	#4P mix w/ PG 64-16	-1.47	0.29	Yes
	Georgia 1/2 inch mix w/ PG 58-34PM	-0.27	0.17	No

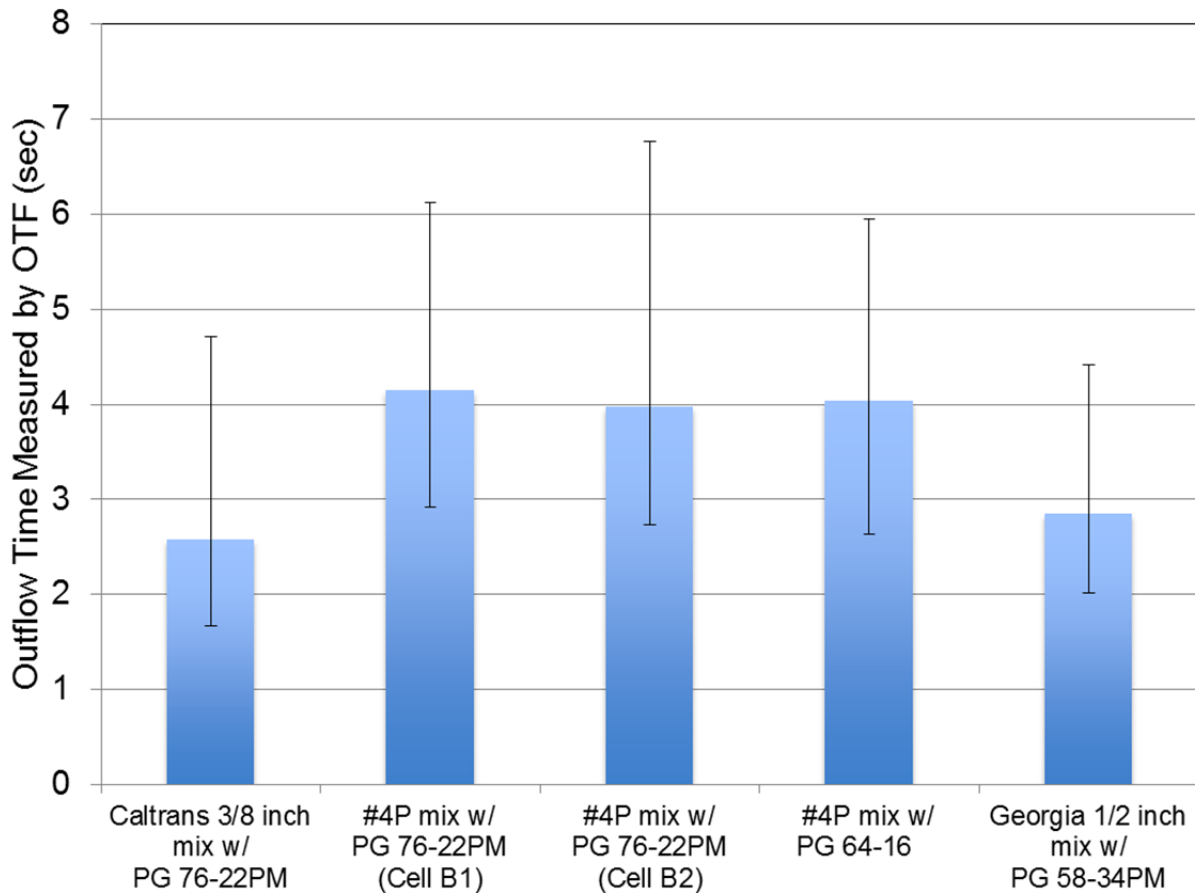


Figure 4.8: Initial outflow time measured by OTF for the different mixes.

A statistical test on the effect of binder type on outflow time measured by the OTF for the two #4P mixes is listed in Table 4.12; it indicates that binder type had no statistically significant effect.

Table 4.12: Statistical Testing on the Effect of Binder Type on Initial Outflow Time

Mix Design	OFT (s)	Count	Std. Dev.	P-value	Difference Significant?
#4P mix w/ PG 64-16 (0.5 in.)	4.04	15	0.976	0.84	No
#4P mix w/ PG 76-22PM (0.5 in.)	3.97	15	0.978		

4.1.5 Caltrans Portable Skid Tester Test Results

The Caltrans Portable Skid Tester (CST) was used to measure the coefficient of friction (COF) on different OGFC surfaces before and after HVS trafficking.

Initial Coefficient of Friction

The initial coefficients of friction measured by the CST for the different mixes are listed in Table 4.13 and plotted in Figure 4.9. Table 4.14 shows a comparison of the initial COF between the different mixes and the control mix. The results indicate that the differences in initial COF between all the mixes and the control mix are statistically significant even though the differences are small.

Table 4.13: COF Values Measured by California Portable Skid Tester (CST) for Different Mixes

Mix Design	COF Value	Count	Std. Dev.
Caltrans 3/8 inch mix w/ PG 76-22PM	0.37	16	0.008
#4P mix w/ PG 76-22PM (Cell B1)	0.40	8	0.010
#4P mix w/ PG 76-22PM (Cell B2)	0.39	18	0.033
#4P mix w/ PG 64-16	0.36	12	0.012
Georgia 1/2 inch mix w/ PG 58-34PM	0.33	8	0.014

Table 4.14: Comparison of COF Values Measured by CST for Different Mixes Against the Control

Control Mix	Mix Type	Mean Difference	Std. Deviation of Difference	Difference Significant?
Caltrans 3/8 inch mix w/ PG 76-22PM	Georgia 1/2 inch mix w/ PG 58-34PM	0.041	0.0053	Yes
	#4P mix w/ PG 76-22PM	-0.022	0.0059	Yes
	#4P mix w/ PG 64-16	0.015	0.0041	Yes

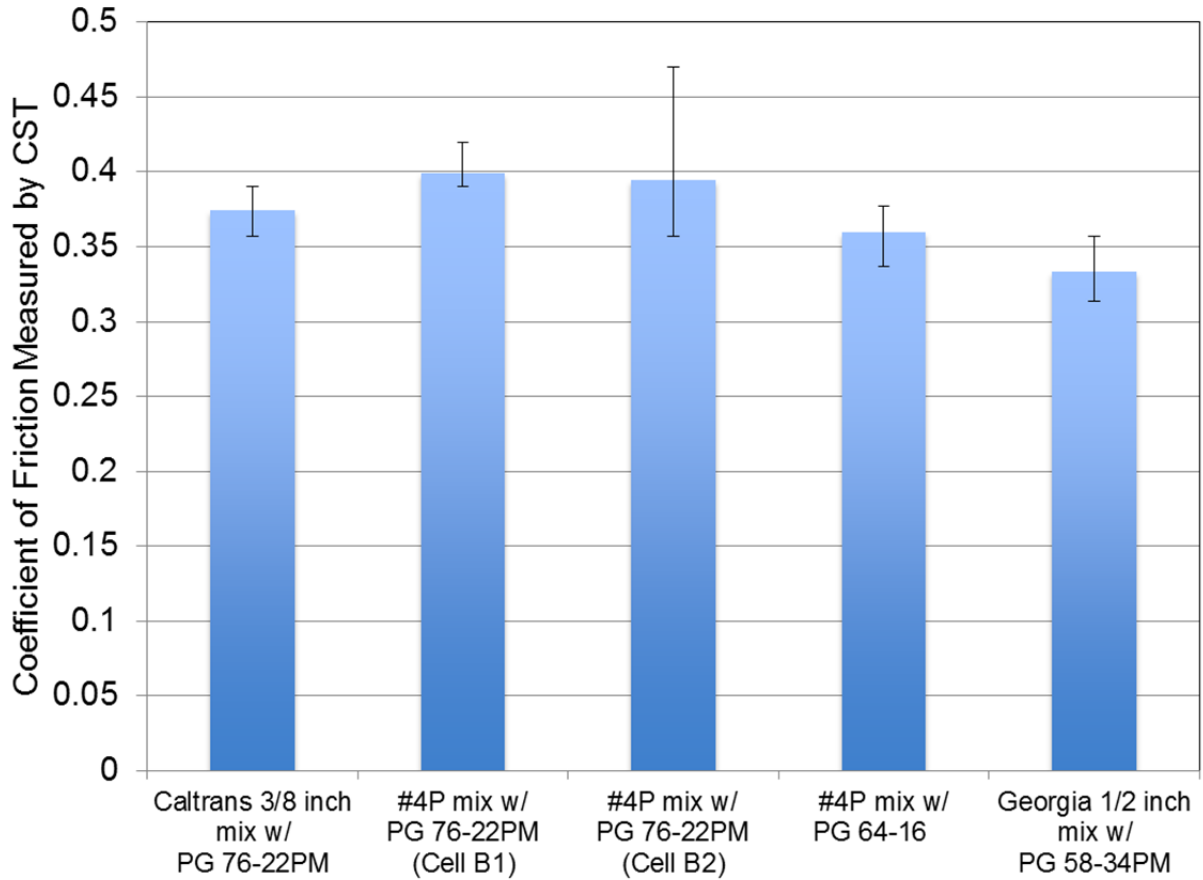


Figure 4.9: Initial coefficient of friction values measured by the California Skid Tester for the different mixes.

A statistical test on the effect of binder type on COF measured by the CST for the two #4P mixes is listed in Table 4.15; it indicates that binder type had a statistically significant effect.

Table 4.15: Statistical Test on the Effect of Binder Type on Initial COF Measured by CST

Mix Design	COF Value	Count	Std. Dev.	P-value	Significant Difference
#4P mix w/ PG 64-16	0.36	12	0.012	0.005	Yes
#4P mix w/ PG 76-22PM (Cell B2)	0.39	18	0.033		

Effect of HVS Trafficking on COF

Figure 4.10 shows the initial and terminal COF values for the different mixes. The terminal values were measured after HVS trafficking was completed. It can be seen that in general the COF values remained constant or increased slightly, and that the terminal values for the different OGFC mixes were roughly the same. An increase in the COF was probably due to wearing away of the surface asphalt covering the aggregate faces, which left the aggregate surface more exposed to traffic and provided better skid resistance. It is believed that

surface friction would eventually decrease after further trafficking due to the smoothing effect of traffic. It should be noted that all mixes were able to provide a minimum COF value of 0.3 required by Caltrans until the pavement structure failed.

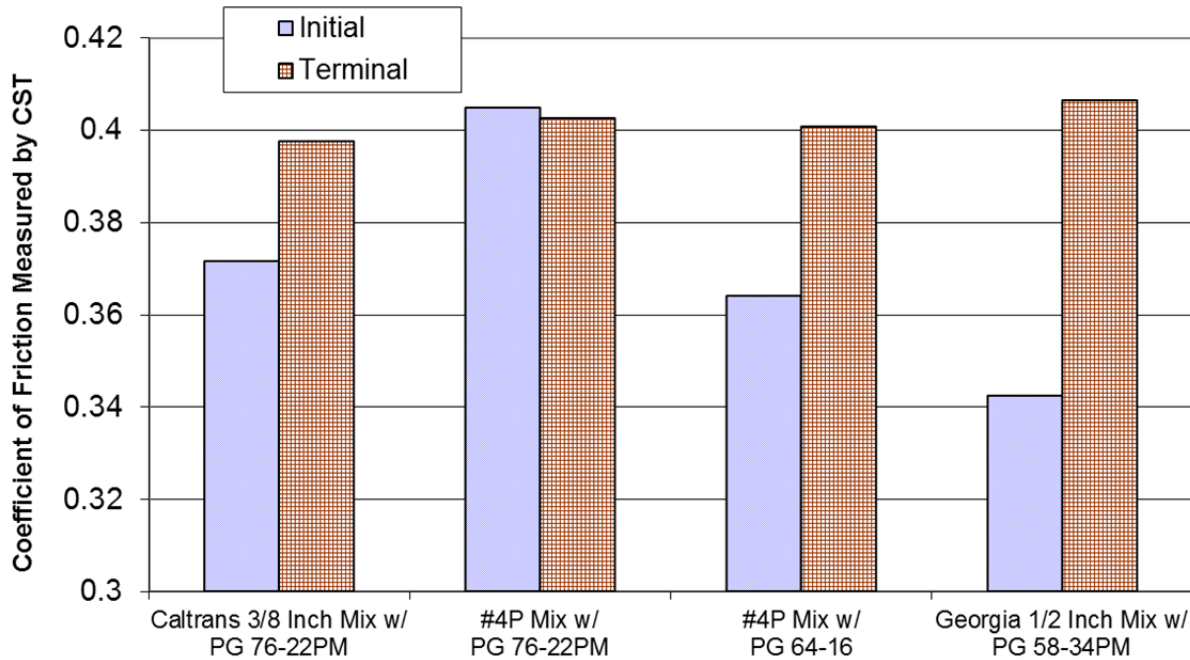


Figure 4.10: Initial and terminal COF values in the wheelpath for the different mixes.

4.1.6 Tire/Pavement Noise Measured by the OBSI Vehicle

Overall Sound Intensity

Figure 4.11 shows the overall sound intensity measured by the UCPRC on-board sound intensity (OBSI) vehicle at 35 mph for the different mixes. Table 4.16 shows the mean and standard deviation of the overall OBSI and for each frequency on each section. No testing was performed on the Georgia 1/2 inch mix because Cell D was too short.

Table 4.16 Mean and Standard Deviation of OBSI on Each Section for Each Frequency

Sound Frequency (Hz)	OBSI (dBA)	Mix Type			
		Caltrans 3/8 Inch Mix w/ PG 76-22PM	#4P Mix w/ PG 76-22PM (Cell B1)	#4P Mix w/ PG 76-22PM (Cell B2)	#4P Mix w/ PG 64-16
Overall	Mean	95.7	94.9	94.3	94.1
	Stdv.	1.8	0.8	0.8	1.0
400	Mean	78.6	79.1	79.8	79.2
	Stdv.	1.6	1.8	1.4	1.3
500	Mean	83.5	84.0	84.1	84.1
	Stdv.	1.9	1.4	1.2	0.9
630	Mean	88.9	88.5	89.0	88.6
	Stdv.	1.9	1.1	0.7	1.0
800	Mean	91.3	89.6	89.6	88.4
	Stdv.	2.5	2.0	0.9	0.8
1,000	Mean	88.4	86.4	87.8	86.8
	Stdv.	2.2	0.9	1.8	0.6
1,250	Mean	86.7	84.0	85.3	83.9
	Stdv.	2.3	0.7	1.7	0.9
1,600	Mean	83.7	79.8	80.3	78.1
	Stdv.	4.3	2.1	1.1	0.9
2,000	Mean	80.8	75.6	77.3	72.9
	Stdv.	4.5	2.3	0.8	1.3
2,500	Mean	75.6	70.0	72.5	66.2
	Stdv.	4.3	2.5	1.7	1.9
3,150	Mean	68.9	67.2	66.9	65.0
	Stdv.	4.0	3.0	2.8	1.9
4,000	Mean	64.9	65.4	62.8	63.6
	Stdv.	4.4	2.6	2.6	1.9
5,000	Mean	62.3	63.3	61.0	60.6
	Stdv.	3.8	2.3	2.4	2.4

The results show that all of the #4P mixes had lower noise levels than the control mix, with the difference ranging between about 0.8 to 1.6 dBA. Table 4.16 indicates that the variability of sound intensity values for the #4P mixes was smaller than that for the control mix. Considering that variability in the measurements can come from small differences in the path taken by the OBSI test vehicle on the test section, the lower standard deviation shown in the table for the #4P mixes could indicate more uniform surfaces. On the other hand, greater differences in tire temperature may have also contributed to the larger variation on the control mix.

Frequency Analysis of Sound Intensity

The noise content for each mix is shown for the 1/3 octave band frequencies in Figure 4.12. Because the OBSI measurements were taken at 35 mph, the frequency content is shifted to lower frequencies (to the left) somewhat from what would have been measured at 60 mph. The peak noise level occurs at a lower frequency (800 Hz) at

35 mph because it is dominated by the interaction of the wheel speed and the length of the tread blocks on the tire. Figure 4.12 shows that all four mixes had the same low frequency noise contents but that the high frequency contents of the four mixes differed significantly. Of all the mixes, the control mix exhibited the highest high-frequency noise, while the #4P mix with PG 64-16 binder showed the lowest high-frequency noise. It is generally assumed that frequency sound intensity is most strongly correlated with surface macrotexture and higher frequency sound intensity is most strongly correlated with surface permeability.

Although the correlations with single frequency OBSI and any single surface characteristic are weak [1], they were checked with the data from this study. No clear correlation could be seen with the few data points between MPD and OBSI at 800 Hz, or between permeability and OBSI at 1,000 Hz, 1,250 Hz, or 1,600 Hz (Figure 4.13 and Figure 4.14(a) through (c), respectively). As has generally been found in UCPRC noise studies, this indicates that the noise at individual frequencies or overall is not a simple phenomenon that can only be explained by a few pavement surface characteristics, and is instead a complex interplay between several factors, such as tire tread block size and shape, and a number of pavement surface characteristics.

Previous research has also indicated that once a minimum level of permeability is present in a mix, there is no correlation between permeability and OBSI [1]. The results presented here indicate that the #4P mixes on the test track have permeability above that minimum required level. The same previous research [1] also indicates that there is a low correlation between MPD and higher frequency OBSI values, and that the correlation diminishes further as frequency increases. The lower MPD of the #4P mixes may have contributed to the lower high-frequency noise values; however, why lower MPD did not reduce the low frequency noise is unknown.

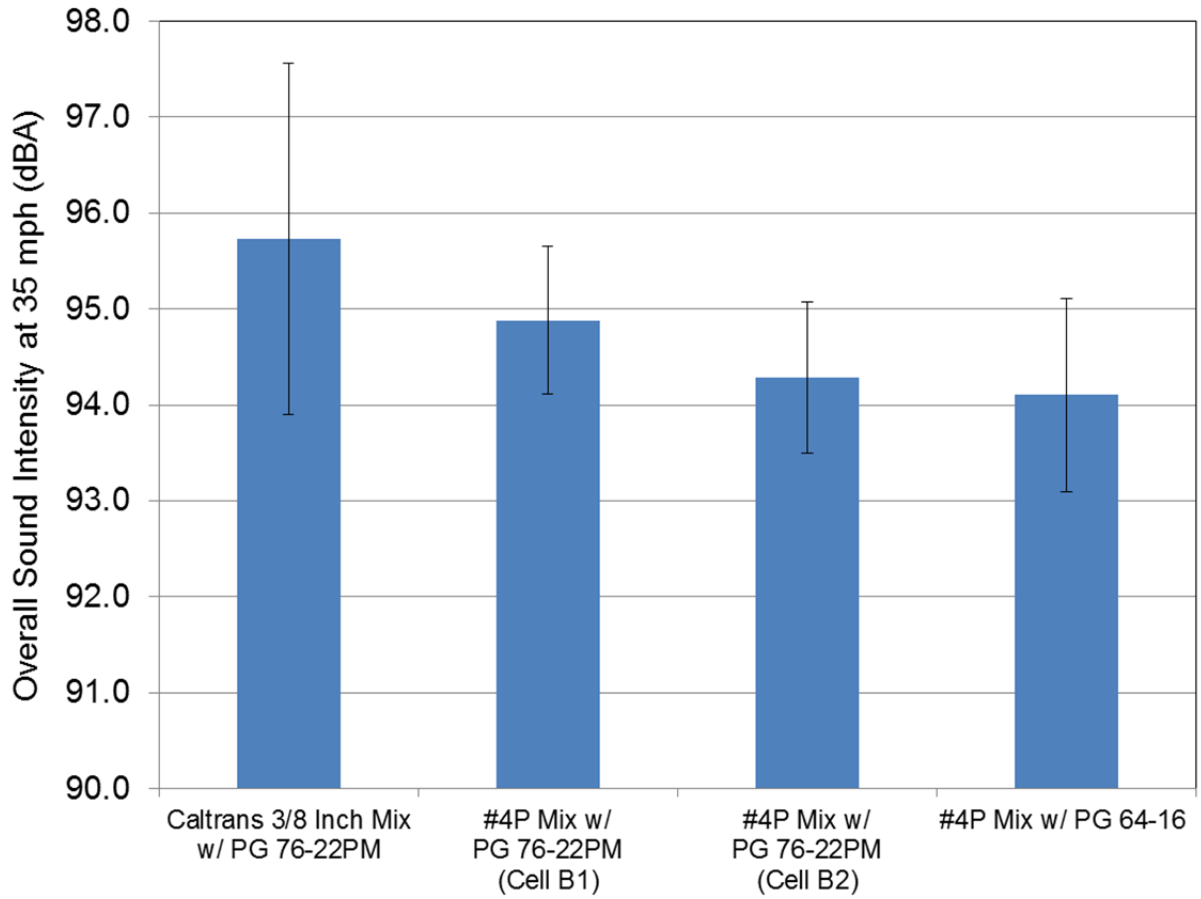


Figure 4.11: Overall sound intensities measured at 35 mph for the different mixes.

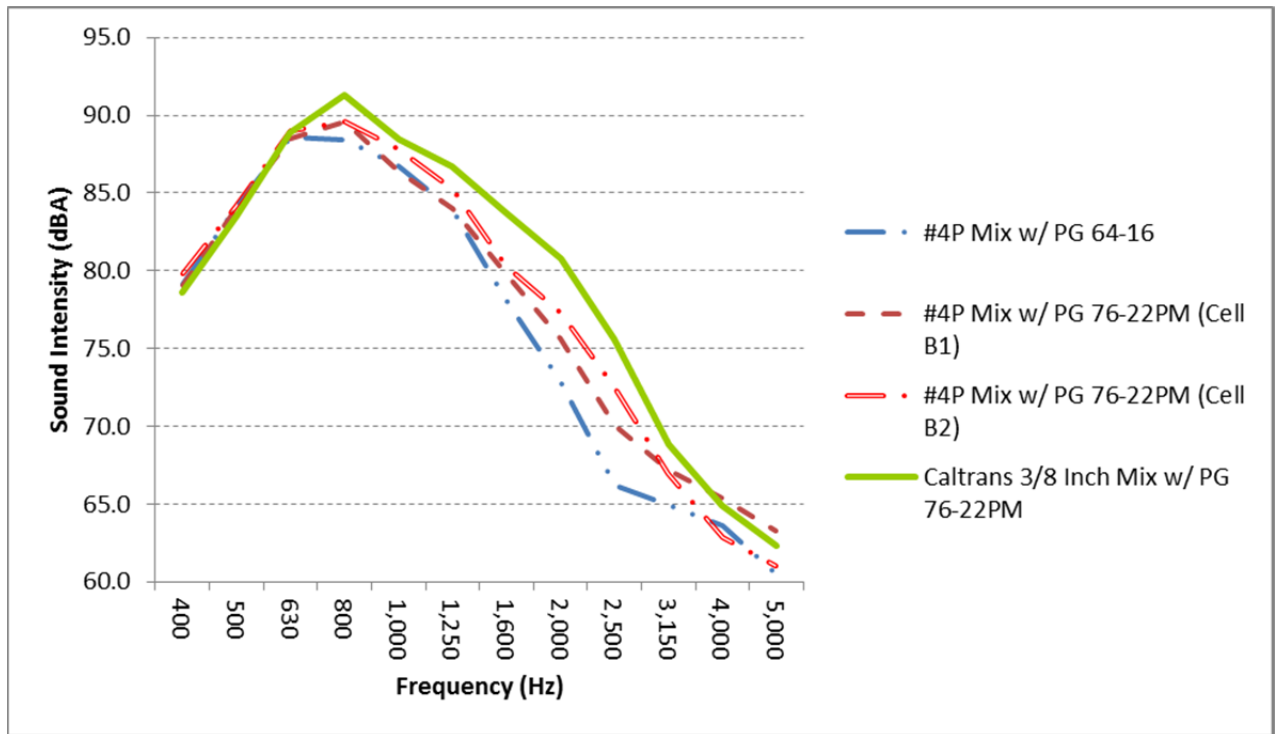


Figure 4.12: 1/3 octave band noise content for the four mixes.

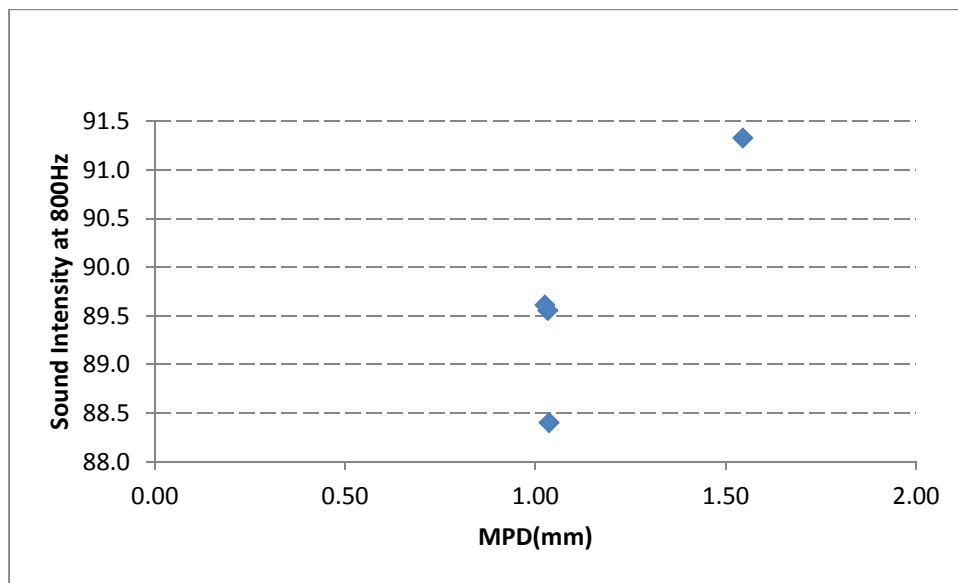
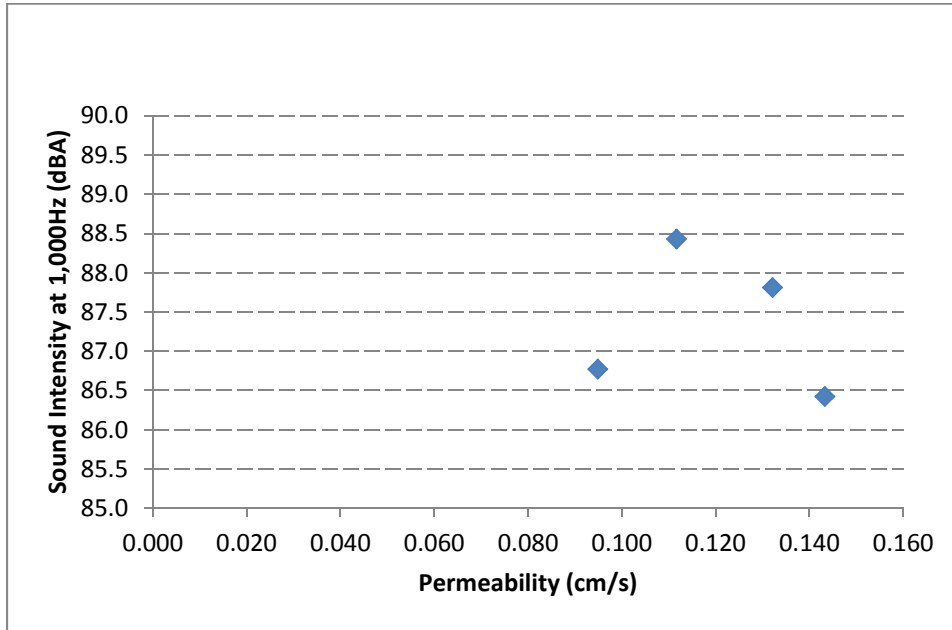
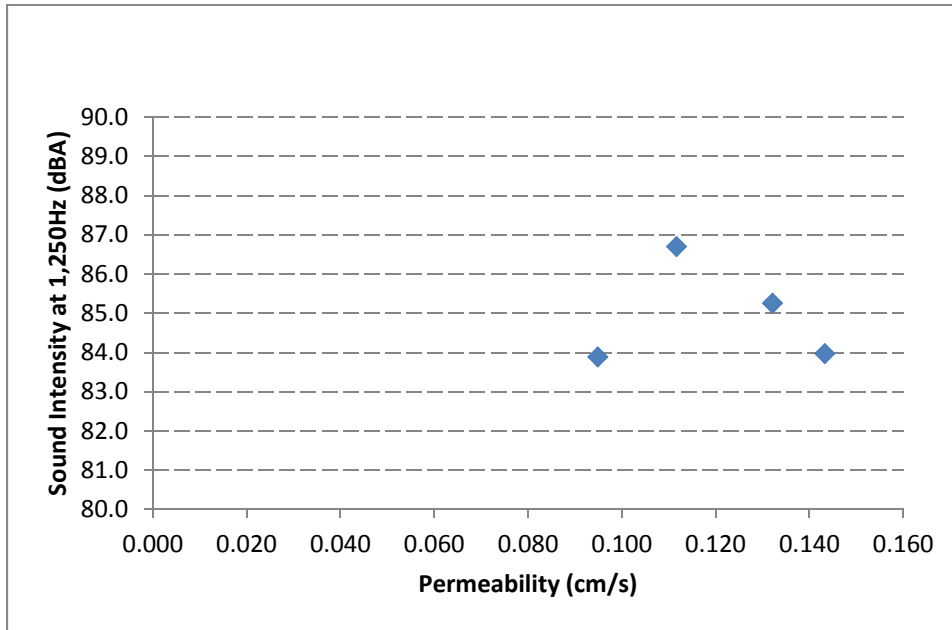


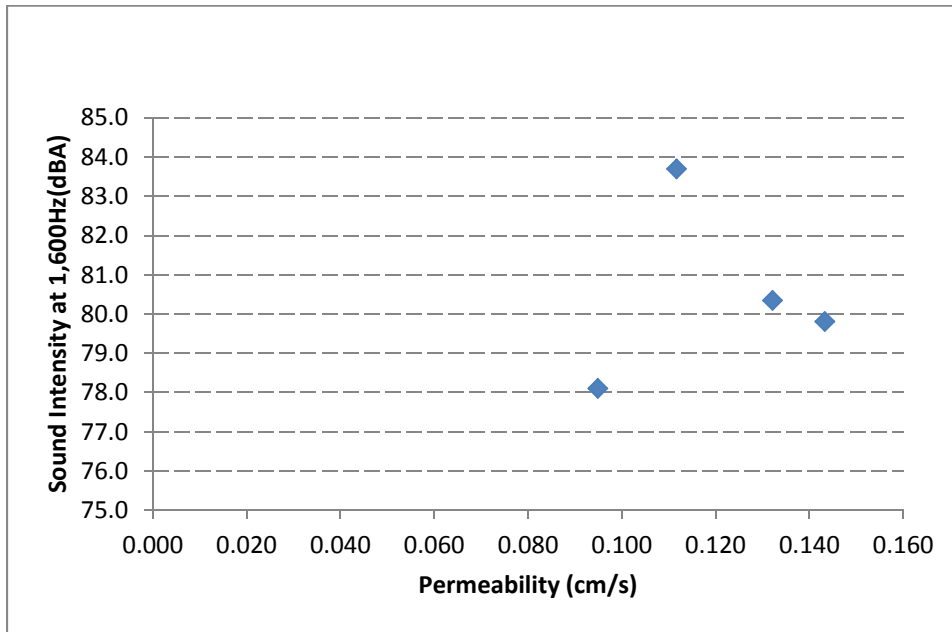
Figure 4.13: Relationship between surface macrotexture and sound intensity at 800 Hz.



(a)



(b)



(c)

Figure 4.14: Relationship between permeability and sound intensity at (a) 1,000 Hz, (b) 1,250 Hz, and (c) 1,600 Hz.

4.1.7 Summary of Surface Texture and Noise Measurements on HVS Test Track

A summary comparing the noise and surface texture measurements on the untrafficked surfaces of the different OGFC mixes to the control mix is shown in Table 4.17. In addition, Figure 4.15 shows the surface friction measurements on the untrafficked test sections made with both the CST and DFT, and Figure 4.16 shows MPD measured by both the CTM and LTS. These figures and tables allow for the following observations:

- All three mixes had lower MPDs, quieter surfaces, and the same or longer outflow times than the control mix. The MPD values for the #4P mixes were approximately 1.1 mm compared with 1.8 mm for the control mix and 1.5 mm for the Georgia 1/2 inch mix. The values for the #4P mixes are within the range of 0.9 to 1.6 mm measured using an inertial profiler on new OGFC and rubberized open-graded mixes across the state as part of the asphalt pavement noise study [1]. The value for the control mix built for this study is high compared to values statewide for similar mixes. The MPD values for the #4P mixes are higher than the 0.4 to 0.7 mm measured on new dense-graded asphalt mixes as part of the same statewide survey.
- The differences in overall OBSI between the control mix and the #4P mixes are between 0.8 and 1.6 dBA, which should be at most minimally perceptible to humans. However, the change in the high frequency content will likely be perceptible.

- Compared to the control mix, all three mixes had higher DFT-measured surface friction. On the other hand, CST measurements indicated that the #4P mix with PG 76-22PM binder had higher friction compared to the control, while the #4P mix with PG 64-16 binder and the Georgia 1/2 inch mix had lower friction than the control.
- While there appears to be some influence of binder type on the friction of the #4P mixes, the differences are not statistically significant.

Table 4.17: Summary of Surface Texture and Noise Measurements on Untrafficked Surfaces of Different OGFC Mixes Relative to Control Mix

Measurement Type	Device	#4P Mix w/ PG 76-22PM	#4P Mix w/ PG 64-16	Georgia 1/2 inch Mix w/ PG 58-34PM
Surface friction	CST	Higher*	Lower*	Lower*
	DFT	Higher*	Higher*	Higher*
Macrotexture (MPD)	CTM	Lower*	Lower*	Lower*
	LTS	Lower*	Lower*	Lower*
Outflow time	OFT	Longer*	Longer*	Same
Tire/pavement noise	OBSI vehicle	Quieter*	Quieter*	Quieter

* Indicates statistically significant difference.

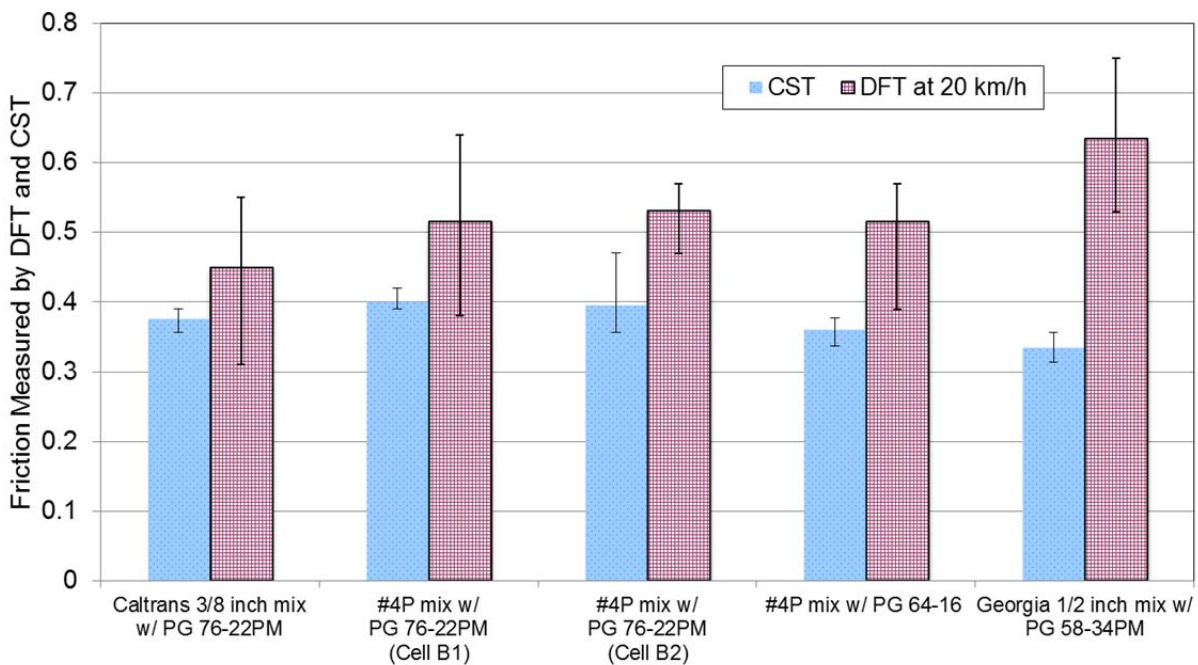


Figure 4.15: Surface friction as measured by the CST and DFT on untrafficked surfaces.

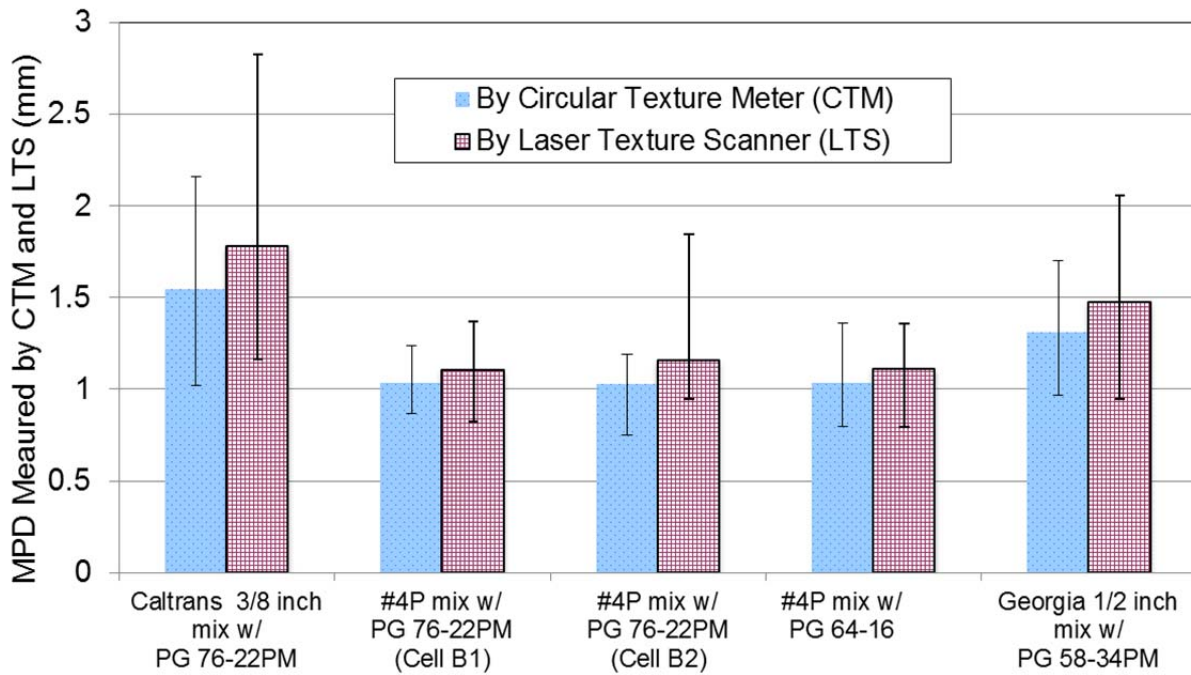


Figure 4.16: Mean profile depth measured by CTM and LTS on untrafficked surfaces.

4.2 Laboratory Test Results

Surface texture measurements were taken on ingot specimens compacted on the day of construction using loose mix sampled from the supply trucks. *Note:* no ingot specimens were prepared using the Georgia 1/2 inch mix because of the problems encountered during construction. DFT-measured surface friction, CTM- and LTS-measured macrotextures, and outflow time measured with the OTF are shown in Figure 4.17 to Figure 4.19 respectively. Error bars in these figures indicate maximum and minimum measurements.

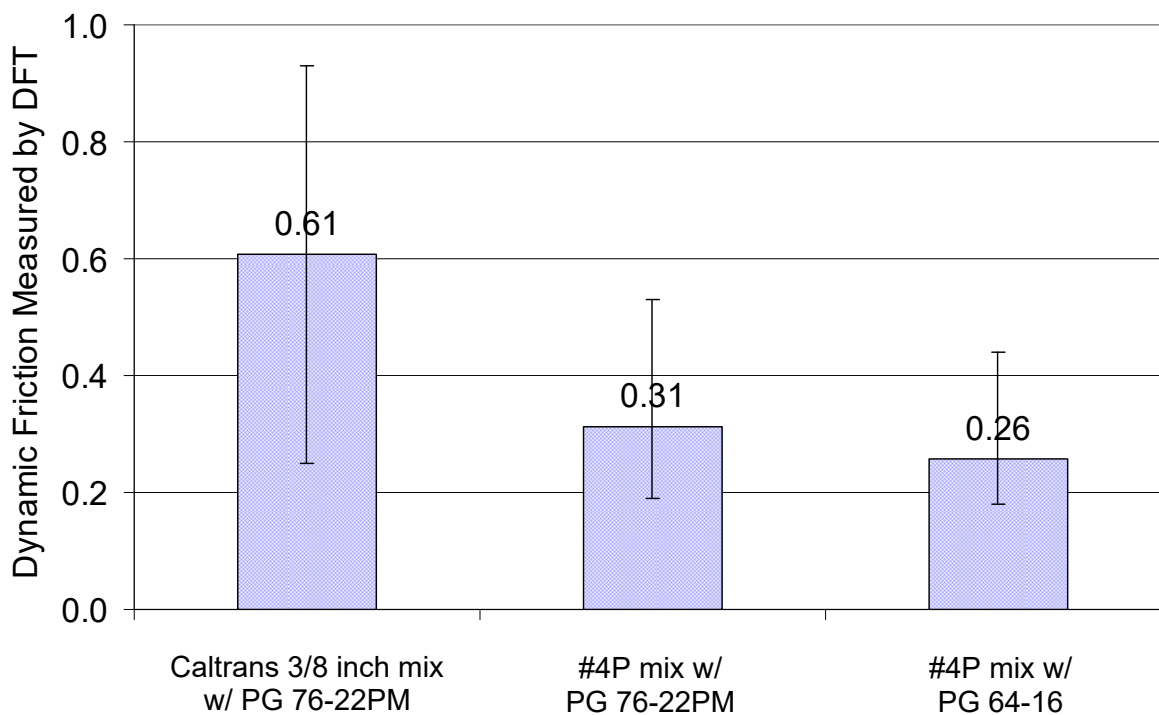


Figure 4.17: Coefficients of friction measured on ingot specimens using the DFT.

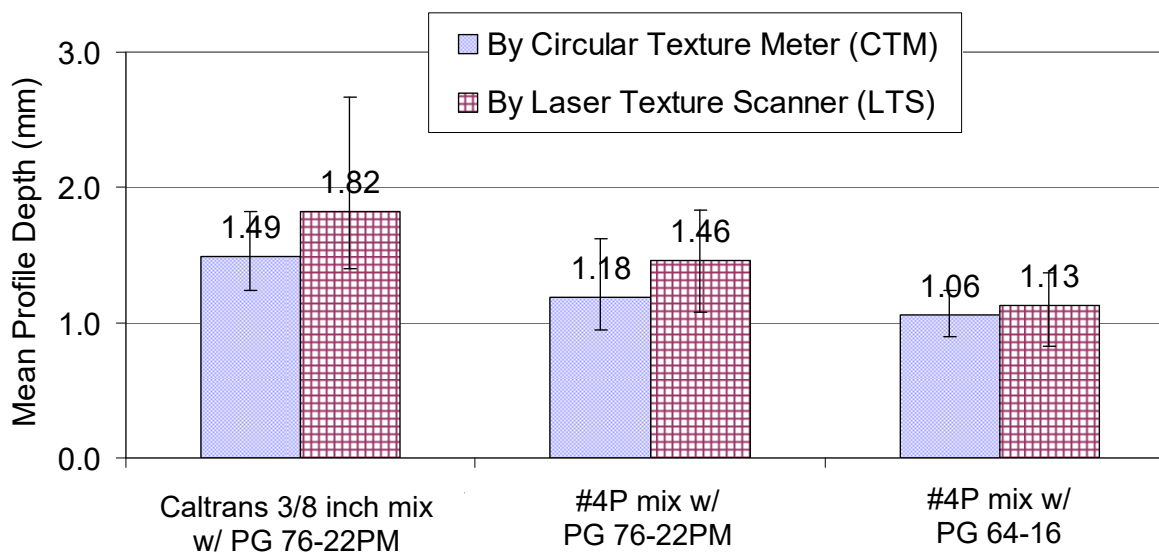


Figure 4.18: Mean profile depths measured on ingot specimens by both CTM and LTS.

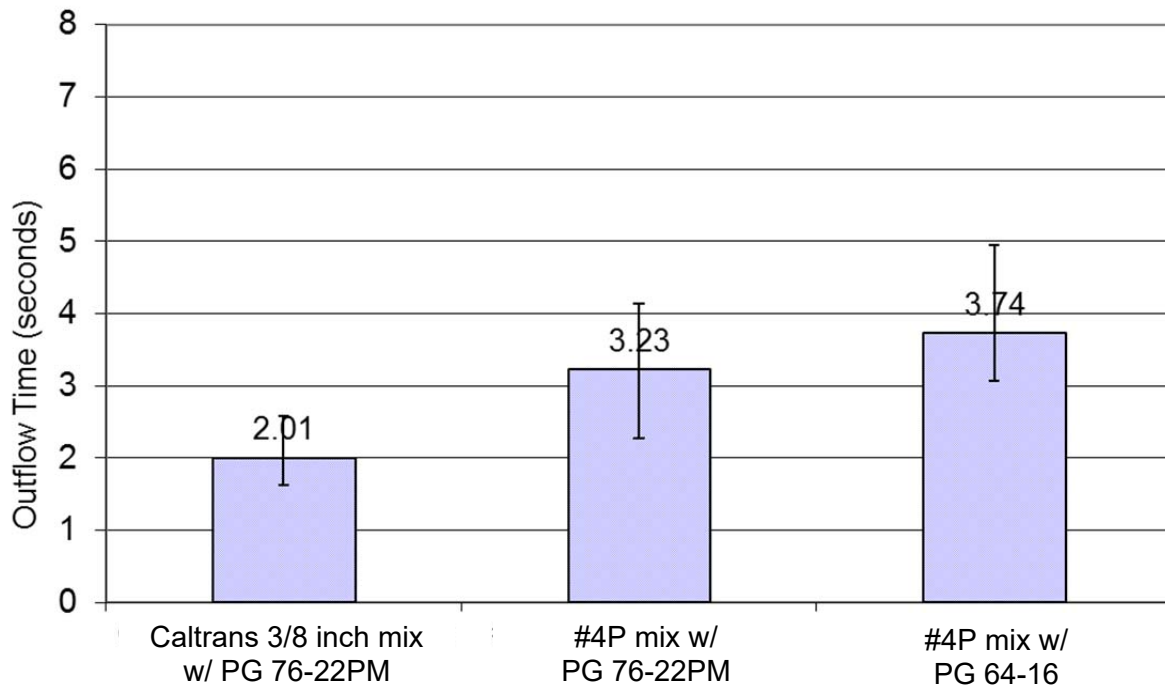


Figure 4.19: Outflow time on ingot specimens measured by the OTF.

Although statistical testing indicates that the differences among the different mixes shown in Figure 4.17 to Figure 4.19 are significant, it is believed that the difference between the two #4P mixes are within measurement errors and are practically negligible. The surface texture measurements from the ingot specimens confirms all of the relevant findings based on measurements taken from the HVS test track (see Table 4.17) except the following:

- Measurements taken on the ingot specimens showed that all the #4P mixes had lower dynamic friction than the control mix, whereas measurements taken on the HVS test track indicate otherwise. This result indicates that some caution should be taken when determining friction based on laboratory-compacted specimens.

5 MOISTURE DAMAGE SUSCEPTIBILITY TEST RESULTS

This chapter presents what was learned from two pilot HVS tests conducted to evaluate the moisture damage susceptibility of the different OGFC mixes. As mentioned in Section 3.3.2, it was found from the two pilot tests that moisture damage could not be induced by HVS trafficking without first causing severe structural failure in the pavements. A decision was therefore made to cancel the remaining moisture damage susceptibility tests.

Both test sections, 652HC and 662HC, were located in Cell A (see Table 3.1 and Figure 3.1), which had the control mix (Caltrans 3/8 inch mix with PG 76-22PM binder).

5.1 Section 652HC: The First Pilot Test

The environmental conditions and loading program for Section 652HC are described in Section 3.3.6. In summary, a total of 178,200 load repetitions at a load level of 40 kN were applied using the HVS between January 25, 2012 and February 14, 2012, with a traffic pattern that included wander. Unheated tap water was fed into the water tank. Pavement temperature was not controlled.

5.1.1 Temperature

Figure 5.1 shows the average hourly air and pavement temperatures during HVS testing period for Section 652HC, and Figure 5.2 shows the test sections' average daily temperatures. The averaging includes all of the temperatures measured irrespective of whether the HVS was running because pavement temperature was not controlled in this test. Figure 5.2 shows that the daily average pavement temperatures ranged between 50°F (10°C) and 59°F (15°C), with a daily variation of 9 to 13°F (6 to 8°C) depending on the measurement depth.

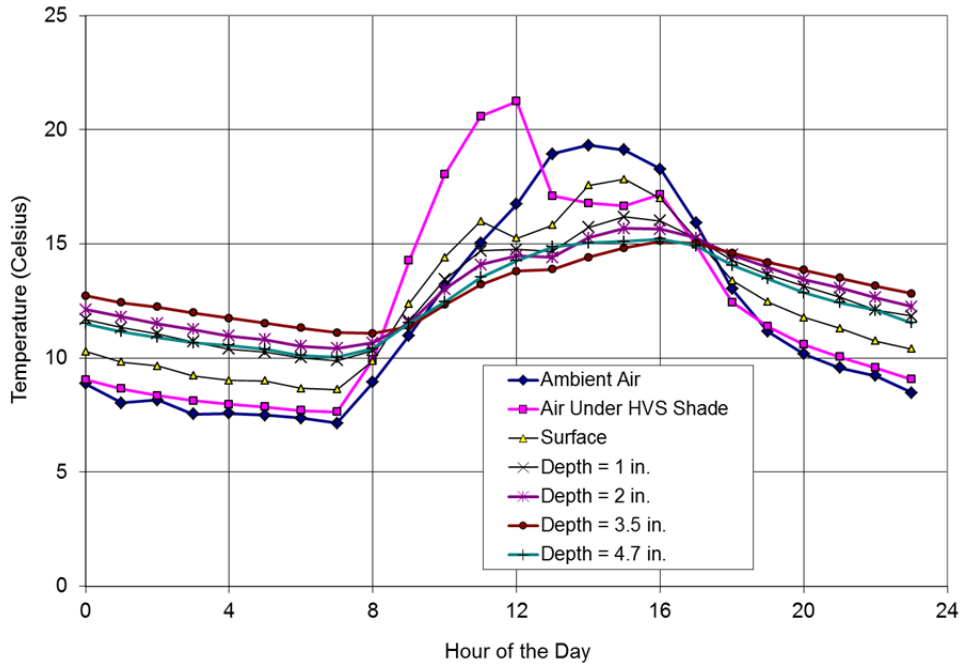


Figure 5.1: Average hourly temperatures for Section 652HC. (Dual wheel, Caltrans 3/8 inch mix with PG 76-22PM binder).

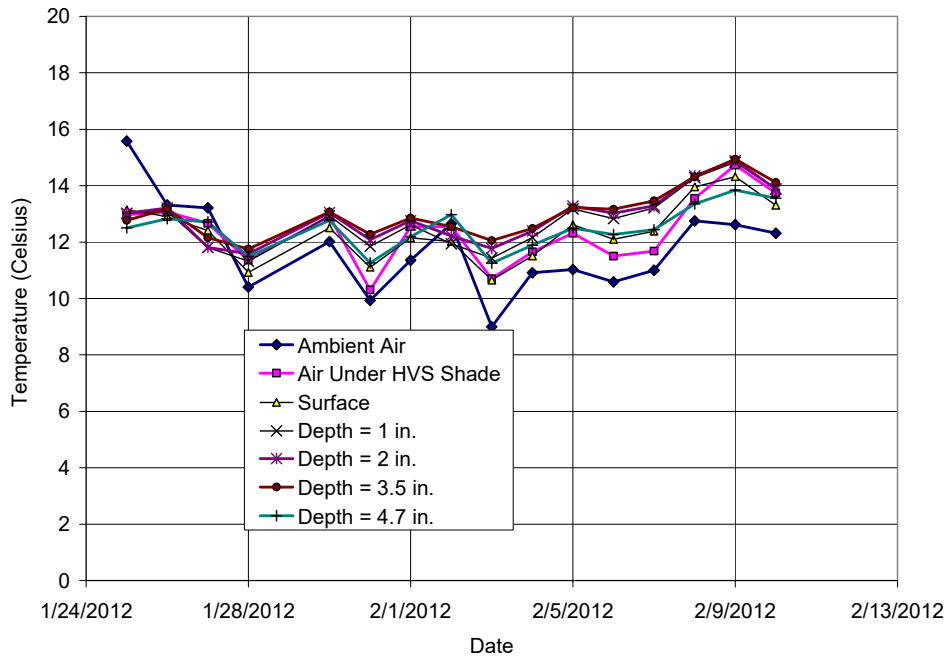


Figure 5.2: Average daily temperatures during HVS testing for Section 652HC. (Dual wheel, Caltrans 3/8 inch mix with PG 76-22PM binder.)

5.1.2 Permanent Deformation

The accumulation of maximum total rut (MTR, as defined in Figure 3.3) with load repetitions for Section 652HC is shown in Figure 5.3. As the figure shows, the rut accumulation rate accelerated after 50,000 load repetitions. Rutting also increased dramatically between the last two measurements, which corresponded with the appearance of significant cracking on the surface.

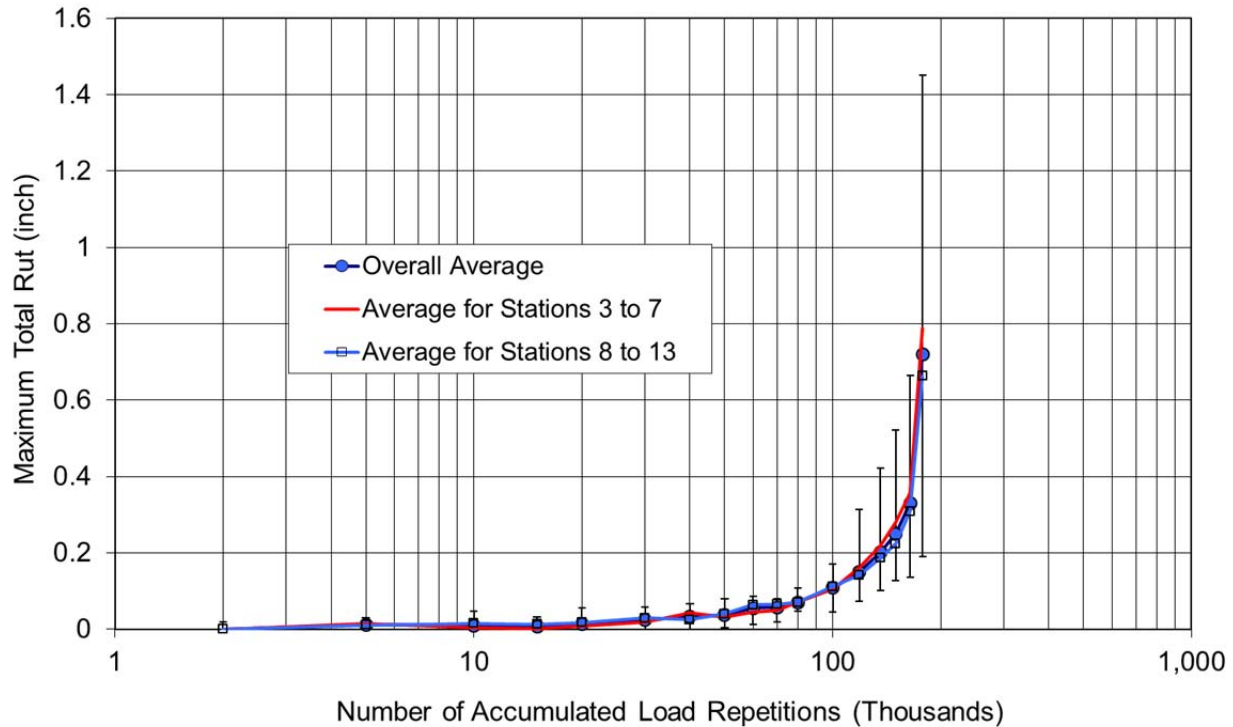


Figure 5.3: Accumulation of maximum total rut with load repetition for Section 652HC. (Caltrans 3/8 inch mix with PG 76-22PM binder.)

5.1.3 Visual Evaluation

The surface of Section 652HC after completion of HVS trafficking appears in Figure 5.4. It shows that the pavement failed by severe subgrade rutting, which in turn led to severe cracking in both the OGFC and the underlying HMA layer. No moisture damage was visible.



(a) Overall view of the failed pavement



(b) A closer look at the test section



(c) Severe cracking and punch down near Station 7



(d) Signs of subgrade rutting and crack initiation near Station 13 but no moisture damage in the asphalt

Figure 5.4: Photos of HVS Test Section 652HC after HVS trafficking showing cracking and subgrade rutting but no moisture damage in the OGFC surface layer.

5.1.4 Summary of Test Results

After application of 178,200 repetitions of 40 kN loading on Section 652HC, no moisture damage was observed on the OGFC surface layer. The pavement failed by severe subgrade rutting that led to severe cracking in both the OGFC layer and the underlying HMA layer. In other words, the pavement failed structurally before noticeable moisture damage to the OGFC layer occurred.

5.2 HVS Test Results for Section 662HC: The Second Pilot Test

Based on observations from Section 652HC, a second pilot test was run to see whether moisture damage could be induced by HVS trafficking before structural failure occurred. The findings from the earlier test indicated that the HVS wheel load needed to be reduced while the moisture attack needed to be more aggressive. Accordingly, the following adjustments were made with respect to the environmental condition and loading programs:

- The HVS wheel load was reduced to 4.5 kips (20 kN) from 9 kips (40 kN).
- Water was heated to a target water temperature of 77°F (25°C) so it would be damaging to the asphalt binder/aggregate interface without inducing unwanted rutting.
- Water was ponded to keep the OGFC constantly soaked.

More aggressive measures, such as adding chemicals to the water, were not adopted because they do not represent realistic scenarios typical on highways. The HVS trafficking was applied between February 22, 2012 and March 26, 2012, with a total of 447,500 load repetitions.

5.2.1 Temperature

Figure 5.5 shows the average hourly air and pavement temperatures for Section 662HC during the HVS testing period. Figure 5.6 displays the average daily temperatures for the section during testing and shows that daily average pavement temperatures ranged between 50°F (10°C) and 64°F (18°C), with a daily variation of 9 to 13°F (6 to 8°C) depending on the measurement depth. The average pavement temperatures were slightly higher than those for Section 652HC, indicating that the heated water had a minimal effect on the pavement temperature.

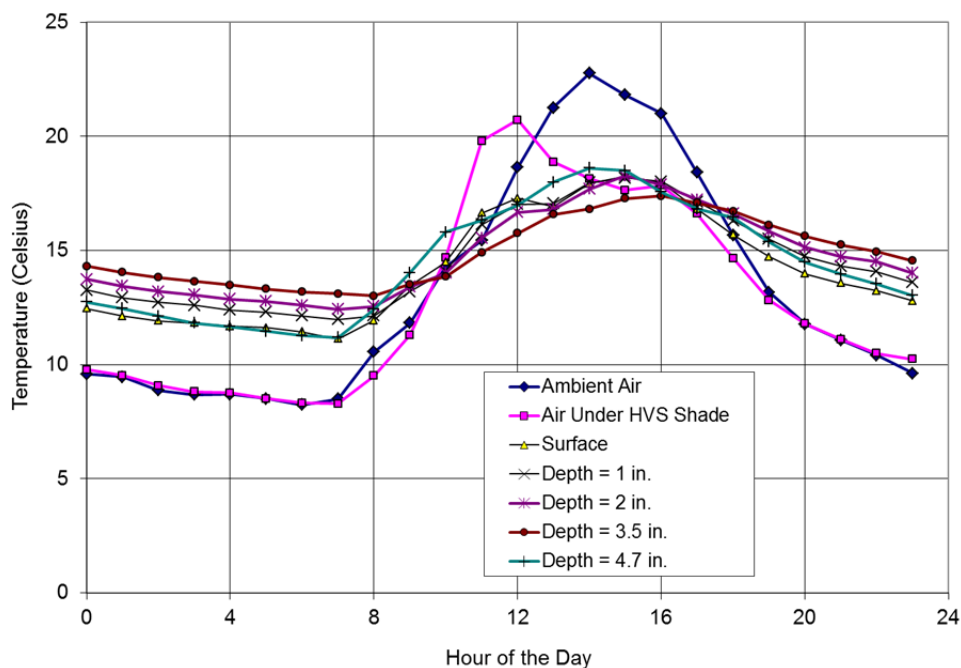


Figure 5.5: Average hourly temperatures for Section 662HC. (Dual wheel, Caltrans 3/8 inch mix with PG 76-22PM binder.)

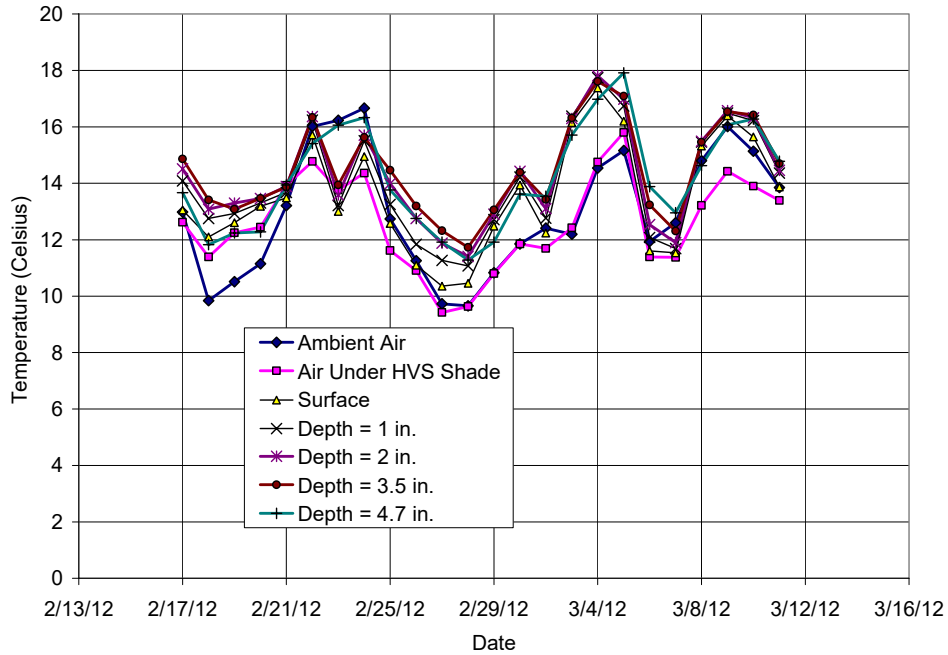


Figure 5.6: Average daily temperatures during HVS testing for Section 662HC. (Dual wheel, Caltrans 3/8 inch mix with PG 76-22PM binder.)

The effect of the heater on water temperature can be seen in Figure 5.7, which shows the average hourly water temperatures during HVS testing for Section 662HC grouped according to whether or not the HVS was operating and the heater was on. The figure shows that the heater maintained the water temperature between 77°F and 86°F (25°C and 30°C) most of the time.



**Figure 5.7: Average hourly water temperatures during HVS testing for Section 662HC grouped by HVS and heater status.
(Section 662HC: dual wheel, Caltrans 3/8 inch mix with PG 76-22PM binder.)**

5.2.2 Permanent Deformation

The accumulation of maximum total rut (MTR, as defined in Figure 3.3) with load repetitions for Section 662HC is shown in Figure 5.8. As the figure shows, the rate of rut accumulation accelerated after 200,000 load repetitions. The pavement had only 0.2 inches of average maximum total rut (AMTR) and did not reach the rutting failure criterion (defined as 0.5 in. of AMTR) by the end of the test.

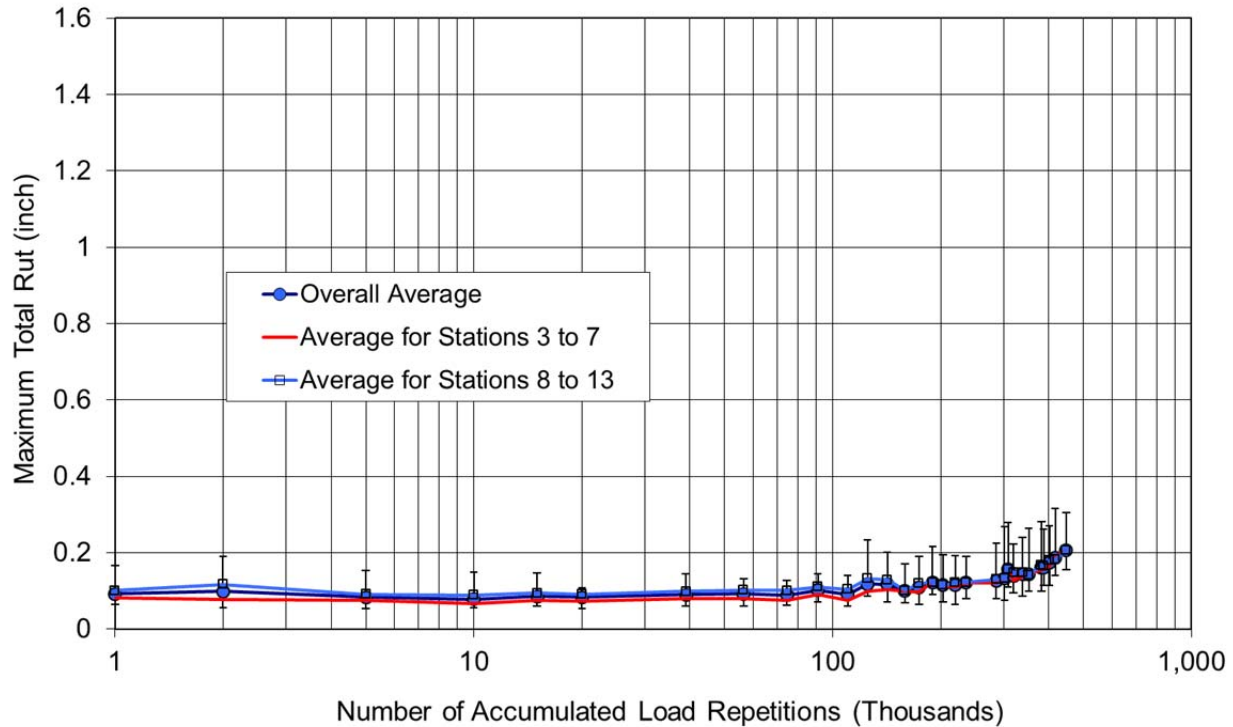


Figure 5.8: Accumulation of maximum total rut with load repetitions for Section 662HC. (Caltrans 3/8 inch mix with PG 76-22PM binder.)

5.2.3 Visual Damage

Figure 5.9 shows the pavement surface of Section 662HC after the completion of HVS trafficking. Figure 5.9b shows where raveling occurred on the OGFC layer due to the use of Ecoflex sealant when permeability measurements were taken. The raveling was initiated by removal of the cured sealant from the pavement surfaces, i.e., the force required to remove the sealant also loosened the aggregates in the OGFC layer. Subsequent HVS trafficking caused the OGFC layer to ravel in the affected area. Other than this unintended raveling, there were no signs of moisture damage or structural failure. Figure 5.9c and Figure 5.9d provide a visual comparison of the surface texture before and after HVS trafficking, and they indicate that there were no noticeable changes.



(a) Overall view of the test section



(b) Damage caused by the use of Ecoflex sealant



(c) Picture at Station 10 before HVS Trafficking



(d) Picture at Station 10 after HVS trafficking

Figure 5.9: Photos of HVS Test Section 662HC after HVS trafficking showing no sign of moisture damage in the OGFC surface layer other than that caused by the removal of Ecoflex sealant while taking permeability measurements.

5.2.4 Summary of Test Results

After five weeks of HVS trafficking with reduced load and heated water that was ponded at a level flush with the pavement surface, no signs of moisture damage were visible in the OGFC layer. The reduced load resulted in a much slower rate of rut accumulation compared to Section 652HC (the first pilot test). Although a heater raised the water temperature to between 77°F and 86°F (25°C and 30°C), the pavement temperatures were only slightly higher than those recorded on Section 652HC. The heated water and ponding were found to be insufficient to induce moisture damage when combined with HVS trafficking.

5.3 Summary of HVS Testing for Moisture Susceptibility

Two pilot HVS tests were conducted to investigate whether it was possible to induce moisture damage in the OGFC surface layer before the pavement failed structurally (i.e., through rutting and/or fatigue cracking).

In the first pilot test, on Section 652HC, a total of 178,200 load repetitions were applied at a 9 kips (40 kN) load level with unheated water flowing over the pavement. The pavement failed due to severe subgrade rutting with no noticeable moisture damage in the form of raveling.

A second pilot test was conducted, on Section 662HC, with adjustments to the environmental conditions and testing programs used in the first pilot test. Specifically, the HVS load was reduced to 4.5 kips (20 kN), and the flowing water was heated to between 77°F and 86°F (25°C and 30°C) and ponded at a level flush with pavement surface. After 447,500 HVS load repetitions, these new conditions were still insufficient to induce moisture damage.

It was concluded from these two pilot tests that the HVS was unsuitable for inducing moisture damage in the OGFC surface layer. As a result, the remaining HVS tests for evaluating moisture damage susceptibility were cancelled.

6 PERMEABILITY AND CLOGGING EVALUATION RESULTS

6.1 Material Characteristics

Table 6.1 identifies the mix types, dust gradation, type of testing, and air-void contents for the cores used in the clogging studies. Note that the air-void contents listed are for the entire core, which includes the OGFC and HMA layers.

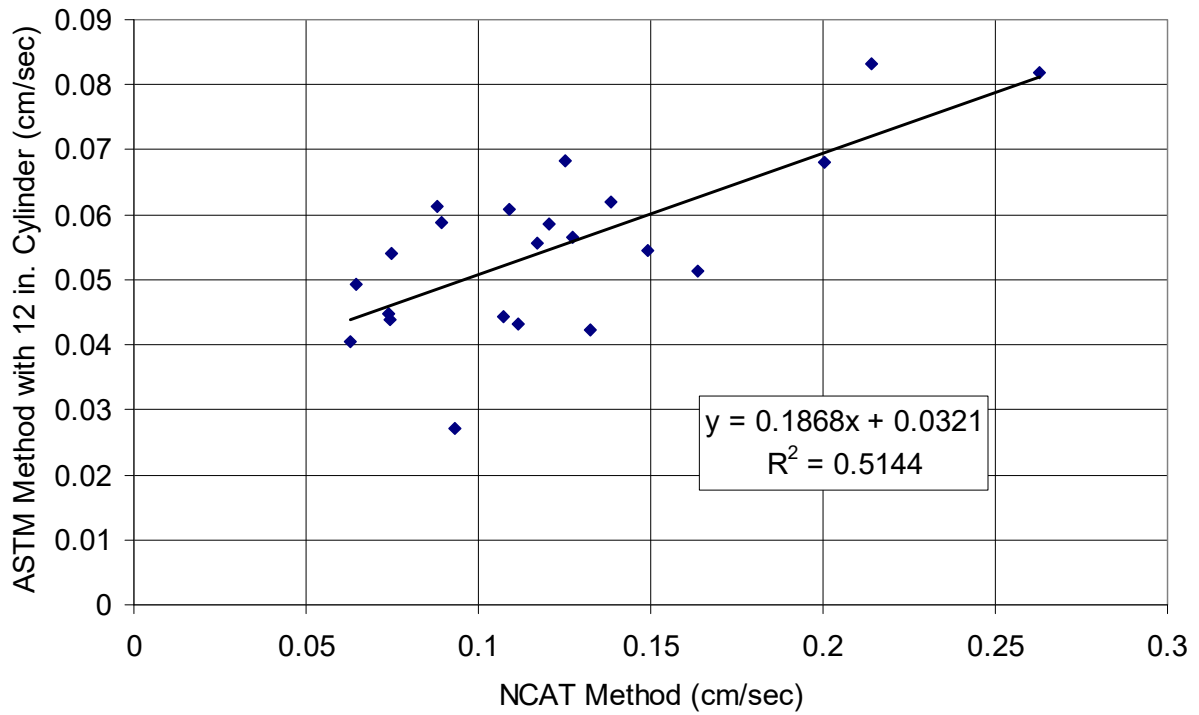
Table 6.1: Measured Air-Void Content of Cores Used for X-Ray CT Imaging

Mix Type	Sample ID	Gradation of Dust Put on Surface	Test Type	AV (%) ¹
Caltrans 3/8 inch mix w/ PG 76-22PM	1-653	<600 micron, wet	Rainfall simulation	11.04
#4P mix w/ PG 76-22PM	1-655	<600 micron, wet	Rainfall simulation	12.13
#4P mix w/ PG 64-16	1-657	<600 micron, wet	Rainfall simulation	13.61
Caltrans 3/8 inch mix w/ PG 76-22PM	2-653	<38 micron, wet	Rainfall simulation	13.29
#4P mix w/ PG 76-22PM	2-655	<38 micron, wet	Rainfall simulation	11.80
#4P mix w/ PG 64-16	2-657	<38 micron, wet	Rainfall simulation	13.43
Caltrans 3/8 inch mix w/ PG 76-22PM	3-653	<38 micron, dry	Rutting	13.94
#4P mix w/ PG 76-22PM	3-655	<38 micron, dry	Rutting	13.61
#4P mix w/ PG 64-16	3-657	<38 micron, dry	Rutting	13.67

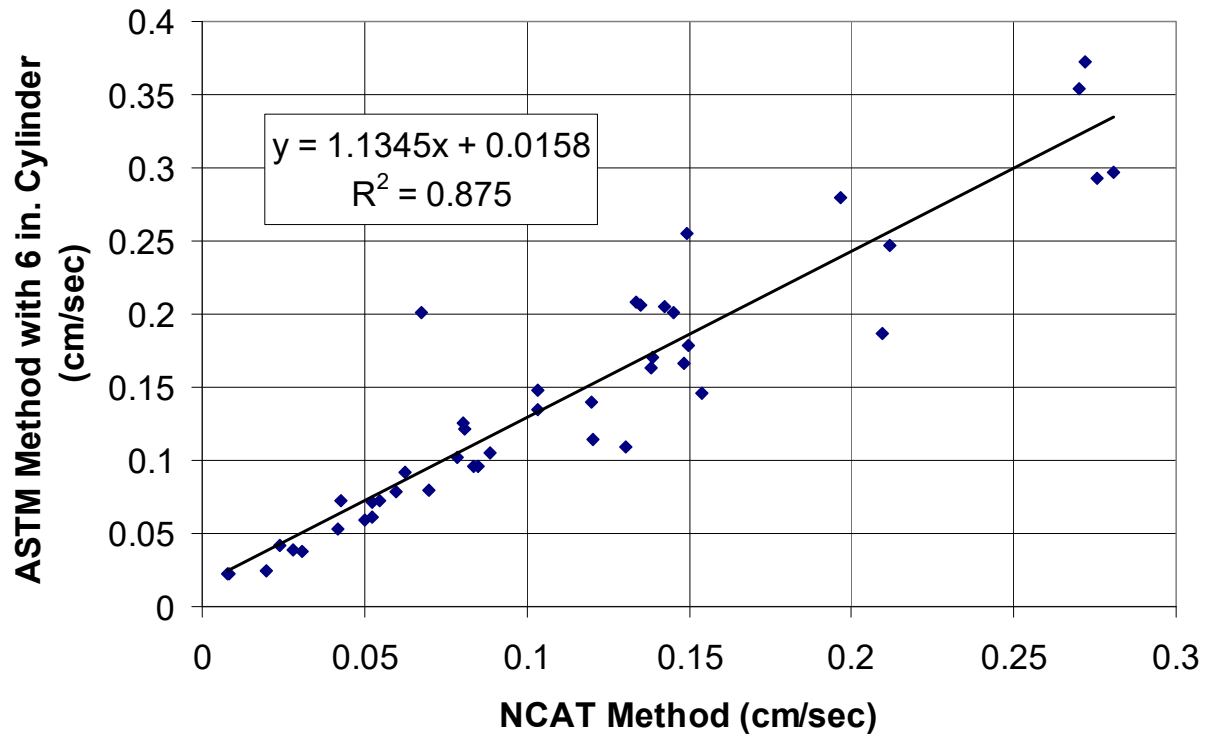
¹ Air-void content of the cores includes both the OGFC and HMA layers.

6.2 Correlation of Permeability Results Measured by ASTM and NCAT Methods

As indicated in Section 3.7.3, permeability measurements were made using both the NCAT permeameter and the ASTM 1701 method. The NCAT permeameter was originally developed for use on asphalt pavement and the ASTM method for use on concrete pavement, although this should not have any bearing on the measured results. The ASTM measurements were made using both the standard ring size (300 mm) and a modified ring size (150 mm). The measured permeability values obtained by the NCAT and ASTM methods were highly correlated for the two different ring sizes for all test sections (see Figure 6.1a). In general, the permeability values measured by the ASTM method with the standard ring size were about 50 percent larger than those measured with the NCAT permeameter (with an R^2 of 0.51). However, when the ASTM-modified ring size (150 mm) was used, permeabilities for the NCAT and ASTM methods were close, with a significantly higher correlation ($R^2=0.88$). This result suggests that ring size controlled the measured permeability. Since the NCAT and ASTM modified ring size permeameters have equal diameters, their permeability measurements appear to be close and highly correlated.



(a) ASTM method using standard cylinder size (12 in.) versus NCAT



(b) ASTM method using modified cylinder size (6 in.) versus NCAT

Figure 6.1: Correlation between the permeability values measured by the ASTM and NCAT methods with standard 12 in. (300 mm) and modified 6 in. (150 mm) cylinder sizes.

From Figure 6.1 it can be concluded that: (1) both methods are useful for permeability measurement and (2) the ASTM method provides a slightly higher permeability reading of the pavement surface than the NCAT method when both methods use a cylinder with a six inch diameter.

Note that in this study, the focus was on the relative permeability of different the OGFC mixes compared to the control mix, Caltrans 3/8 inch mix w/ PG 76-22PM. That is, the relative change in permeability was more important than the absolute values.

6.3 Permeability Before HVS Trafficking

Permeability of the different OGFC mixes measured on the HVS test track before HVS trafficking are plotted in Figure 6.2, with their statistics listed in Table 6.2. The results from both NCAT and ASTM measurements indicate the following:

- The two #4P mixes had roughly the same permeability as the control mix, while the Georgia 1/2 inch mix had much higher permeability than the control mix.
- Permeability measurements are highly variable. Although most of the COV values (coefficient of variance) on the different mixes was less than 0.5, COV for measurements taken on the Caltrans control mix was as high as 1.03.

It is believed that the greater thickness (0.15 ft) used for the Georgia 1/2 inch mix was the main reason it had significantly higher permeability compared to all the other OGFC mixes, whose layer thicknesses were between 0.05 and 0.07 ft (see Table 2.9).

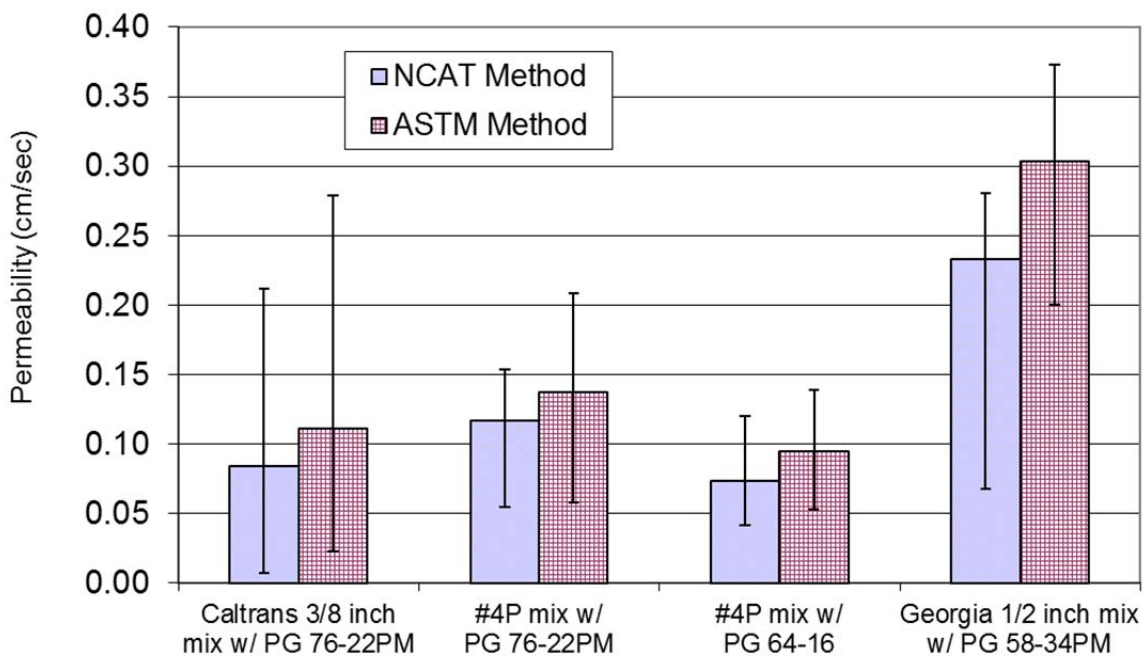


Figure 6.2: Permeability for different OGFC mixes before HVS trafficking.

Table 6.2: Statistics of Permeability for Different OGFC Mixes before HVS Trafficking

Method	Quantity	Caltrans 3/8 inch Mix w/ PG 76-22PM	#4P Mix w/ PG 76-22PM	#4P Mix w/ PG 64-16	Georgia 1/2 inch Mix w/ PG 58-34PM
NCAT	Avg.	0.084	0.103	0.074	0.233
	Count	11	20	11	5
	Std. Dev.	0.087	0.046	0.024	0.093
	COV	1.03	0.45	0.32	0.40
ASTM	Avg.	0.112	0.138	0.095	0.304
	Count	11	22	11	5
	Std. Dev.	0.106	0.049	0.032	0.067
	COV	0.95	0.35	0.34	0.22

6.4 Rutting and Airborne Dust-Related Clogging

6.4.1 Visual Indication

It is expected that rutting caused by HVS trafficking will affect pavement permeability. In this study, this phenomenon is referred to as *rutting-related clogging*. A 0.17 in. (4.3 mm) rain event on March 13, 2012, at Davis, California, led to a clear visual indication of rutting-related clogging. Figure 6.3 shows photos of two HVS test sections during the rain. Both sections had been tested with the HVS and had about 0.5 inches of total rut. The rutted portion of Section 651HB (0.15 ft of Georgia 1/2 inch mix with PG 58-34PM binder [Figure 6.3a]) drained well and showed no signs of standing water on its surface. On the other hand, the rutted area in the wheelpath created by the NGWBT on Section 669HB (0.07 ft of #4P mix with PG 76-22PM binder) drained poorly and filled with standing water. The fact that the unrutted area of Section 669HB (Figure 6.3b) still drained properly indicates that the clogging was due to rutting.



(a) 651HB: Georgia 1/2 inch mix with PG 58-34PM binder, OGFC thickness = 0.15 ft



(b) Section 669HB: #4P mix with PG 76-22PM binder, OGFC thickness = 0.07 ft

Figure 6.3: Surface photos of two sections previously tested with the HVS showing different residual permeability during a 0.17 in. (4.3 mm) rain.

6.4.2 *Effect of Rutting on Permeability*

The variation of normalized residual permeability with a normalized number of load repetitions is shown in Figure 6.4, in which the permeability was normalized by the corresponding initial readings while load repetitions were normalized by the rutting life for each section shown in Table 7.1. In addition, Figure 6.5 shows the normalized residual permeability with the average maximum total rut. The following observations are made from the figures:

- In general, 20 to 30 percent of permeability was lost during the first 10 percent of rutting life (Figure 6.4). In the worst case (667HB: #4P mix with PG 64-16 binder), 60 percent of the permeability was lost in the first 5 percent of rutting life.
- The normalized permeability roughly decreased linearly with the amount of rut (Figure 6.5), although the rate at which it decreased was not constant across the different test sections.

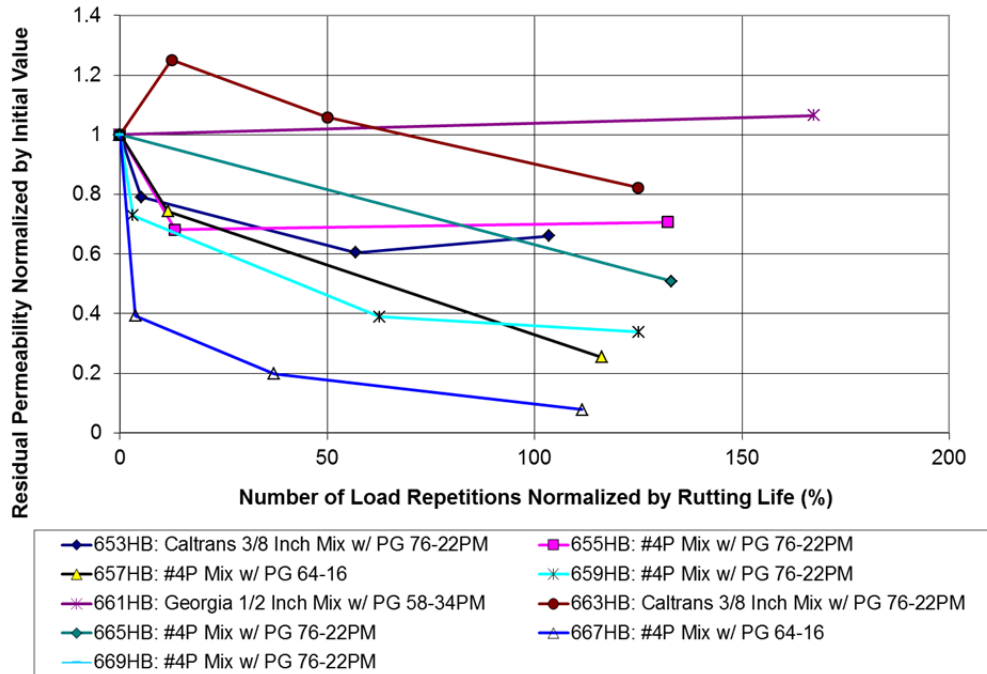


Figure 6.4: Variation of normalized residual permeability measured with the NCAT method with a normalized number of load repetitions for each test section. (No data were available for Section 651HB.)

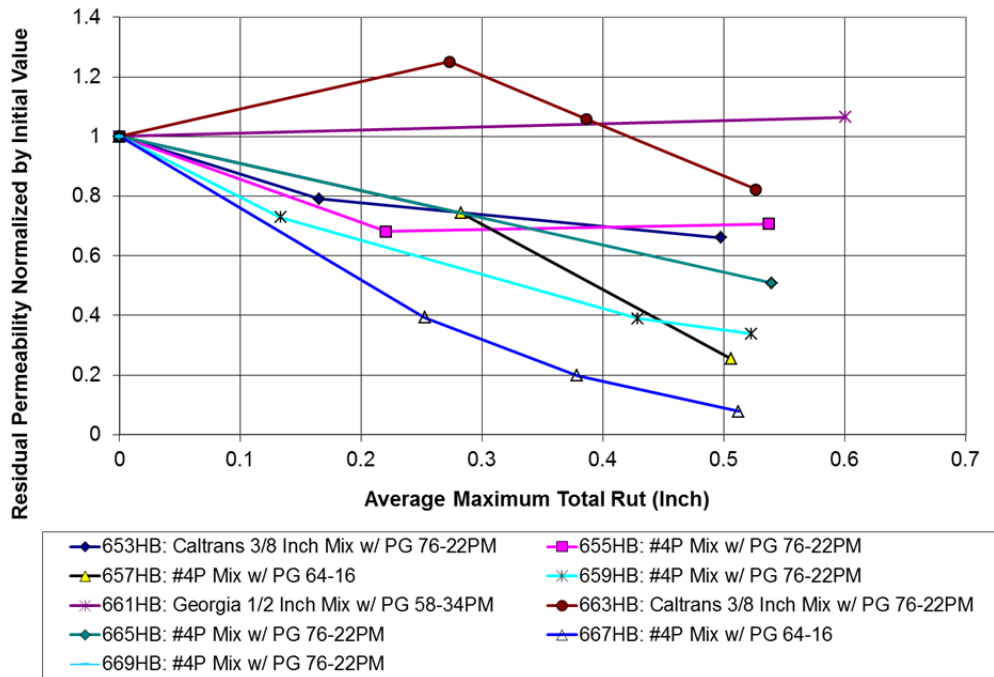


Figure 6.5: Variation of normalized residual permeability measured with the NCAT method with average maximum total rut for each test section. (No data were available for Section 651HB.)

Figure 6.6 shows the average percent reduction in permeability caused by HVS-induced rutting grouped by OGFC mix type. The two #4P mixes show greater reduction in permeability (i.e., clogging) than the control mix (Caltrans 3/8 inch mix with PG 76-22PM binder), while the Georgia mix shows roughly the same as or less clogging than the control.

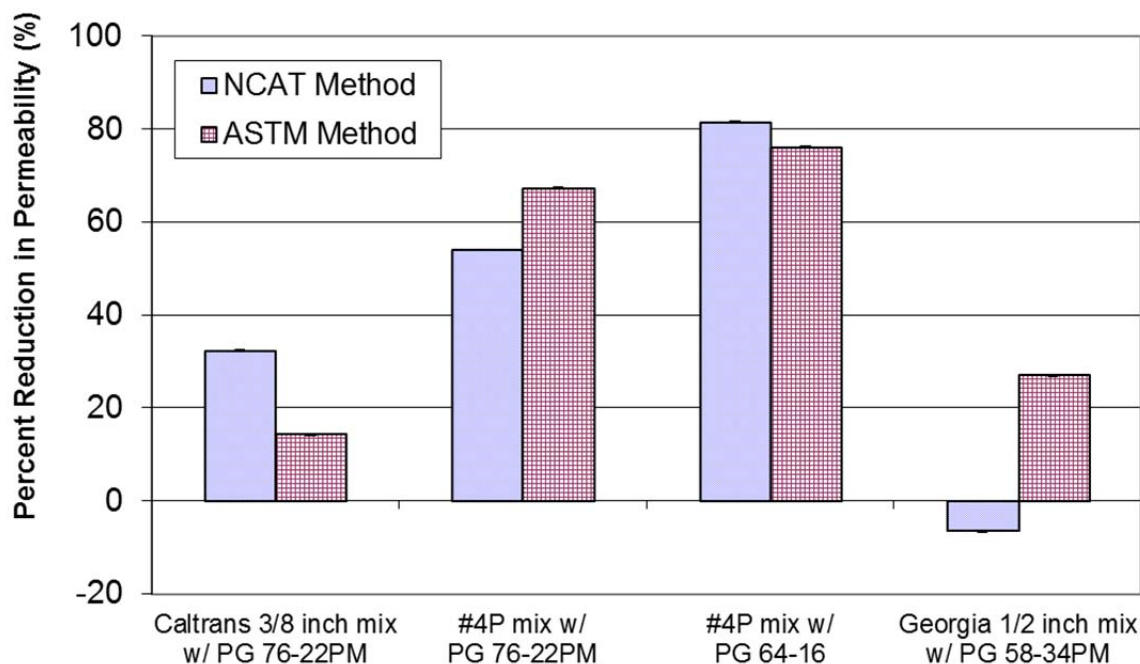


Figure 6.6: Percent reduction in permeability for the different OGFC mixes after HVS trafficking, which led to approximately 0.5 in. of average maximum total rut.

6.4.3 Effect of Airborne Dust on Permeability Reduction

Figure 6.7 shows a comparison of percent permeability reductions measured by both the NCAT and ASTM methods under different conditions with respect to airborne dust application. The figure shows that there was no consistent effect of airborne dust application on the reduction in permeability. With this finding, it can be concluded that the reduced permeability was mostly due to rutting-related clogging.

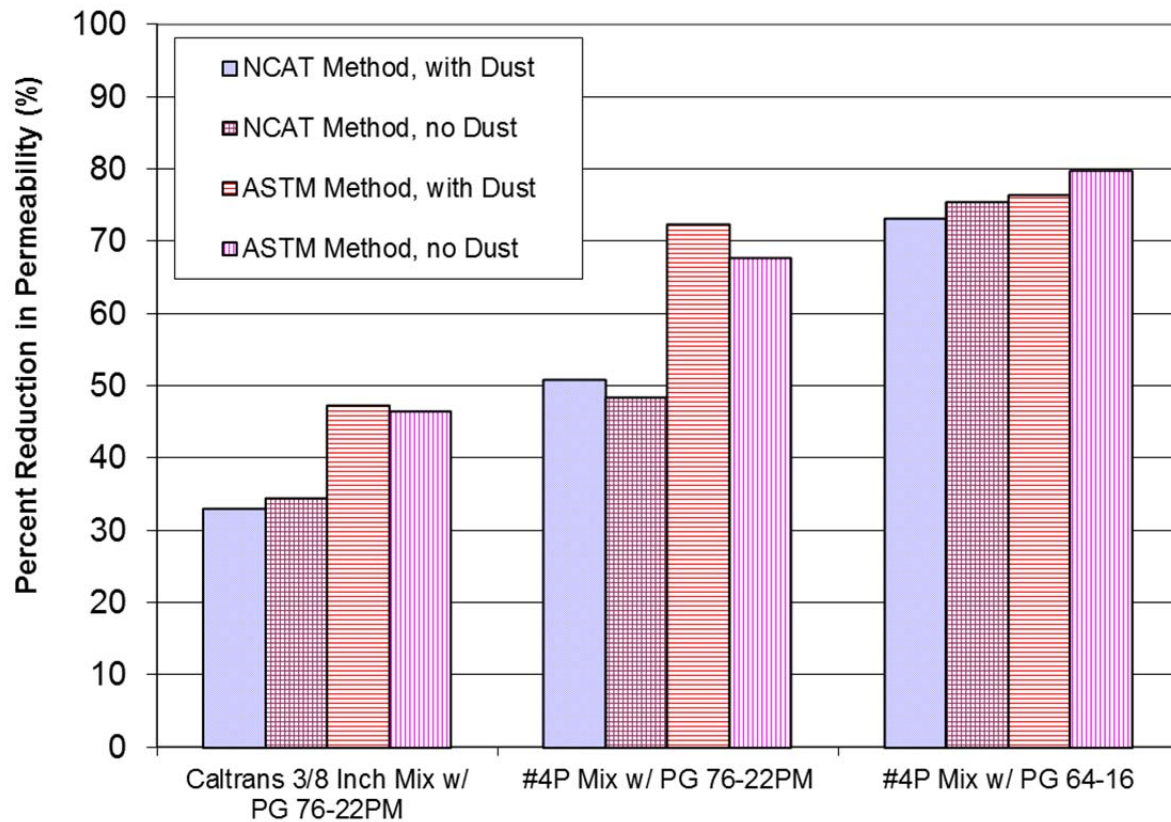


Figure 6.7: Comparison of percent reductions in permeability measured by both the NCAT and ASTM methods under different conditions with respect to airborne dust application.

6.4.4 Change in Air-Void Content and Distribution

Figure 6.8 shows the HVS-induced rutting-related changes in air void profiles of three core samples. The figure is based on x-ray CT images that were taken on the same cores both immediately before and after HVS trafficking. The reductions in air-void content shown were obtained by subtracting the air-void contents measured after testing from those measured before testing. The figure shows that there were significant reductions in OGFC layer air-void contents after the rutting tests. In addition, it can be seen that while higher levels of air void reduction were accumulated at the bottom of the open-graded layers, there was also noticeable air void reduction in the upper part of the layers. The residual air-void content of the OGFC layers after HVS testing generally ranged from 10 percent to 30 percent.

The average percent reduction in air-void contents for the OGFC layers of Sections 653HB (Caltrans 3/8 inch mix with PG 76-22PM binder), 655HB (#4P mix with PG 76-22PM binder), and 657HB (#4P mix with PG 64-16 binder) were calculated to be 8.2 percent, 8.8 percent, and 10.9 percent, respectively. The normalized residual permeability for Sections 653HB, 655HB, and 657HB was 0.66, 0.71, and 0.25, respectively. The greater air void reduction for Section 657HB is believed to be the main reason it lost more permeability than the other two sections.

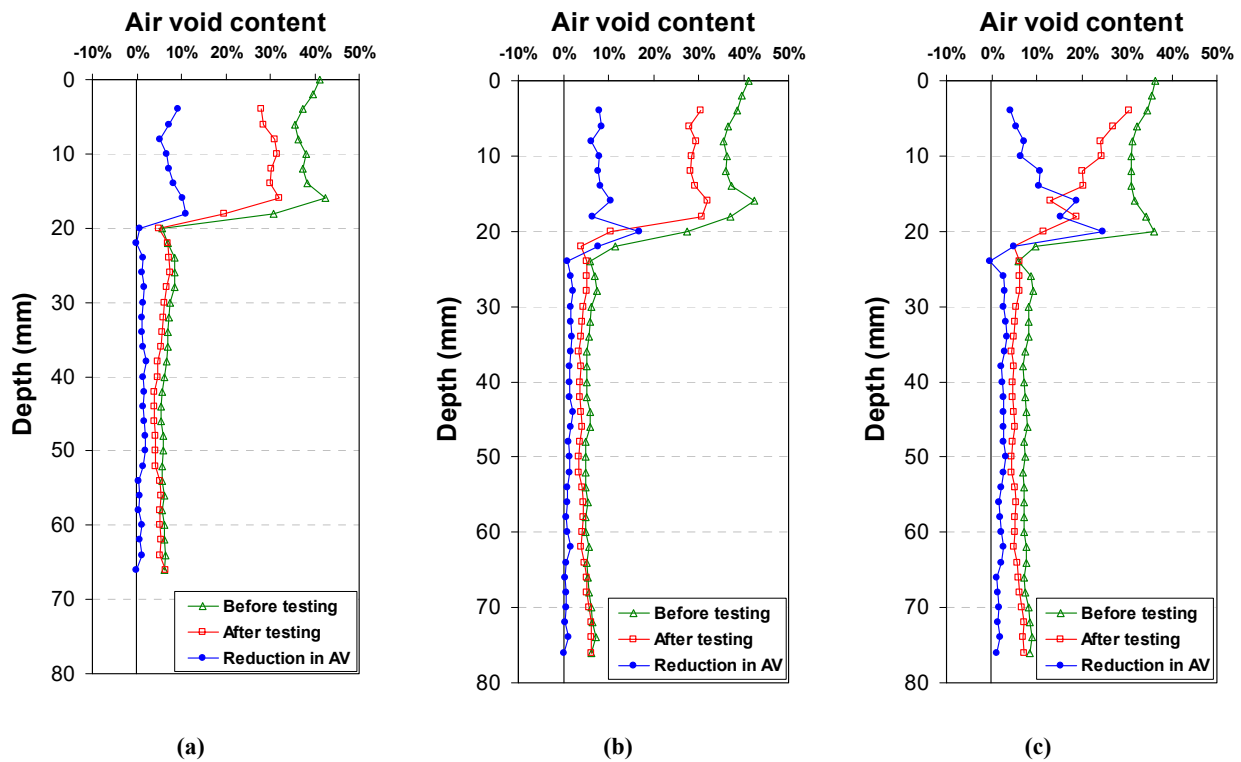


Figure 6.8: Air-void content distributions of three asphalt cores before and after rutting tests, depth = 0 for the OGFC surface.
(a) Section 653HB: Caltrans 3/8 inch mix with PG 76-22PM binder; (b) Section 655HB: #4P mix with PG 76-22PM binder; and (c) Section 657HB: #4P mix with PG 64-16 binder.

6.4.5 Summary of Rutting-Related Clogging Test Results

The permeability test results can be summarized as follows:

- The two #4P mixes showed more severe reductions in permeability than the control mix (Caltrans 3/8 inch mix with PG 76-22PM binder), while the Georgia 1/2 inch with PG 58-34PM binder showed less reduction than the control mix.
- The reduction in permeability was found to have an approximately linear correlation with the amount of accumulated total rut.
- Larger reductions in permeability were found to coincide with a larger reduction in air-void content for the OGFC layer.
- Since rutting typically increases much faster in the early ages of a pavement due to densification, one can expect a significant reduction in permeability soon after trafficking begins. Specifically, an approximately 20 percent to 30 percent reduction in permeability can be expected to occur within the first 10 percent of the rutting life of a pavement.
- The addition of airborne dust did not significantly contribute to a reduction in permeability (i.e., clogging).

6.5 Runoff-Related Clogging

An evaluation of clogging due to runoff drainage was performed using rainfall simulations that included solids of known concentration and particle size distribution. In this evaluation, vertical air void distributions of several cores were measured with an x-ray CT image scanner before and after the application of simulated rainfall, which contained particles of <38 micron gradation. The difference in the air void distributions rendered by the CT images before and after the tests provided a measure of the changes due to runoff-related clogging. The results are shown in Figure 6.9. Note that these cores contain OGFC at the top and HMA at the bottom.

The air-void contents shown in Figure 6.9 for the OGFC layers vary between 30 and 40 percent, which are consistently higher than the as-built air-void contents listed in Table 2.9. This discrepancy was caused partly by the different sampling locations and partly by differences in air void identification errors between the two layers. Nevertheless, it is believed that the observations made with respect to the changes in air void distribution are valuable because the before and after HVS trafficking analyses had the same amount of error.

Since none of these specimens were subjected to HVS loading, it was anticipated that any change in air-void content after the rainfall simulation would be the result of clogging caused by the addition of particles from the runoff drainage. However, as Figure 6.9 shows, the addition of particles through the rainfall simulation did not significantly change the air-void distributions, and the air-void content of the OGFC layer for Section 657HB (#4P mix with PG 64-16 binder) even increased slightly after the rainfall simulation. It is believed that the increased air-void content is due to the higher initial air-void content and to the washing away of initially trapped particles from the air voids by the simulated rainfall. The air void profiles shown in Figure 6.9 also indicate that the reduction in air-void content appeared mostly in the bottom 0.1 to 0.25 inches (2 to 6 mm) of the OGFC layers, while the air-void content of the upper part did not change significantly.

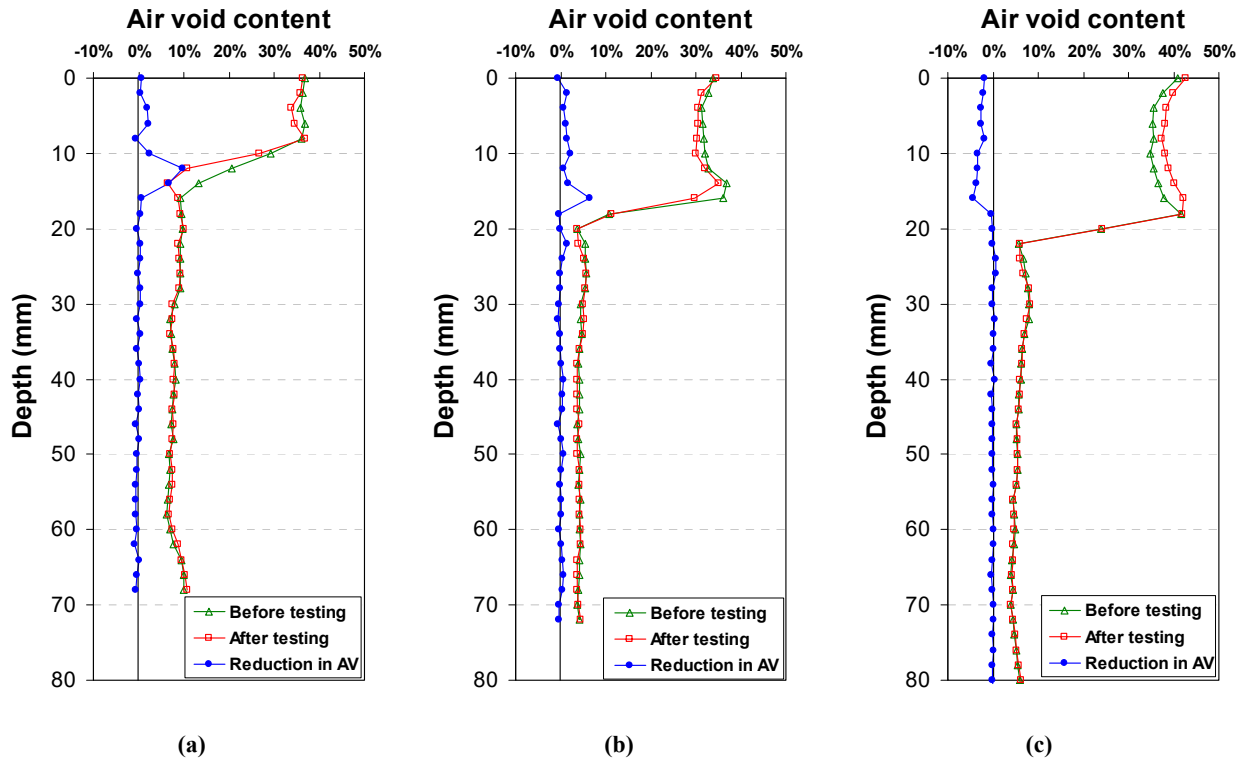


Figure 6.9: Air-void content distributions of cores before and after rainfall simulations with <38 micron particle gradation (depth = 0 for the surface OGFC layer).
(a) Caltrans 3/8 inch mix with PG 76-22PM binder, (b) #4P mix with PG 76-22PM binder, and (c) #4P mix with PG 64-16 binder.

Figure 6.10 presents the results of measurements of the air-void content distributions of the asphalt cores before and after rainfall simulation experiments performed with soil particles less than 600 microns. As shown in the figure, a relatively higher reduction in air-void ratio occurred in the bottom 0.15 to 0.25 inches (4 to 6 mm) of the OGFC layer while the air-void contents of the upper 0.5 inches (12 mm) of the layer did not significantly change. This result suggests that most of the added particles penetrated the OGFC layer and accumulated at the bottom.

In summary, the rainfall simulations using particles with both gradations did not cause severe clogging in the upper portion of the open-graded pavement when it was not subjected to HVS trafficking. The majority of particle accumulation occurred in the bottom 1/8 to 3/16 inches (3 to 4 mm) of the OGFC layer, and hence the particles added during the rainfall simulation did not affect the functionality of the permeable layer.

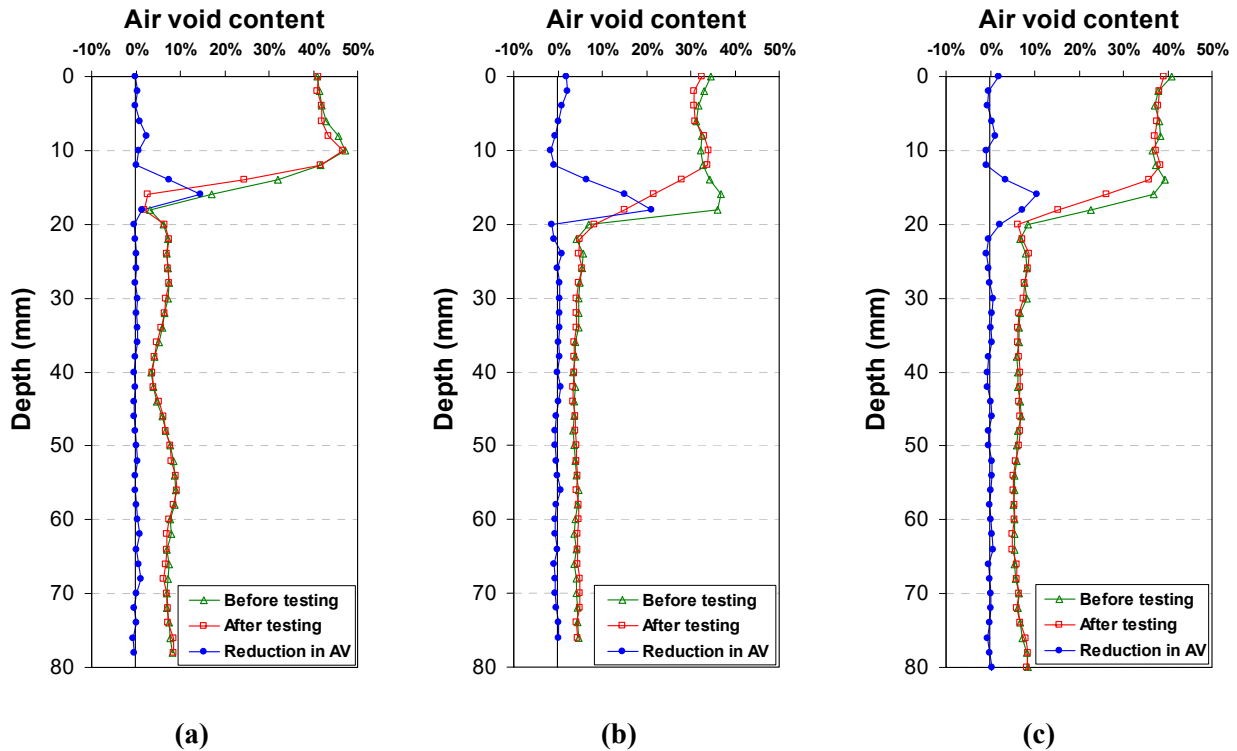


Figure 6.10: Air-void content distributions of cores before and after rainfall simulations with <600 micron particle gradation (depth = 0 mm is the surface of the OGFC layer).
(a) Caltrans 3/8 inch mix with PG 76-22PM binder; (b) #4P mix with PG 76-22PM binder; and (c) #4P mix with PG 64-16 binder.

Figure 6.9 and Figure 6.10 indicate that the clogging susceptibilities of the two OGFC mixes (#4P mix with PG 76-22PM binder and #4P mix with PG 64-16 binder) were lower or roughly the same as that of the control mix (Caltrans 3/8 inch mix with PG 76-22PM binder) under simulated rainfall. The observed reduction in void ratio due to runoff drainage was significantly lower than the reduction in air-void contents observed due to rutting, hence rutting-related clogging is believed to more critical than runoff-related clogging.

6.6 Summary of Permeability and Clogging Evaluation Results

Results obtained from this portion of the study showed the following:

- The two #4P mixes had similar initial permeability compared to the control mix (Caltrans 3/8 inch mix with PG 76-22PM binder), while the Georgia 1/2 inch mix showed significantly higher initial permeability than the control mix.
- Sections with thinner OGFC layers were more prone to clogging due to rutting, with after-HVS permeabilities close to zero.
- The majority of the reduction in permeability values (40 to 60 percent) occurred after about 2,000 repetitions (less than 4 mm downward rut depth) and in most cases the permeability was reduced to near

zero after 5,000 to 30,000 repetitions. The results of X-ray CT image processing revealed a significant reduction in the air-void content of core samples after HVS rutting tests. The highest air-void reduction was concentrated at the bottom of the OGFC layers. Permeability measurements also showed a 40 to 90 percent reduction in permeability after HVS trafficking. X-ray CT image processing of core samples that had been tested under simulated rainfall showed air-void content reduction concentrated in the lower part (0.1 to 0.25 inches [2 mm to 6 mm] from the bottom) of the OGFC layers as a result of particle accumulation.

- The addition of dust particles (<38 microns) did not significantly change the permeability of OGFC layers, indicating that the loss of permeability was mostly due to permanent deformation accumulated during HVS operation. Most of the particles accumulated at the bottom of the OGFC layer and did not affect surface permeability.
- For the reasons listed above, the rutting performance of OGFC pavements should be considered in assessing the long-term effectiveness of permeable pavements in stormwater runoff control and management. The results also indicate that OGFC mixes can trap particles, which may reduce their ability to allow water to flow water to the shoulder without overtopping, but which may also trap pollution in the pavement that would otherwise flow to the side of the road [33].
- Permeability measured by the ASTM and NCAT methods were correlated, but generally the values measured by the ASTM method were larger than those obtained by the NCAT method.

7 RUTTING PERFORMANCE

As discussed in Chapter 3, the rutting performance of the different OGFC mixes was evaluated through HVS testing on the test track and with Hamburg Wheel Track Testing (HWTT) in the laboratory. As noted earlier, specimens for HWTT were prepared using loose mix collected during construction of the HVS test track.

7.1 HVS Testing Results

This section presents the data collected during HVS testing, including testing temperatures and rut accumulation.

7.1.1 Temperature

Pavement temperature was controlled by a thermostat with a target temperature of 122°F (50°C) at 2 in. (50 mm) depth. As an example, Figure 7.1 shows the average hourly temperatures measured at different depths while the HVS trafficked Section 657HB (dual wheel, #4P mix with PG 64-16 binder).

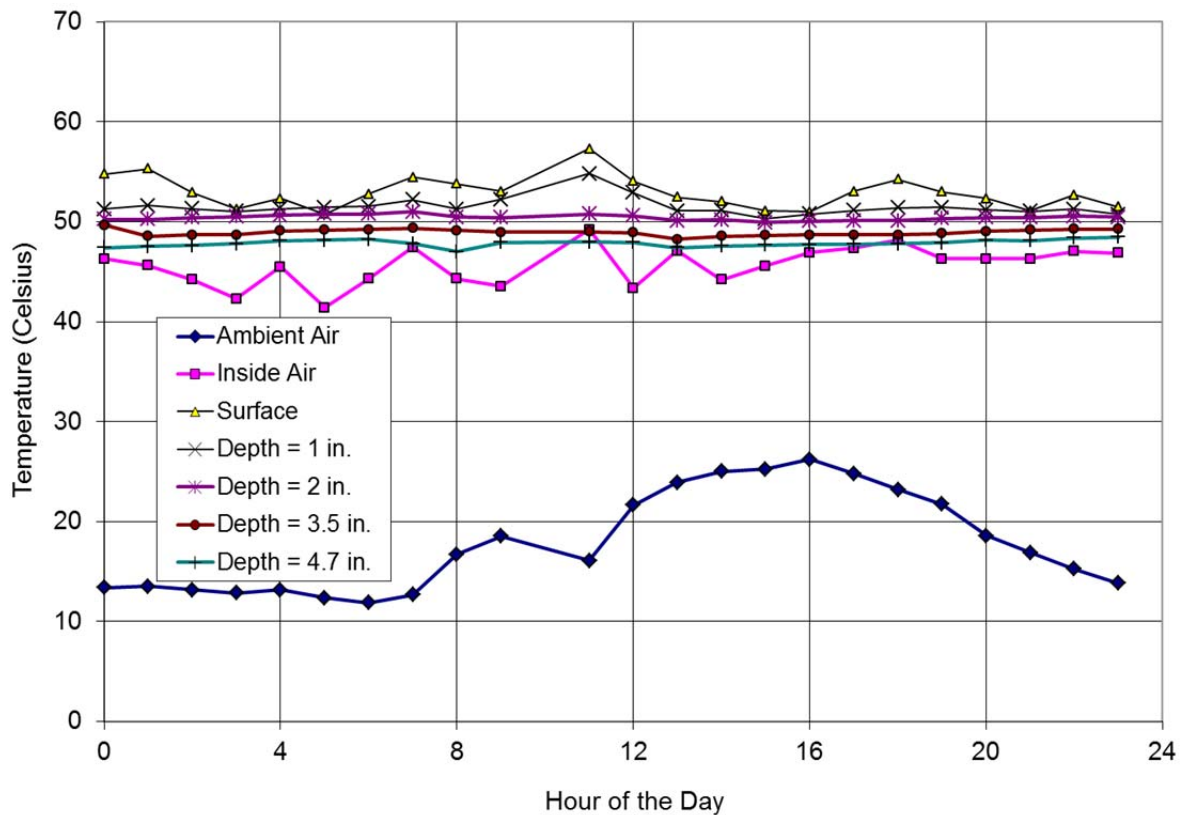


Figure 7.1: Hourly average temperatures while trafficking for Section 657HB (dual wheel, #4P mix with PG 64-16 binder).

7.1.2 Visual Observation

Surface photos of all the HVS rutting test sections after trafficking are shown in Figure 7.2 to Figure 7.6. All the photos show visible surface ruts that were mostly caused by permanent deformation in the asphalt-bound layers. The treads and grooves on the HVS tires left ridges in the wheelpaths because of the channelized traffic pattern on all the test sections, but the ridges were especially pronounced on the sections tested with dual wheels. These ridges affected surface texture measurements and had to be accounted for during data analyses.



(a) Section 651HB, tested with dual wheels



(b) Section 661HB, tested with NGWBT

Figure 7.2: Surface photos of Sections 651HB and 661HB (Georgia 1/2 inch mix with PG 58-34PM binder, Cell D) after HVS trafficking.



(a) Section 653HB, tested with dual wheels



(b) Section 663HB, tested with NGWBT

Figure 7.3: Surface photos of Sections 653HB and 663HB (Caltrans 3/8 inch mix with PG 76-22PM binder, Cell A) after HVS trafficking.



(a) Section 655HB, tested with dual wheels



(b) Section 665HB, tested with NGWBT

Figure 7.4: Surface photos of Sections 655HB and 665HB (#4P mix with PG 76-22PM binder, Cell B1) after HVS trafficking.



(a) Section 657HB, tested with dual wheels



(b) Section 667HB, tested with NGWBT

Figure 7.5: Surface photos of Sections 657HB and 667HB (#4P mix with PG 76-22PM binder, Cell B2) after HVS trafficking.



(a) Section 659HB, tested with dual wheels



(b) Section 669HB, tested with NGWBT

Figure 7.6: Surface photos of Sections 659HB and 669HB (#4P mix with PG 64-16 binder, Cell C) after HVS trafficking.

7.1.3 Permanent Deformation

The accumulation of average maximum total rut caused by HVS trafficking is shown in Figure 7.7 for the sections tested with the dual wheel and in Figure 7.8 for the sections tested with the Next Generation Wide Base Tire (NGWBT). The rutting life, defined as the number of load repetitions needed to reach 0.5 inches (12.5 mm) of average maximum total rut, is listed in Table 7.1 for each HVS test section. Table 7.2 shows the ratio between the load repetitions to a 0.5 inch rut for each mix relative to the control mix. Ratios are shown for both the dual tire and NGWBT tests.

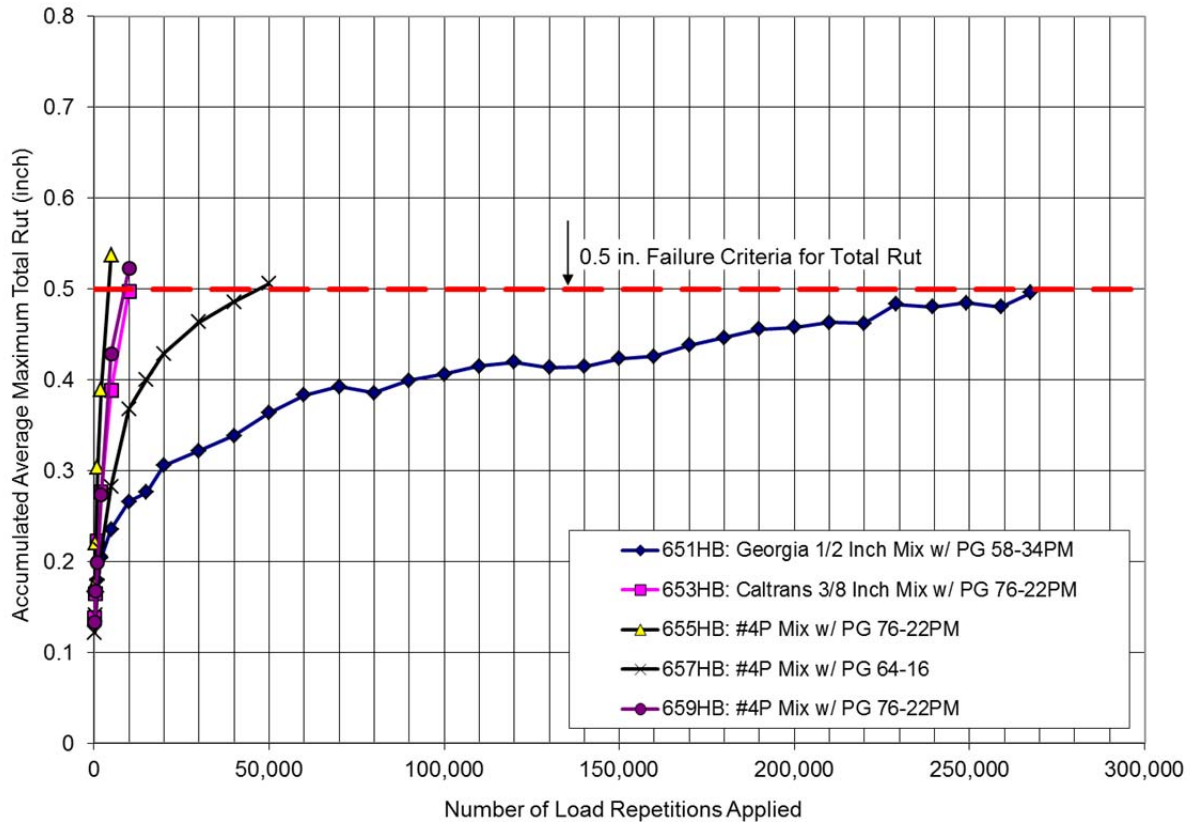


Figure 7.7: Accumulation of total rut for the HVS sections tested under dual-wheel traffic.

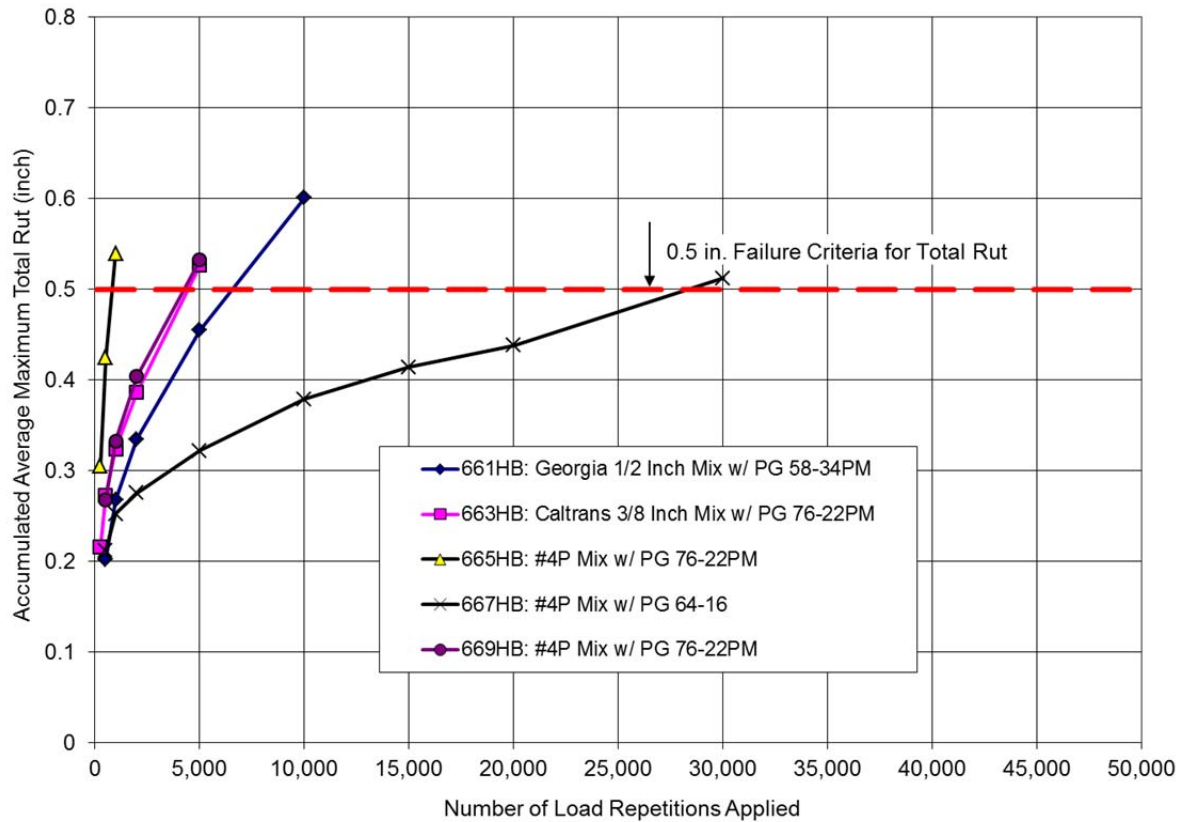


Figure 7.8: Accumulation of total rut for the HVS sections tested under next generation wide base tire (NGWBT) traffic.

Table 7.1: Rutting Life of Test Sections

Section	Mix Type	Test Cell	Wheel Type	Rutting Life	Life Ratio vs. Control Mix
651HB	Georgia 1/2 inch mix with PG 58-34PM	Cell D	Dual wheel	261,032	26.99
653HB	Caltrans 3/8 inch mix with PG 76-22PM	Cell A	Dual wheel	9,671	1.00
655HB	#4P mix with PG 76-22PM	Cell B1	Dual wheel	3,783	0.39
657HB	#4P mix with PG 64-16	Cell C	Dual wheel	43,058	4.45
659HB	#4P mix with PG 76-22PM	Cell B2	Dual wheel	7,993	0.83
661HB	Georgia 1/2 inch mix with PG 58-34PM	Cell D	NGWBT ¹	5,978	1.49
663HB	Caltrans 3/8 inch mix with PG 76-22PM	Cell A	NGWBT	4,001	1.00
665HB	#4P mix with PG 76-22PM	Cell B1	NGWBT	752	0.19
667HB	#4P mix with PG 64-16	Cell C	NGWBT	26,917	6.73
669HB	#4P mix with PG 76-22PM	Cell B2	NGWBT	3,757	0.94

¹: NGWBT = Next generation wide base tire.

Table 7.2: Comparison of Rutting Life for Different Wheel Types

Mix Type	Test Cell	Rutting Life		
		Dual Wheel	NGWBT	Dual Wheel Ratio
Georgia 1/2 inch mix with PG 58-34PM	Cell D	261,032	5,978	43.7
Caltrans 3/8 inch mix with PG 76-22PM	Cell A	9,671	4,001	2.4
#4P mix with PG 76-22PM	Cell B1	3,783	752	5.0
#4P mix with PG 64-16	Cell C	43,058	26,917	1.6
#4P mix with PG 76-22PM	Cell B2	7,993	3,757	2.1

According to an x-ray CT imaging study of Sections 653HB, 655HB, and 657HB [34], approximately 52 percent of the downward rut in the wheelpath occurred in the OGFC layer; this ratio of contribution is relatively consistent across the different OGFC mixes.

Based on the HVS rutting test results, the following observations can be made with respect to the rutting performance of different OGFC mixes compared to the control mix (Caltrans 3/8 inch mix with PG 76-22PM):

- *Effect of mix type:* The Georgia 1/2 inch mix with PG 58-34PM binder and #4P mix with PG 64-16 binder performed better than the control mix, while the #4P mix with PG 76-22PM binder showed equal or worse rutting performance than the control mix.
- *Effect of wheel type:* Rutting life under the dual wheel was typically 1.5 to 5.0 times longer than the corresponding rutting life under the NGWBT.
- *Effect of binder type:* The #4P mix with PG 64-16 binder had a much longer rutting life than the #4P mix with PG 76-22PM binder.

7.2 Hamburg Wheel-Track Testing Results

7.2.1 Material Characteristics of Specimens

Table 7.3 shows the air-void contents of the specimens for each mix tested with the HWTT, along with the as-built air-void contents copied from Table 2.9. Given that the compaction effort of 65 gyrations was the same across all four mixes, the Georgia 1/2 inch mix with PG 58-34PM binder had the highest air-void contents. Table 7.3 also indicates that the Georgia 1/2 inch mix was the only mix with HWTT specimen air-void contents that were significantly different from the as-built air-void content.

Table 7.3: Air-Void Contents of HWTT Specimens

Test No.	Caltrans 3/8 inch Mix w/ PG 76-22PM	#4P Mix w/ PG 76-22PM	#4P Mix w/ PG 64-16	Georgia 1/2 inch Mix w/ PG 58-34PM
1	28.2	26.8	26.9	29.9
	28.3	26.2	26.5	29.2
2	28.2	26.7	26.2	29.9
	28.2	26.0	26.4	29.1
3	28.6	26.2	26.9	
	28.1	24.1	26.8	
4	28.6	25.1	26.7	
	28.6	24.7	28.2	
Average	28.4	25.7	26.8	29.5
Std. Dev.	0.2	1.0	0.6	0.4
As-built Average*	26.7	26.8	29.5	21.0

*: The as-built average air-void contents are copied from Table 2.9.

7.2.2 Visual Observations

Figure 7.9 shows example specimens of each OGFC mix after HWTT was completed. The pictures show (a) relatively small rut depths in specimens of the two mixes with PG 76-22PM binder compared to specimens with the other two mixes and (b) that in addition to large rut depth, the specimens with #4P mix with PG 64-16 binder exhibited signs of crumbling, which indicates moisture damage in the specimen.



(a) Caltrans 3/8 inch mix w/ PG 76-22PM



(b) #4P mix w/ PG 76-22PM



(c) #4P mix w/ PG 64-16



(d) Georgia 1/2 inch mix w/ PG 58-34PM

Figure 7.9: Examples of specimens of each OGFC mix after HWTT testing.

7.2.3 Test Results

Rut accumulation after completion of HWTT for the different mixes is compared in Figure 7.10. The results plotted are the averages of four replicate tests, except for the Georgia mix, which had only two replicates.

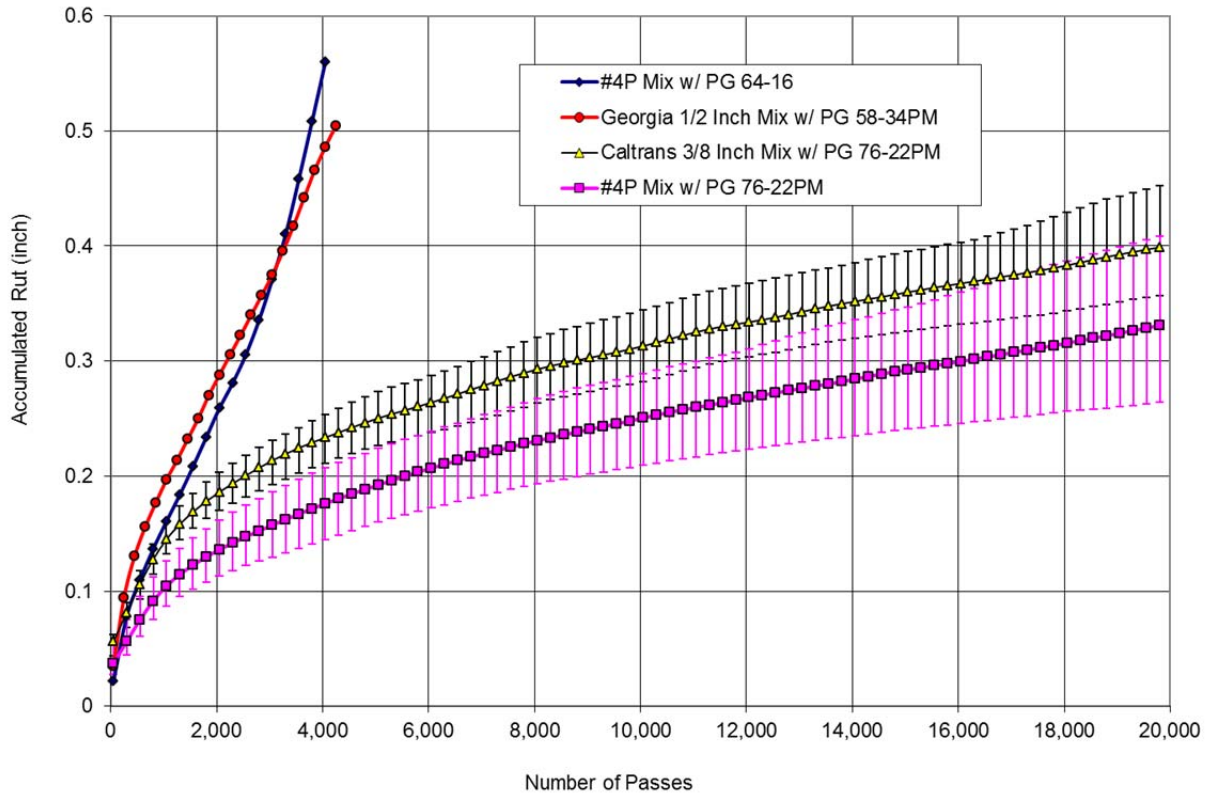


Figure 7.10: Comparison of rut accumulation in HWTT results for the different mixes; the results plotted are the average of four replicates except for the Georgia mix, which had only two replicates. Error bars for the Caltrans 3/8 inch mix with PG 76-22PM binder and the #4P mix with PG 76-22PM binders are also shown to indicate the range of test results.

Figure 7.10 indicates that both the Georgia 1/2 inch mix and the #4P mix with PG 64-16 binder had worse rutting performance than the control mix (Caltrans 3/8 inch mix with PG 76-22PM binder). On the other hand, the #4P mix with PG 76-22PM binder had slightly better rutting performance than the control mix. A summary of the characteristics of the HWTT rut accumulation curves appears in Table 7.4.

Table 7.4: Summary of Characteristics of the HWTT Rut Accumulation Curves

Quantity	Caltrans 3/8 inch Mix w/ PG 76-22PM	#4P Mix w/ PG 76-22PM	#4P Mix w/ PG 64-16	Georgia 1/2 inch Mix w/ PG 58-34PM
Creep Slope	0.00022 (0.21)*	0.00021 (0.33)*	0.0037 (0.33)*	0.0023 (0.36)*
Inflection Point	>20,000	>20,000	2,928 (0.12)*	4,730 (0.49)*
Strip Slope	N/A	N/A	0.0062 (0.08)*	0.0031 (0.34)*

*: Numbers in parentheses indicate the corresponding coefficient of variation.

7.3 Shear Stiffness Test Results

7.3.1 Material Characteristics of Specimens

Table 7.5 shows the air-void contents of the specimens of each mix used in shear stiffness tests, along with the as-built air-void contents listed in Table 2.9. As shown in the table, the #4P mix with PG 64-16 binder had air-void contents similar to the as-built average. The other two mixes—the Caltrans 3/8 inch mix and the #4P mix with PG 76-22PM binder—had air-void contents between 5 to 7 percent lower than the as-built averages.

Table 7.5: Air-Void Contents of Shear Stiffness Testing Specimens

Test No.	Caltrans 3/8 inch Mix w/ PG 76-22PM	#4P Mix w/ PG 76-22PM	#4P Mix w/ PG 64-16
1	30.3	32.1	31.1
2	31.0	32.1	28.0
3	33.6	35.1	29.6
Average	31.6	33.1	29.6
Standard Deviation	1.7	1.7	1.6
As-built average*	26.7	26.8	29.5

*: The as-built average air-void contents are copied from Table 2.9. The value for the #4P mix with PG 76-22PM binder is the average of cells B1 and B2.

7.3.2 Shear Stiffness of Different OGFC Mixes

The variations in shear stiffness with loading frequency for the different mixes at 131°F (55°C) are shown in Figure 7.11; the results indicate that both #4P mixes were slightly softer than the control mix. Of the three mixes, the #4P mix with PG 64-16 binder had the lowest stiffness.

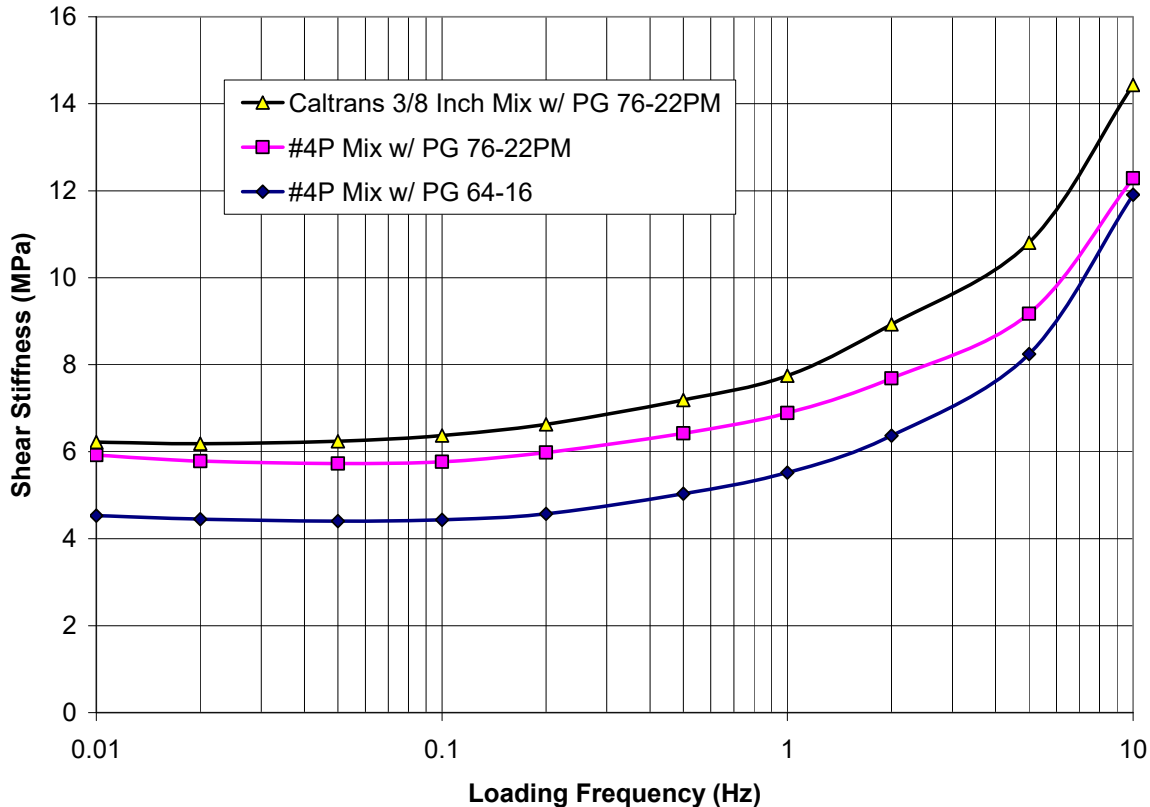


Figure 7.11: Shear stiffness of different OGFC mixes tested at 131°F (55°C) under different loading frequencies.

7.4 Summary of Rutting Test Results

The rutting performance of the different OGFC mixes were evaluated using the HVS on the test track and with HWTT on cores in the laboratory. Shear stiffnesses were also determined in the laboratory following AASHTO T 320 with the Superpave Simple Shear Tester (SST). A summary of the rutting and shear stiffness results for the different OGFC mixes relative to the control mix appears in Table 7.6. The table indicates that there was no correlation among the three types of test results.

The following factors are believed to have led to the inconsistency between the HWTT and HVS rutting performances:

- *Differences in testing conditions:* HWTT specimens were submerged in water during testing while HVS test sections were mostly dry. Crumbling found in #4P mix specimens with PG 64-16 binder indicates that the mix has a strong susceptibility to moisture damage, which would likely lead to poor rutting performance in the HWTT, even though this mix had the best performance of the three #4P sections in HVS tests for rutting under dry conditions.
- *Differences in material characteristics:* HWTT specimens were prepared in the lab after reheating the loose mix sampled during construction. This difference in preparation method between the HWTT specimens and HVS test tracks may have led to differences in properties of the mixes. Similarly, it is believed that the rutting performance of the Georgia 3/8 inch mix in HWTT was worse than in HVS testing because the laboratory specimens had higher air-void contents than the as-built values used in the test track.

Table 7.6: Summary of Rutting and Shear Stiffness for Different OGFC Mixes Relative to the Control Mix (Caltrans 3/8 inch Mix with PG 76-22PM Binder)

Measurement Type	Device	Condition	#4P Mix w/ PG 76-22PM	#4P Mix w/ PG 64-16	Georgia 1/2 inch Mix w/ PG 58-34PM
Rutting	HVS	Dry, 122°F	Same or worse	Better	Better
Rutting	HWTT	Submerged, 122°F	Slightly better	Worse	Worse
Shear Stiffness	SST	Dry, 131°F	Softer	Softer	<Not tested>

Since the Georgia 1/2 inch mix showed poor rutting performance in the HWTT results, it is believed that lime treatment and mineral fiber additive (both of which are part of its standard preparation according to GDOT guidelines) are critical for the resistance of the mix to moisture damage and should be required for field applications of the mix.

The HVS test results also suggest that there are significant effects of binder type and wheel type on the rutting performance of OGFC mixes.

8 MICROSTRUCTURE CHANGES UNDER HVS TRAFFICKING

X-ray CT images were taken of blocks of the two #4P mixes and the Caltrans control mix before and after they were subjected HVS trafficking. Results pertaining to the densification of the asphalt layers, relative contributions to rutting by the various layers of the test sections, and particle movement within the pavement sections are discussed below.

8.1 Densification of Asphalt Bound Layers

Figure 8.1 shows the reductions in air-void content, i.e., densification, caused by HVS trafficking that were determined for the wheelpath and hump areas, respectively. Figure 8.2 shows the calculated distributions of rutting caused by densification for all the HVS test sections. In these figures, the interface between the OGFC and HMA layers is shown by horizontal lines. Details about how these figures were developed are presented in Section 3.4.3.

From Figure 8.1 and Figure 8.2 it can be seen that densification was concentrated at the bottom of the OGFC layers for all the test sections except for Section 657HB (#4P mix with PG 64-16 binder), which had a significant amount of densification at the top part of the OGFC layers as well. Due to the low initial air-void content at the start of the tests, reductions in the air-void contents of the HMA layers were significantly smaller than those of the OGFC layers.

Section 657HB shows more severe densification at the top part of the OGFC layer than Sections 653HB (Caltrans 3/8 inch mix with PG 76-22PM) and 655HB (#4P mix with PG 76-22PM), and it is believed that this led to lower residual permeability (see Figure 6.4). This result suggests that although Section 657HB showed better rutting performance (See Figure 7.7), it may have lost its drainage functionality (permeability) due to rutting.

Figure 8.2 also shows air-void reduction in the hump areas of the OGFC layers, with only a negligible change in air-void contents in the hump areas of the HMA layers.

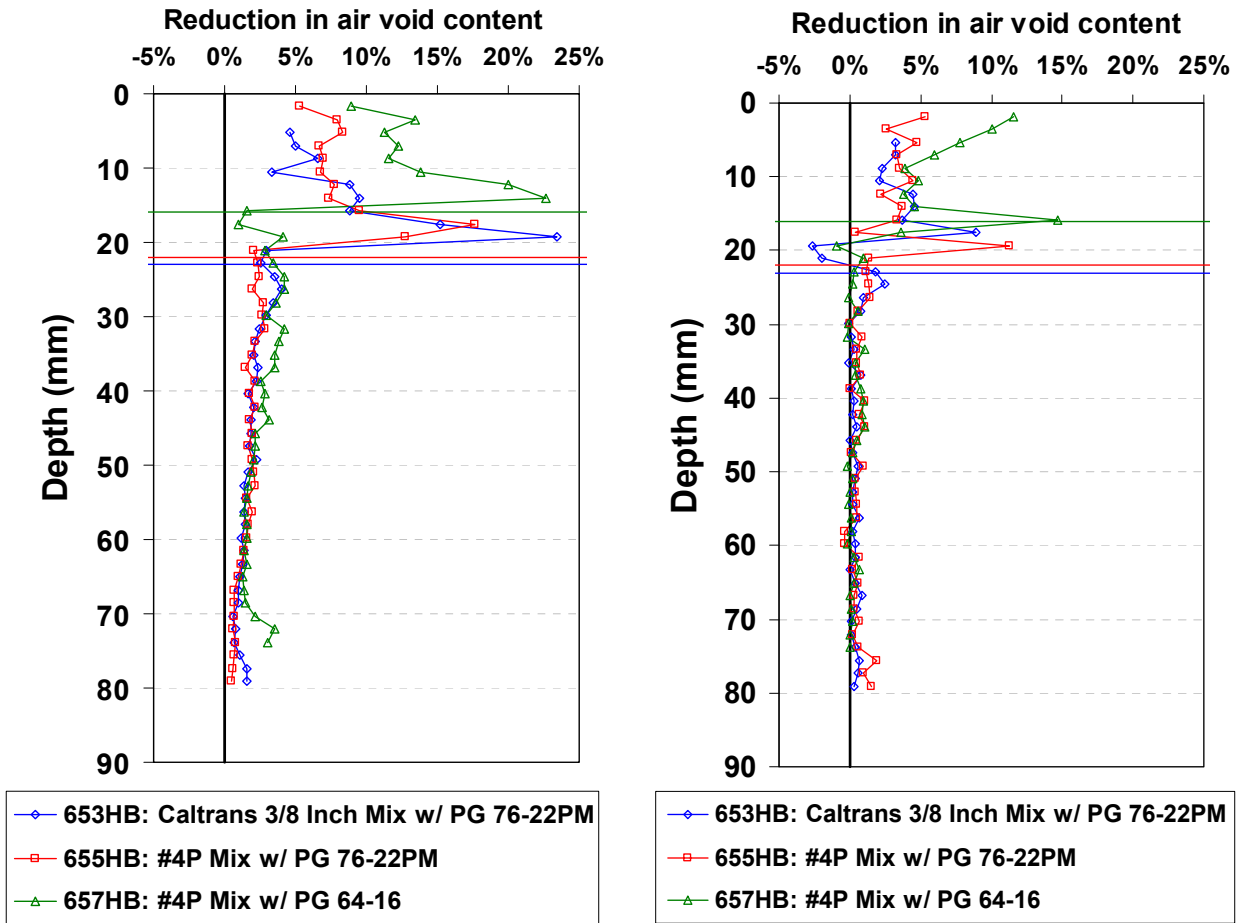


Figure 8.1: Reductions in air-void content caused by HVS trafficking (a) in the wheelpath area and (b) in the hump area (b).

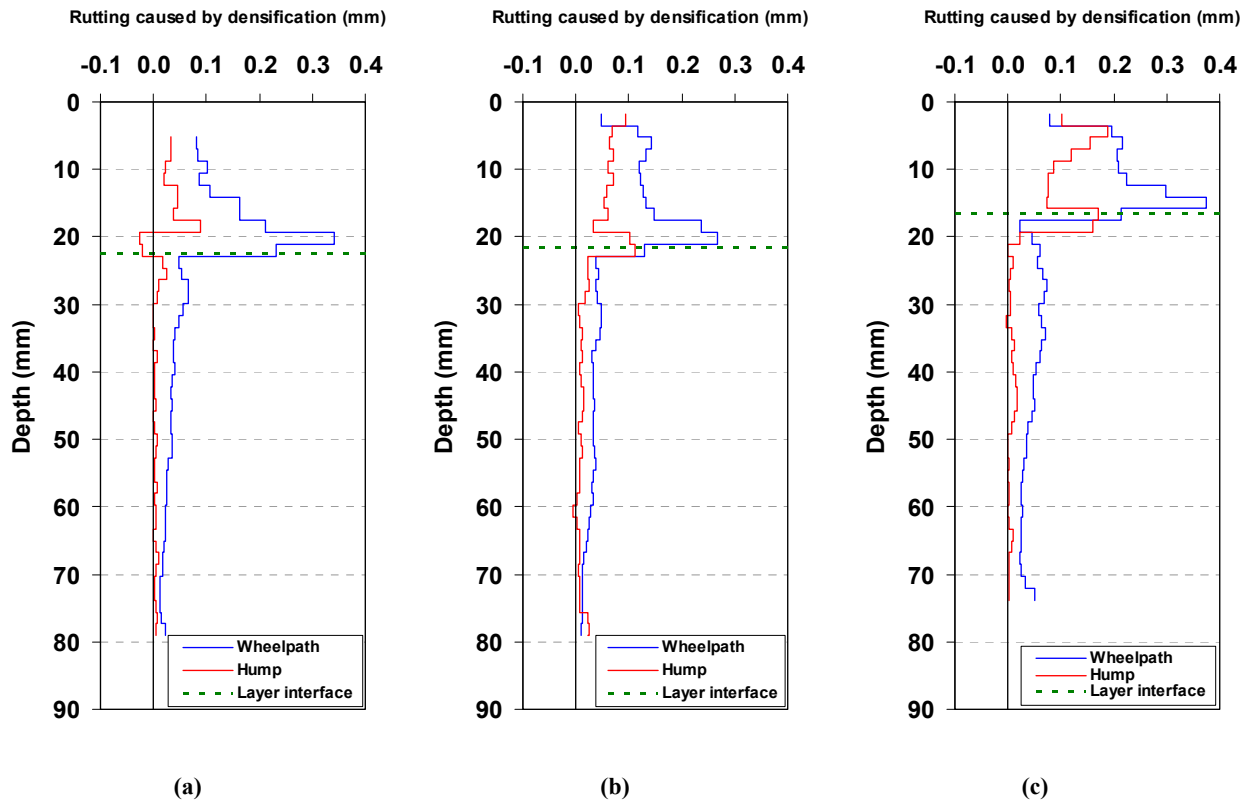


Figure 8.2: Rutting distributions caused by air void reductions in (a) Section 653HB (Caltrans 3/8 inch mix with PG 76-22PM binder), (b) Section 655HB (#4P mix with PG 76-22PM binder), and (c) Section 657HB (#4P mix with PG 64-16 binder).

Densification-related rut for each layer calculated from the data shown in Figure 8.2 is also given in Table 8.1. It can be seen that the OGFC and HMA layers both contribute significantly to the total densification-related rut.

Table 8.1: Downward Rut Caused by Air Void Reduction from X-Ray CT Images (mm)

Section	Mix Type	OGFC Thickness	OGFC Layer		HMA Layer	
			Hump	Wheelpath	Hump	Wheelpath
653HB	Caltrans 3/8 inch mix w/ PG 76-22PM	23 mm	0.28	1.57	0.15	1.07
655HB	#4P mix w/ PG 76-22PM	22 mm	0.85	1.72	0.34	0.96
657HB	#4P mix w/ PG 64-16	16 mm	1.05	2.02	0.34	1.46

8.2 Decomposition of Surface Downward Rut

Following the technique described in Section 3.4.3, the total surface downward rut was separated into the contributions from unbound layer rut, densification in the OGFC layer, shear in the OGFC layer, densification in the HMA layer, and shear in the HMA layer. The decomposition of surface downward rut was determined for the three HVS test sections and the results are listed in Table 8.2. Note that the surface downward rut under discussion here is less than the maximum downward rut along the transverse profile measured on top of the blocks by the laser profilometer because the blocks were not wide enough (see Figure 3.12).

Table 8.2 shows that the relative contributions to the surface downward rut from the unbound layer, the HMA layer, and the OGFC layer were consistent across the three HVS test sections: roughly 10 percent from the unbound layers, 52 percent from the OGFC layer, and 38 percent from the HMA layer. It shows that the OGFC layer was the major contributor to surface downward rut even though the layer was relatively thin compared to the underlying HMA layer.

Table 8.2 also shows that the contribution of densification to the total asphalt-bound layer rut was 69 percent, 79 percent, and 90 percent for Sections 653HB, 655HB, and 657HB, respectively. This suggests that densification is the major factor controlling rutting of the OGFC layers.

Table 8.2: Calculated Contributions of Shear, Densification, and Unbound Layer-Related Rutting to the Total Surface Rutting for OGFC and HMA Layers

Layer or Component	653HB (Caltrans 3/8 inch Mix w/ PG 76-22PM)		655HB (#4P Mix w/ PG 76-22PM)		657HB (#4P Mix w/ PG 64-16)	
	Rut (mm)	Ratio	Rut (mm)	Ratio	Rut (mm)	Ratio
Unbound	0.38	0.09	0.46	0.12	0.48	0.11
OGFC-D*	1.57	0.37	1.72	0.45	2.02	0.47
OGFC-S*	0.57	0.14	0.21	0.05	0.27	0.08
HMA-D*	1.07	0.25	0.96	0.25	1.46	0.33
HMA-S*	0.61	0.15	0.50	0.13	0.10	0.01
Total	4.2	1.0	3.85	1.0	4.33	1.00
OGFC		0.51		0.50		0.54
HMA		0.40		0.38		0.35
D/(S+D) ^x		0.69		0.79		0.90

*: OGFC-D = densification in OGFC layer, OGFC-S = shear in OGFC layer, HMA-D = densification in HMA layer, and HMA-S = shear in HMA layer

^x: $D/(S+D) = (OGFC-S + HMA-S) / (OGFC-S + HMA-S + OGFC-D + HMA-D)$

8.3 Aggregate Movement Caused by HVS Trafficking

Using CT image scans of asphalt concrete blocks that were taken before and after HVS trafficking, Figure 8.3 shows the distribution of the permanent displacement vectors within the blocks. These visualizations were improved for the figure by limiting the view to one 0.8 in. (20 mm) segment of each of the asphalt concrete block. The following can be seen from these images:

- Although most of the permanent displacements occurred in the OGFC layers, the permanent displacements in the HMA layer were also significant.
- No significant shear flow was observed in the OGFC layers.
- In addition to densification in the vertical direction, the HVS wheel pushed the OGFC asphalt mix from under the tire to the sides, creating densification at the humps as well. This result explains the high densification observed in the OGFC humps measured by x-ray CT imaging (Figure 8.2).

- Particles in the HMA layers were pushed away from the HVS tire creating two shear flow patterns. Most of the shear flow at the HMA layers appeared to be in the downward direction, while the upward shear flow to the humps, previously observed by Coleri et al. for thick rubberized gap-graded mixes [8], was not observed. This result suggests that shear flow at the HMA layers did not significantly increase the height of the humps or affect maximum total rutting.

In order to quantitatively evaluate the particle movements, cumulative distributions of the vertical particle displacements under the HVS wheelpaths were calculated and are shown in Figure 8.4. From the figure, the following can be observed:

- Although most of the permanent displacements occurred in the OGFC layers, the permanent displacements in the HMA layers were also significant (see Figure 8.4).

The amount of permanent particle movement under the HVS wheelpaths was similar for all the test sections (see Figure 8.4).

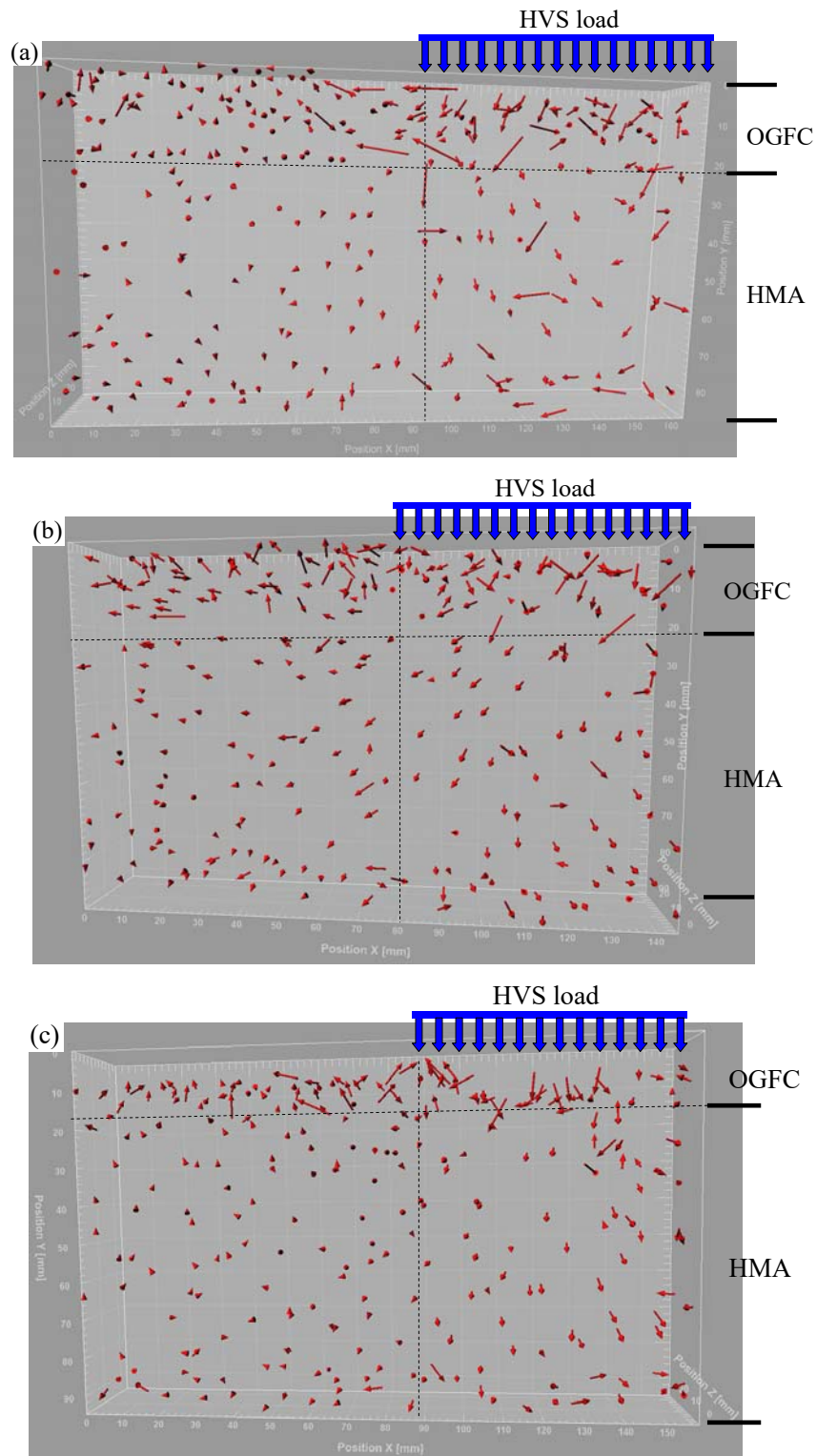
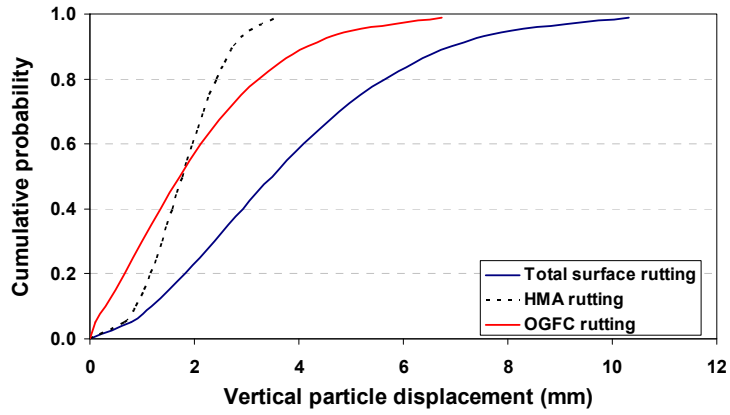
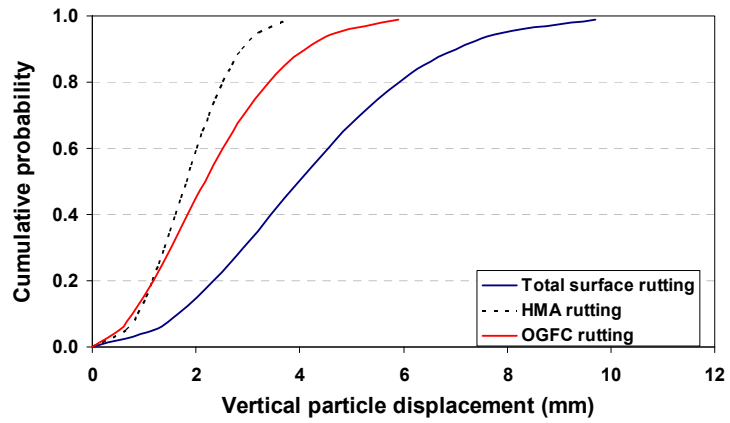


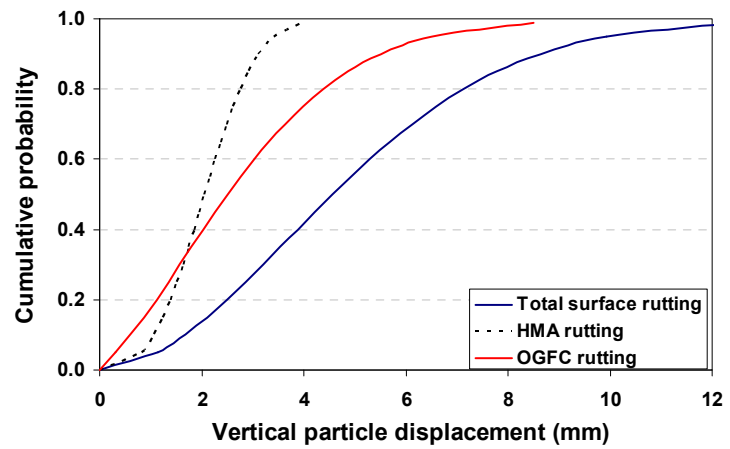
Figure 8.3: Displacement vectors for one 0.8 in. (20 mm) segment of each of the asphalt concrete blocks (front view): (a) Section 653HB (Caltrans 3/8 inch mix with PG 76-22PM binder), (b) Section 655HB (#4P mix with PG 76-22PM binder), and (c) Section 657HB (#4P mix with PG 64-16 binder). Note: Direction of HVS traffic is out of the page.



(a) Section 653HB (Caltrans 3/8 inch mix with PG 76-22PM binder)



(b) Section 655HB (#4P mix with PG 76-22PM binder)



(c) Section 657HB (#4P mix with PG 64-16 binder)

Figure 8.4: Cumulative distribution functions of the vertical particle displacements.

8.4 Summary of Results

The material discussed in this chapter aimed to identify the permanent deformation accumulation mechanisms of OGFC mixes under full-scale loading. Microstructural changes in the OGFC and underlying HMA layers under full-scale trafficking were determined using x-ray CT images taken before and after HVS testing. Image processing and particle-tracking methods were used to identify changes in air-void and aggregate distributions to evaluate the rutting mechanisms of multilayered (OGFC on HMA) asphalt concrete sections. Densification of the OGFC was observed to be the major factor controlling rutting on test sections, followed by densification of the HMA layer below, while shear-related deformation in both asphalt layers was only a minor contributor. Displacement vector distributions for the OGFC layers appeared to be larger than the distributions for the HMA layers due to the high initial air-void content of the OGFC layers. However, significant deformation of the HMA layers confirmed that underlying HMA layers may also contribute to early rutting failures.

9 MIX DURABILITY

This chapter presents results from Cantabro testing, which reflects the durability of the different mixes against mechanical tumbling.

9.1 Material Characteristics of Specimens

Table 9.1 shows the average air-void contents, and the standard deviation, for the specimens used in Cantabro testing.

Table 9.1: Percent Air-Void Content and Percent Weight Loss of Cantabro Test Specimens

Mix Type	Number of Specimen	Air-Void Content	Weight Loss
Caltrans 3/8 inch mix w/ PG 76-22PM	6	29.2 (0.8)*	78 (8.9)*
#4P mix w/ PG 76-22PM	6	25.2 (0.9)	41 (10)
#4P mix w/ PG 64-16	6	24.4 (1.0)	31 (3.5)

*: Average with standard deviation in parentheses.

9.2 Test Results

The averages and standard deviations of percent weight loss measured from Cantabro testing for the different OGFC mixes are listed in Table 9.1. Figure 9.1 shows examples of the residual specimens of the three mixes used in this study.

The results rank the mixes in the following order in terms of mechanical durability from best to worst:

1. #4P mix with PG 64-16
2. #4P mix with PG 76-22PM
3. Caltrans 3/8 inch mix with PG 76-22PM

Using the individual test results, Student's *t*-tests were conducted assuming test results for the different mixes were unmatched and had unknown and unequal variances. The above ranking was found to be statistically significant at a significance level of 0.05.

In summary, the #4P mixes had better durability than the control mix (Caltrans 3/8 inch mix with PG 76-22PM binder) in Cantabro testing.

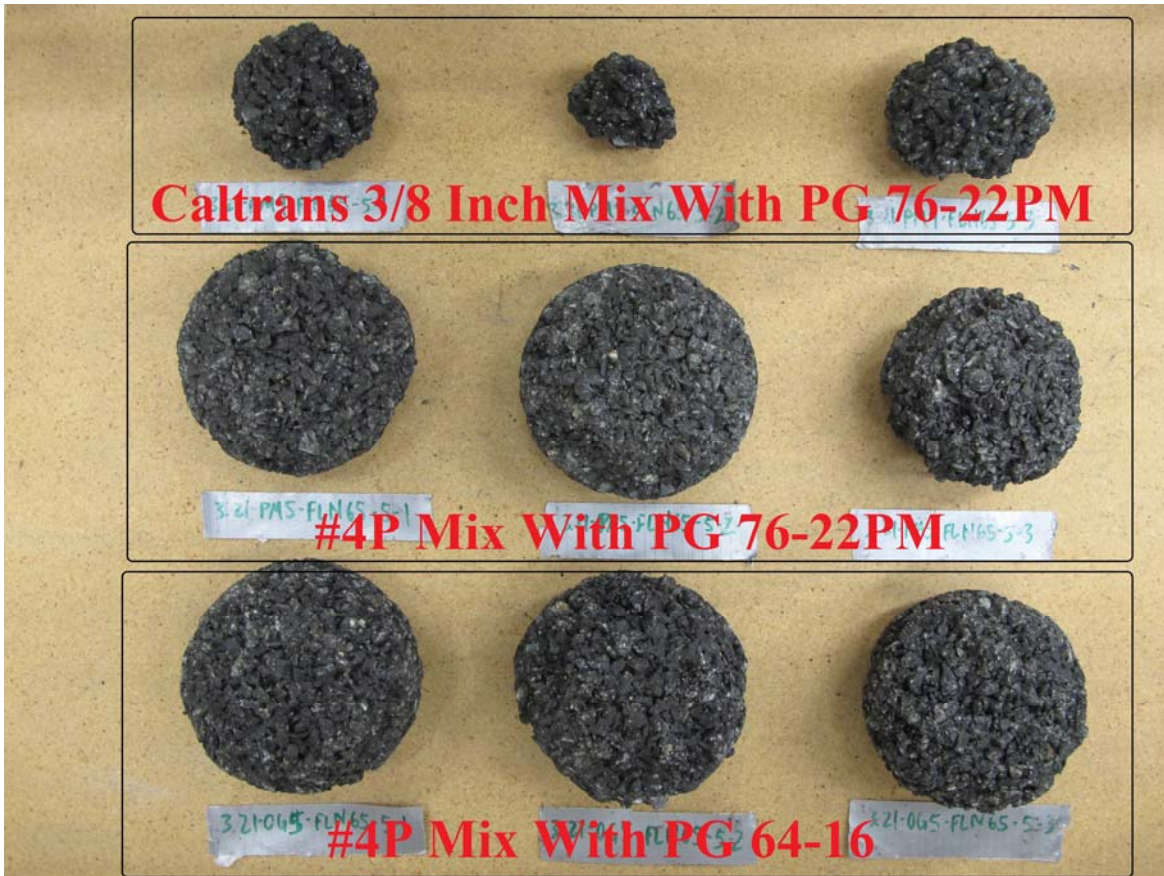


Figure 9.1: Examples of residual specimens after Cantabro testing of the different OGFC mixes. (Note that each original specimen had a diameter of 4 inches [100 mm].)

10 SUMMARY, OBSERVATIONS, AND RECOMMENDATIONS

10.1 Summary

This study is part of a long-term effort that started in 2005 to develop the specifications, guidelines, standardized laboratory and field test methods, and other information needed for quieter pavement research to be incorporated into standard Caltrans practices, and lead to quieter pavements.

Based on an earlier laboratory study, several open-graded friction course (OGFC) mixes were selected for further evaluation with accelerated pavement testing using the Heavy Vehicle Simulator (HVS) and laboratory testing on plant-produced materials. These selected mixes had showed good overall laboratory performance in terms of durability and sound absorption, which is correlated with tire/pavement noise. Specifically, the following HVS test cells were constructed for this experiment:

- Cell A: Caltrans 3/8 inch mix with PG 76-22PM binder, average as-built thickness = 0.06 ft
- Cell B1: #4P mix with PG 76-22PM binder, average as-built thickness = 0.06 ft
- Cell B2: Same mix as Cell B1, average as-built thickness = 0.07 ft
- Cell C: #4P mix with PG 64-16 binder, average as-built thickness = 0.05 ft
- Cell D: Georgia 1/2 inch mix with PG 58-34PM, average as-built thickness = 0.15 ft

The #4P mixes had nominal maximum aggregate size of 4.75 mm (#4 sieve) with “P” indicating a coarser aggregate gradation identified in the earlier laboratory study [2]. The five test cells included three new OGFC mixes, with the Caltrans 3/8 inch mix serving as the control mix.

The construction, HVS testing, and relevant laboratory testing in this current study were conducted under Partnered Pavement Research Center Strategic Plan Element (PPRC SPE) 3.21. The study examined the performance of the selected OGFC mixes in terms of their constructability, rutting performance, moisture damage susceptibility, surface texture, permeability, clogging susceptibility, clogging and rutting mechanisms, and tire/pavement noise.

10.2 Observations

The following items summarize several important observations made about mix constructability and the relative performance of the different OGFC mixes compared to the control mix:

- Constructability:
 - The #4P gradation was selected because the original #4 gradation could not be produced in northern California with current crushed rock bin size gradations without excessive waste of

unused aggregate. If there is a market for the #4P mixes, producers indicated a potential willingness to produce additional bin sizes to economically produce this gradation.

- The lime treatment and mineral fiber additive required for the Georgia 1/2 inch mix (according to GDOT specifications) were not readily available for the mixing plants near Davis, California, and therefore they were not added to the mixes.
 - The design thicknesses of the OGFC layers ranged from 0.05 to 0.08 ft but all were constructed with roughly the same thickness, an indication of the difficulty in meeting such a fine distinction in thickness specifications using conventional paving equipment.
 - As with all OGFC construction, paving at cool temperatures can cause difficulties in paving. It may be worthwhile to increase the minimum surface temperature and air temperatures in the standard specifications when paving thin layers of OGFC.
- Rutting performance:
 - Based on the HVS testing results, the #4P mix with PG 64-16 binder and the Georgia 1/2 inch mix with PG 58-34PM performed better than the control mix, while the #4P mix with PG 76-22PM binder performed either the same as or worse than the control.
 - Based on Hamburg Wheel-Tracking Test (HWTT) results, the #4P mix with PG 76-22PM binder was slightly better than the control mix, while the #4P mix with PG 64-16 binder and the Georgia 1/2 inch mix with PG 58-34PM were worse than the control.
 - HWTT and HVS testing yielded results that were completely opposite in terms of rutting performance ranking. It is believed this occurred due to their different testing conditions, with the submersion in water in the HWTT affecting the performance of the PG 64-16 mix, and that this indicates the importance of HVS testing for rutting.
 - Moisture damage susceptibility:
 - The HVS was found to be ineffective for evaluating the moisture damage susceptibility of OGFC mixes.
 - The crumbling of finished HWTT specimens that contained the #4P mix with PG 64-16 binder indicates that this mix is much more susceptible to moisture damage than the control mix.
 - Surface texture:
 - The three OGFC mixes had lower mean profile depths (MPD), and the same or longer outflow times than the control mix. The MPD values for the #4P mixes were within the range of MPD values measured using an inertial profiler on new OGFC and rubberized open-graded mixes across the state as part of the asphalt pavement noise study. The value for the control mix built for this study is high compared to values statewide.

- California Portable Skid Tester (CST) measurements taken after HVS trafficking indicated that all three new OGFC mixes had roughly the same coefficient of friction.
- Based on dynamic friction tester (DFT) measurements taken on the HVS test track, all three new mixes showed higher surface friction than the control mix. On the other hand, laboratory-prepared ingot specimens of the two #4P mixes showed lower DFT surface friction than the control mix.
- MPD, dynamic friction measured by the DFT, and coefficient of friction measured by the CST for all mixes satisfied the minimum requirements throughout HVS testing,
- Mechanical Durability:
 - The two #4P mixes had better durability than either the control mix or the Georgia 1/2 inch mix under mechanical tumbling in Cantabro testing.
- Permeability before being subjected to environmental or traffic loading:
 - The two #4P mixes had roughly the same permeability as the control mix, while the Georgia 1/2 inch mix had much higher permeability compared than the control mix.
- Clogging susceptibility:
 - After HVS trafficking, the two #4P mixes showed more a severe reduction in permeability caused by rutting than the control mix, while the Georgia 1/2 inch with PG 58-34PM binder showed a smaller reduction compared to the control mix.
 - Clogging from simulated rainfall with suspended solids induced a similar amount of air void reduction in all three mixes compared to the control.
 - Airborne dust was not found to lead to clogging in any of the OGFC mixes.
- Tire/pavement noise:
 - All three new #4P OGFC mixes had lower noise levels than the control mix. Noise was not tested on the Georgia 1/2 inch mix due to the short length of the section. The overall OBSI noise reduction of the #4P mixes ranged between 0.8 and 1.6 dBA, which would be barely perceptible in terms of loudness, if at all, for human hearing. All of the reduction in noise was at higher frequencies, and the change in frequency content of the noise would likely be perceptible to humans.

10.3 Recommendations

Table 10.1 summarizes the comparative performance of the three new OGFC mixes and the control mix. The table shows, all three new #4P mixes had pros and cons compared to the control mix. The study did validate that the pavements using these new OGFC mixes had lower tire/pavement noise. Considering the fact that all of the mixes satisfied the surface texture requirements, the following recommendations are made based on Table 10.1:

- For #4P mix with PG 76-22PM binder: This mix is recommended for places where rutting is not an issue. Clogging of this mix can mostly be avoided by limiting rutting.
- For #4P mix with PG 64-16 binder: This mix is recommended for places where moisture damage can be avoided. The mix had good rutting performance but is prone to moisture damage.
- For Georgia 1/2 inch mix with PG 58-34PM binder: This mix is recommended if lime treatment and mineral fiber additives can be accommodated, and the cost is determined to be feasible.
- When all of the mixes are feasible for a given project, the preliminary indications are:
 - The #4P mixes offer superior noise and mechanical durability compared with the control mix. Their skid resistance, as measured by Caltrans Test 342 (CST), and surface permeability are similar. The #4P mixes have less macrotexture than the control, but more than dense-graded mixes. A rubberized binder may improve moisture sensitivity and rutting performance, which were better or worse than the control mix depending on the binder type.
 - The Georgia 1/2 inch mix is likely to provide superior skid resistance and rutting performance compared to the control mix, although it could not be fully investigated in this project due to difficulties in getting it produced as designed by local plants. It is also likely to cost more because of the lime treatment and fibers in addition to the polymer-modified binder.
- Based on the results from this study, it is recommended that several pilot sections be placed using a rubberized binder. For these mixes to be placed, the gradations may need to be adjusted somewhat to be producible using current crushed stone bin gradations.
- Consideration should be given to increasing the minimum surface and air temperatures for paving of open-graded mixes.

**Table 10.1: Summary of Performances of New OGFC Mixes Relative to the Control Mix
(Caltrans 3/8 inch Mix with PG 76-22PM Binder)**

Performance Type	Evaluation Method	#4P Mix w/ PG 76-22PM	#4P Mix w/ PG 64-16	Georgia 1/2 inch Mix w/ PG 58-34PM
Constructability	Construction log	0	0	–
Tire/pavement noise	OBSI vehicle	+	+	Not evaluated
Initial permeability	Permeameters	0	0	+
Clogging susceptibility due to rutting	HVS	–	–	+
Durability	Cantabro test	+	+	Not evaluated
Rutting performance	HVS	–	+	+
	HWTT	+	–	?
Surface friction	CST (CT 342)	0	0	0
	Dynamic Friction Tester	?	?	+
Macrotexture (MPD)	Circular Texture Meter	–	–	–
	Laser Texture Scanner	–	–	–
	Greater than dense- graded asphalt?	Yes	Yes	Yes
Initial Outflow Time	Outflow Meter	–	–	0

Notes: 0 means about the same performance as the control mix; + means better performance than the control mix, – means worse performance than the control mix; and ? indicates inconclusive performance difference.

REFERENCES

1. Ongel, A., et al. Investigation of Noise, Durability, Permeability, and Friction Performance Trends for Asphaltic Pavement Surface Types: First- and Second-Year Results. 2008, University of California Pavement Research Center. (UCPRC-RR-2007-03)
2. Lu, Q., P. Fu, and J. Harvey. Laboratory Evaluation of the Noise and Durability Properties of Asphalt Surface Mixes.. 2009. University of California Pavement Research Center. (UCPRC-RR-2009-07)
3. California Department of Transportation. Standard Specifications. 2010, State of California Business, Transportation and Housing Agency, Department of Transportation.
4. Guada, I., A. Rezaei, J.T. Harvey, and D. Spinner, Evaluation of Grind and Groove (Next Generation Concrete Surface) Pilot Projects in California. 2013, University of California Pavement Research Center. (in progress). (UCPRC-RR-2013-01)
5. California Department of Transportation. Test Method 368: Standard Method for Determining Optimum Bitumen Content (OBC) for Open Graded Asphalt Concrete. 2003.
6. Watson, D., A. Johnson, and D. Jared. Georgia Department of Transportation's Progress in Open-Graded Friction Course Development. *Transportation Research Record: Journal of the Transportation Research Board*, 1998. 1616(1): p. 30-33.
7. Jones, D. Quality Management System for Site Establishment, Daily Operations, Instrumentation, Data Collection and Data Storage for APT Experiments. 2005, CSIR Transportek: Pretoria, South Africa.
8. Coleri, E., J.T. Harvey, K. Yang, and J.M. Boone., A Micromechanical Approach to Investigate Asphalt Concrete Rutting Mechanisms. *Construction and Building Materials*, Vol. 30(0), 2012, p. 36-49.
9. Simpleware Ltd. *ScanIP and ScanFE* software. 2010. Innovation Centre, Rennes Drive. Exeter EX4 4RN, UK.
10. American Association of State Highways Transportation Officials. Bulk specific gravity and density of compacted asphalt mixtures using automatic vacuum sealing method. 2009.
11. Bitplane. *Imaris: 3D and 4D Real-Time Interactive Data Visualization*. Version 7.2.
12. Choubane, B., C.R. Holzschuher, and S. Gokhale. Precision of Locked-Wheel Testers for Measurement of Roadway Surface Friction Characteristics. *Transportation Research Record: Journal of Transportation Research Board*, 2004(1869).
13. Kummer, H.W. and W.E. Meyer. Penn State Road Surface Friction Tester as Adapted to Routine Measurement of Pavement Skid Resistance, in 42nd Annual Meeting of Road Surface Properties Conference. 1963.
14. American Society for Testing and Materials. Annual Book of ASTM Standards. Vol. 04.03. 2007, West Conshohocken, PA.

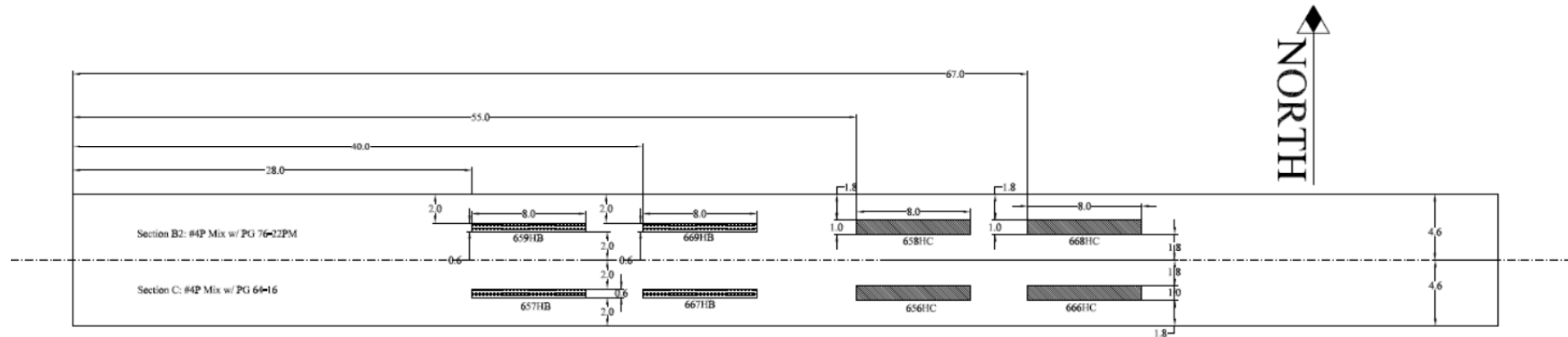
15. Hall, J.W., L.T. Glover, K.L. Smith, L.D. Evans, J.C. Wambold, T.J. Yager, and Z. Rado. Guide for Pavement Friction, Project No. 1-43, Final Guide. 2006. National Cooperative Highway Research Program, Transportation Research Board, National Research Council, Washington, D.C.
16. Hogervorst, D., Some Properties of Crushed Stone for Road Surfaces. Bulletin of the International Association of Engineering Geology, 1974. 10(1).
17. Lu, Q., E. Kohler, J. Harvey, and A. Ongel. Investigation of Noise and Durability Performance Trends for Asphaltic Pavement Surface Types: Three-Year Results. 2009, University of California Pavement Research Center. UCPRC-RR-2009-01.
18. Sandberg, U. and J.A. Ejsmont, Tyre-road Noise Reference Book. 2002: Informex.
19. TICS Ltd. Circular Track Texture Meter. 2012. (Accessed August 23, 2012.) Available from: <http://www.tics.hu/CTMeter.htm>.
20. Rezaei, A., E. Masad, and A. Chowdhury. Development of a Model for Asphalt Pavement Skid Resistance Based on Aggregate Characteristics and Gradation. ASCE Journal of Transportation Engineering, 2011. 137(12): p. 863-783.
21. AMES Engineering. Laser Texture Scanner Specification Manual. 2012. (Accessed August 23, 2012.) Available from: <http://www.amesengineering.com/amestexturescanner.html>.
22. Moore, D.F. Prediction of Skid Resistance Gradient and Drainage Characteristics for Pavements. Highway Research Record: Journal of Highway Research Board, 1966(131): p. 181-203.
23. Lu, Q. and B. Steven. Friction Testing of Pavement Preservation Treatments: Literature Review. 2006. University of California Pavement Research Center. (UCPRC-TM-2006-10)
24. Kayhanian, M. and B. Givens. Processing and Analysis of Roadway Runoff Micro (<20 μm) Particles. Journal of Environmental Monitoring. 2011. 13(10): p. 2,720-2,727.
25. Li, H., M. Kayhanian, and J. Harvey. Comparative Field Permeability Measurement of Permeable Pavements Using ASTM C1701 and NCAT Permeameter Methods. Journal of Environmental Management (to be published).
26. Kayhanian, M., D. Anderson, J.T. Harvey, D. Jones, and B. Muhunthan. Permeability Measurement and Scanning Images to Investigate Clogging of Pervious Concrete Pavements in Parking Lots. Journal of Environmental Management, 2012. 95(1): p. 114-123.
27. Kayhanian, M., C. Suverkropp, A. Ruby, and K. Tsay. Characterization and Prediction of Highway Stormwater Pollutant Event Mean Concentrations. Environmental Management, 2007. 85(2): p. 279-295.
28. McDaniel, R.S. and W. Thornton. Field Evaluation of a Porous Friction Course for Noise Control, in Annual Meeting CD-ROM for Transportation Research Board. 2005, National Research Council: Washington, D. C.



29. Kobayashi, T. Application Example of Porous Asphalt as Low Noise Pavement, in Proceedings for Specified Subjects, the 22nd Japan Road Conference. 1997. p. 35-36.
30. Rezaei, A., J. Harvey, and Q. Lu. Investigation of Noise and Durability Performance Trends for Asphaltic Pavement Surface Types: Five-Year Results. 2011. (UCPRC-RR-2012-04) Report prepared by UCPRC for the Caltrans Department of Research and Innovation.
31. Bloem, D. L. Skid-Resistance: The Role of Aggregates and Other Factors. 1971. *National Sand and Gravel Association Circular 109*, Silver Spring, MD.
32. Weissmann, J., and M.M. Martino., Evaluation of Seal Coat Performance by Using Macrotecture Measurements, in 88th Annual Meeting of the Transportation Research Board. 2009: Washington, D.C.
33. Barrett, M., C. Shaw. 2008. Benefits of Porous Asphalt Overlay on Storm Water Quality. *Transportation Research Record 2025*. pp. 127-134.
34. Coleri E., J. T. Harvey, K. Yang, J. M. Boone. Micromechanical investigation of open-graded asphalt friction courses' rutting mechanisms. *Construction and Building Materials* 2013, 44(0):25-34.

APPENDIX: TEST TRACK LAYOUT

HVS Section Layout on the North Outer Track for OGAC Study

Revision: 2/14/2012



-  Moisture damage sections
-  Rutting sections

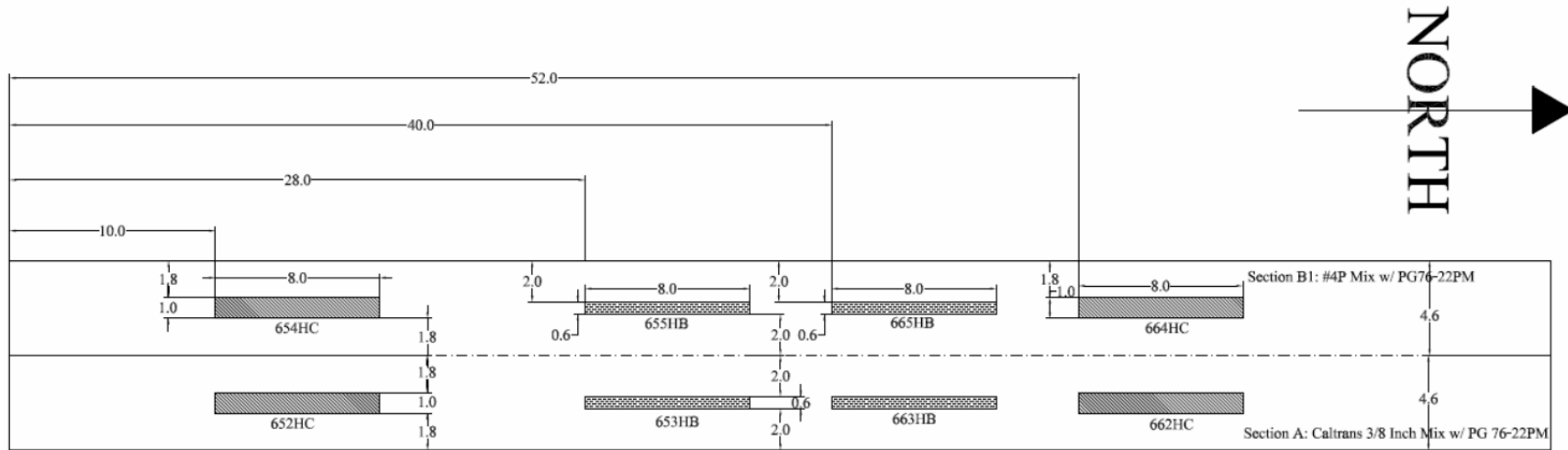
General Notes:

1. Rutting Sections are 8.0 m x 1.0 m.
2. Moisture Damage Tests are 8.0 m x 1.0 m
3. Each lane is 4.6 m wide
4. Starting point (i.e., west end) of the test track should be the same as the one used for outflow testing.

Figure A.1: HVS section layout on the north outer track for OGAC study.

HVS Section Layout on the West Outer Track for OGAC Study

Revision: 2/15/2012



General Notes:

1. Rutting Sections are 8.0 m x 1.0 m.
2. Moisture Damage Tests are 8.0 m x 1.0 m
3. Each lane is 4.6 m wide
4. Starting point (i.e., south end) of the test track should be the same as the one used for outflow testing.

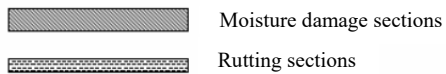


Figure A.2: HVS section layout on the west outer track for OGAC study.